Department
of
APPLIED MATHEMATICS

Nonlinear Effects During Transient
Fluid Flow in Reservoirs as
Encountered in Well-Test Analysis

by
Sigurd Ivar Aanonsen

Report no.79   March 1985

UNIVERSITY OF BERGEN
Bergen, Norway

Departement of Applied Mathematics

University of Bergen

5000 Bergen

Norway

Nonlinear Effects During Transient

Fluid Flow in Reservoirs as

Encountered in Well-Test Analysis

by

Sigurd Ivar Aanonsen

March 1985
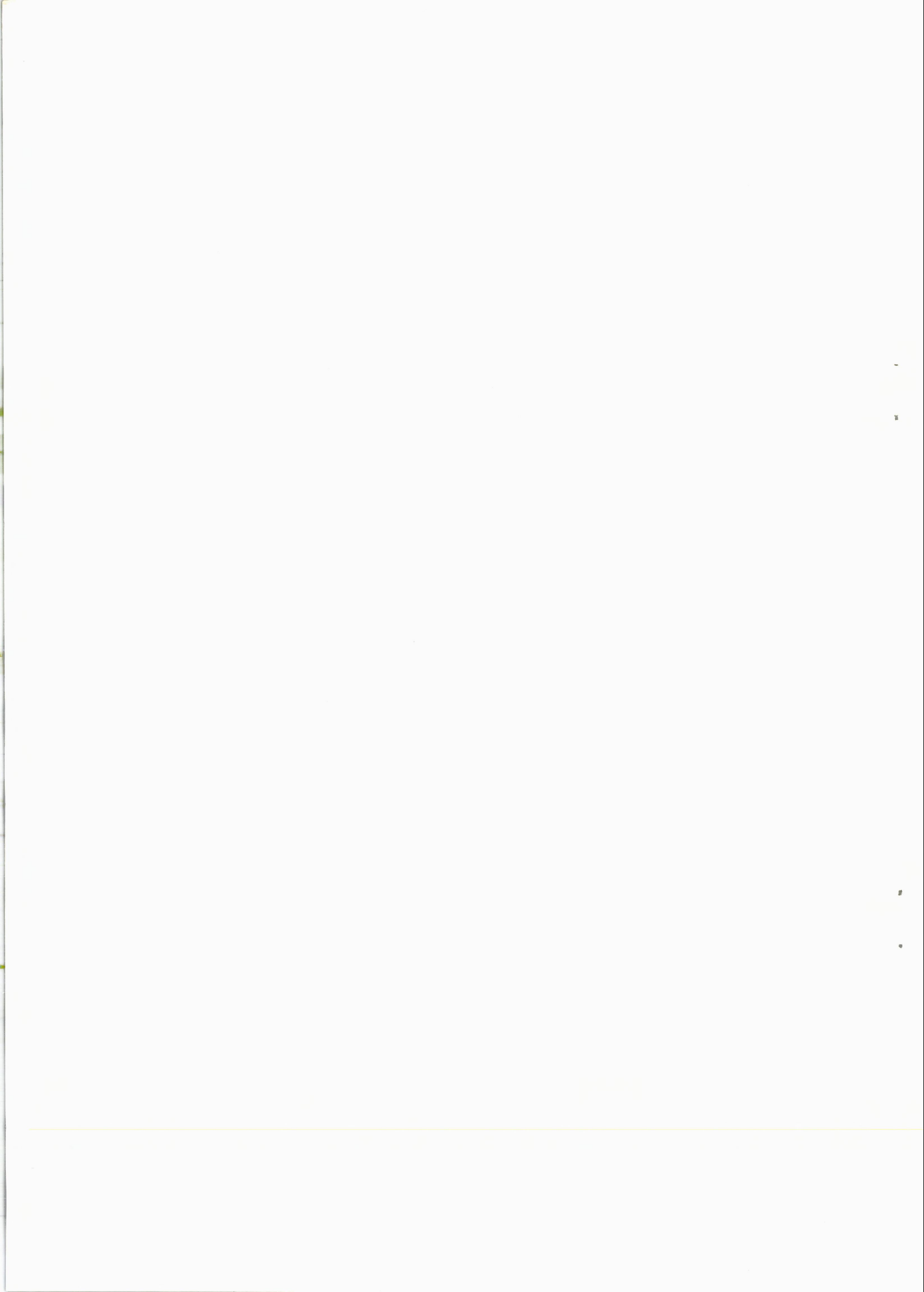
PREFACE

Flow of single-phase oil through porous media is generally accepted to be described by a linear diffusion equation, and in well-test analysis, which is a special case of the inverse problem, a number of methods have been developed based on solutions of this equation. Gas flow and two-phase flow is, however, much more complicated, and even though several methods have been proposed to analyse gas and two-phase well tests, the mathematical verification is often limited.

This report is a major part of my work for the degree Dr.Scient., and the background for the project was research on two-phase flow performed at Rogaland Research Institute in Stavanger. The object has been a study of the non-linear equations governing two-phase flow of oil and gas through porous media with emphasis on obtaining analytical solutions applicable to well-test analysis. However, since the problems occuring in two-phase pressure-test analysis are very similar to those encountered when analysing gas-well tests, and several questions in connection with gas flow was unanswered, a natural approach to the problem was to start with the nonlinear equation describing real gas flow. The different nonlinear effects in two-phase flow could then be identified. For that reason my research has been concentrated on two different problems which is discussed in Part 2 and Part 3 of this report, respectively. Part 2 describes single-phase gas flow, and in Part 3, two-phase flow is considered with emphasis on investigating whether the theory for gas flow can be applied also to that case. To present a basis for part 2 and 3, the general model equations are presented in Part 1. In addition, I also felt it useful to review some of the basic theory for single-phase flow of slightly compressible liquids.

For practical reasons, a separate list of references is placed at the end of each part. The same is done with the list of symbols. However, as far as possible the use of symbols is consistent throughout the report. Unless otherwise stated, all equations are written in absolute units.

Bergen, March 1985

Sigurd Ivar Aanonsen

T A B L E   O F   C O N T E N T S

PART 1

GENERAL THEORY

1.1 INTRODUCTION

Reliable information about in-situ reservoir conditions - rock, fluid, and well properties - is important in many phases of petroleum engineering. Pressure transient testing techniques, which includes generating and measuring pressure variations with time in wells, are an important tool for obtaining such information. Of the practical information obtainable from transient testing is wellbore volume, damage, and improvement; average reservoir pressure; permeability; porosity; reserves; and reservoir and fluid discontinuities.

Of the several hundred publications considering the subject of pressure tests in oil and gas wells, all but a handful assume that the reservoir fluids obey the linear diffusivity equation; an assumption which is strictly valid only for slightly compressible fluids. Most of the testing techniques are thus based on the constant terminal rate solution of this equation, together with the principle of super-position. Detailed description of these solutions and the different techniques may be found in Refs.[1,2,3,4].

For gas reservoirs and reservoirs where multiphase-flow effects are prevailing, the assumption of a slightly compressible fluid will not be valid, and the main object of this report is to study the nonlinear effects that arrise in these cases. The validity of and connections between previous theories are discussed, and some new solutions and methods are presented. Part 1 states the basic model equations describing the fluid flow in the reservoir, and some general considerations are discussed. In Part 2, single-phase gas flow is studied, and Part 3 is concerned with the special problems occuring when both oil and gas are flowing simultaneously in the reservoir.

1.2 MULTIPHASE FLOW IN POROUS MEDIA. N-COMPONENT MODEL. 3-COMPONENT MODEL

In the general compositional model describing fluid flow in porous media, three distict phases; gas, oil, and water, each satisfying Darcy's law, is assumed to exist in the reservoir. The reservoir fluid is assumed to consist of n chemical components; n-1 hydrocarbon components and water. In principle, a finite amount of each chemical component can be in the gas phase and the two liquid phases. However, the water phase will consist mainly of the chemical component water, and usually mass transfer between the water phase and the two hydrocarbon phases is neglected.

The model is described for instance by Peaceman [5], and will be presented only briefly here.

The system is assumed to be described by 3n+24 unknown variables (Large letter subscripts will be used for the phases, and small letter subscripts for the chemical components. Vector functions in R^3 are underlined):

- The filtration velocities of the three phases, $\underline{u}_G$, $\underline{u}_O$, $\underline{u}_W$ (9)

- Mass fractions of the individual components of the total mass of gas, oil, and water phase, respectively, C_{iG}, C_{iO}, C_{iW} (3n)

- Pressures, p_G, p_O, p_W (3)

- Phase densities, ϱ_G, ϱ_O, ϱ_W (3)

- Viscosities, μ_G, μ_O, μ_W (3)

- Saturations, S_G, S_O, S_W (3)

- Relative permeabilities, k_{rG}, k_{rO}, k_{rW} (3)

The corresponding equations are:

Continuity equations for each component:

$$\nabla \cdot \{ \ c_{iG} \varrho_G \underline{u}_G \ + \ c_{iO} \varrho_O \underline{u}_O \ + \ c_{iW} \varrho_W \underline{u}_W \ \}$$

(1.2.1)

$$+ \ \frac{\partial}{\partial t} \{ \ \varphi (\ c_{iG} \varrho_G S_G \ + \ c_{iO} \varrho_O S_O \ + \ c_{iW} \varrho_W S_W \ ) \ \} = 0$$

$$i = 1, 2, \ldots, n$$

Darcy's law for each phase:

$$\underline{u}_G = - \ \frac{k_{rG}}{\mu_G} \ K \cdot \{ \ \nabla p_G \ - \ \varrho_G \underline{g} \ \}$$

(1.2.2)

$$\underline{u}_O = - \ \frac{k_{rO}}{\mu_O} \ K \cdot \{ \ \nabla p_O \ - \ \varrho_O \underline{g} \ \}$$

$$\underline{u}_W = - \ \frac{k_{rW}}{\mu_W} \ K \cdot \{ \ \nabla p_W \ - \ \varrho_W \underline{g} \ \}$$

Elementary relations:

(1.2.3)

$$S_G + S_O + S_W = 1$$

(1.2.4)

$$\sum_{i=1}^{n} c_{iG} = 1$$

$$\sum_{i=1}^{n} c_{iO} = 1$$

$$\sum_{i=1}^{n} c_{iW} = 1$$

Equations of state:

$$f_1 (\varrho_G, p_G, c_{1G}, \ldots, c_{nG}) = 0$$

(1.2.5)

$$f_2 (\varrho_O, p_O, c_{1O}, \ldots, c_{nO}) = 0$$

$$f_3 (\varrho_W, p_W, c_{1W}, \ldots, c_{nW}) = 0$$

$$f_4(\mu_G, p_G, C_{1G}, \ldots, C_{nG}) = 0$$

(1.2.6) $\quad f_5(\mu_O, p_O, C_{1O}, \ldots, C_{nO}) = 0$

$$f_6(\mu_W, p_W, C_{1W}, \ldots, C_{nW}) = 0$$

Relative permeabilities:

$$k_{rG} = f_7(S_G, S_O, S_W)$$

(1.2.7) $\quad k_{rO} = f_8(S_G, S_O, S_W)$

$$k_{rW} = f_9(S_G, S_O, S_W)$$

Capillary pressures:

$$p_G - p_O = p_{cGO}(S_G, S_O, S_W)$$

(1.2.8)

$$p_O - p_W = p_{cOW}(S_G, S_O, S_W)$$

Phase equilibrium:

$$\frac{C_{iG}}{C_{iO}} = K_{iGO}(T, p_G, p_O, C_{1G}, \ldots, C_{nG}, C_{1O}, \ldots, C_{nO})$$

(1.2.9)

$$\frac{C_{iG}}{C_{iW}} = K_{iGW}(T, p_G, p_W, C_{1G}, \ldots, C_{nG}, C_{1W}, \ldots, C_{nW})$$

The temperature T is assumed to be constant. The tensor K gives the absolute permeability of the formation.

The fractions K_{iGO} and K_{iGW} in Eq.(1.2.9) are called K-values, equilibrium ratios, or equilibrium constants, even if the quantities are definitely not constants; and in this model it is assumed that the mass transfer in the reservoir is rapid relative to the fluid movement. A thorough discussion of state equations and relative compositions of petroleum fluids may be found in Ref.[6]. Relative permeabilities and capillary effects are described in Ref.[7] or [8], e.g., and Standing presents correlations for relative permeabilities in his notes from 1974 [9].

Numerical methods to simulate these equations have been presented, and much effort is made to improve the efficiency of compositional simulators. However, to date most work - numerically, and some analytically - has been on a simplified three-component system. Three chemical components, gas, oil, and water, are then defined as the parts of the reservoir fluid being in the respective phases at standard conditions, $p = p_{sc}$ and $T = T_{sc}$ <1>

Assume that the gas component consists of the chemical components $1, 2, \ldots, j$, the oil component of the components $j+1, \ldots, n-1$, and that component n is the water component. 9 new mass fractions may then be defined as:

$$C_{gG} = \sum_{i=1}^{j} C_{iG} \qquad C_{gO} = \sum_{i=1}^{j} C_{iO} \qquad C_{gW} = \sum_{i=1}^{j} C_{iW}$$

$$(1.2.10) \qquad C_{oG} = \sum_{i=j+1}^{n-1} C_{iG} \qquad C_{oO} = \sum_{i=j+1}^{n-1} C_{iO} \qquad C_{oW} = \sum_{i=j+1}^{n-1} C_{iW}$$

$$C_{wG} = C_{nG} \qquad C_{wO} = C_{nO} \qquad C_{wW} = C_{nW}$$

Eqs.(1.2.2), (1.2.3), (1.2.7), and (1.2.8) are valid also for this simplified system. Eq.(1.2.1) reduces directly to three new continuity equations for the new components by summation, and Eq.(1.2.4) simplifies to sums of three terms. However, it is not generally possible to generate new state equations and phase equilibrium equations from the old ones, and these have to be determined independently for the new system assuming that they can be written as functions only of the new reduced number of mass fractions.

<1>   Usually, p and T are taken to be 1 atm and $520\,^{\circ}R$ ($\approx 16\,^{\circ}C$).

The new gas/oil phase equilibrium equations become:

$$\frac{C_{gG}}{C_{g0}} = K_g(p, C_{gG}, C_{g0}, C_{oG}, C_{o0}; T)$$

(1.2.11)

$$\frac{C_{oG}}{C_{o0}} = K_o(p, C_{gG}, C_{g0}, C_{oG}, C_{o0}; T)$$

The so-called "β-model" may now be obtained by introducing the formation volume factors for gas and oil, B_G and B_0 and the solubility factors R_{so} and r_{sg}, where R_{so} is the solubility of gas in oil phase, and r_{sg} is the volatility of oil:

$$B_G \equiv \frac{\varrho_g^{\,s}}{\varrho_G} \; \frac{1}{C_{gG}} \qquad\qquad B_0 \equiv \frac{\varrho_o^{\,s}}{\varrho_0} \; \frac{1}{C_{o0}}$$

(1.2.12)

$$R_{so} \equiv \frac{\varrho_0 B_0}{\varrho_g^{\,s}} \, C_{g0} = \frac{\varrho_o^{\,s}}{\varrho_g^{\,s}} \, \frac{C_{g0}}{C_{o0}}$$

$$r_{sg} \equiv \frac{\varrho_G B_G}{\varrho_o^{\,s}} \, C_{oG} = \frac{\varrho_g^{\,s}}{\varrho_o^{\,s}} \, \frac{C_{oG}}{C_{gG}}$$

$\varrho_g^{\,s}$ and $\varrho_o^{\,s}$ are densities at standard conditions.

In the following, gravity, capillary effects, and mass transfer between the water phase and the two hydrocarbon phases will be neglected. In addition, the water phase is assumed to be incompressible with a constant saturation S_{iw}. However, all these effects can easily be included in the β-model.

The following equations are then obtained:

$$\nabla \cdot \left\{ \frac{\underline{u}_G}{B_G} + R_{so}\frac{\underline{u}_O}{B_O} \right\} + \frac{\partial}{\partial t} \left\{ \varphi\left(\frac{S_G}{B_G} + R_{so}\frac{S_O}{B_O} \right) \right\} = 0 \quad \text{gas component}$$

$$\nabla \cdot \left\{ \frac{\underline{u}_O}{B_O} + r_{sg}\frac{\underline{u}_G}{B_G} \right\} + \frac{\partial}{\partial t} \left\{ \varphi\left(\frac{S_O}{B_O} + r_{sg}\frac{S_G}{B_G} \right) \right\} = 0 \quad \text{oil component}$$

(1.2.13)

$$\underline{u}_G = - \frac{k_{rG}}{\mu_G} K \cdot \nabla p \qquad\qquad\qquad \text{gas phase}$$

$$\underline{u}_O = - \frac{k_{rO}}{\mu_O} K \cdot \nabla p \qquad\qquad\qquad \text{oil phase}$$

$$S_G + S_O = 1 - S_{iw}$$

or

$$\nabla \cdot \left\{ \left(\frac{k_{rG}}{\mu_G B_G} + R_{so}\frac{k_{rO}}{\mu_O B_O} \right) K \cdot \nabla p \right\} = \frac{\partial}{\partial t} \left\{ \varphi\left(\frac{S_G}{B_G} + R_{so}\frac{S_O}{B_O} \right) \right\} \quad \begin{matrix} \text{gas} \\ \text{component} \end{matrix}$$

$$\nabla \cdot \left\{ \left(\frac{k_{rO}}{\mu_O B_O} + r_{sg}\frac{k_{rG}}{\mu_G B_G} \right) K \cdot \nabla p \right\} = \frac{\partial}{\partial t} \left\{ \varphi\left(\frac{S_O}{B_O} + r_{sg}\frac{S_G}{B_G} \right) \right\} \quad \begin{matrix} \text{oil} \\ \text{component} \end{matrix}$$

(1.2.14)

$$S_G + S_O = 1 - S_{iw}$$

If the phase densities, viscosities, and K-values are independent of composition, B_G, B_O, R_{so}, and r_{sg} will be functions of pressure and the parameter T only. Eq.(1.2.14) is then a system of three equations in the three unknowns S_G, S_O, and p.

For solution gas drive reservoirs, this simplified model is generally accepted as a good description of the reservoir processes. r_{sg} is then set equal to zero, i.e., no oil component (also called stock tank oil) is assumed to exist in gas phase. The model is then usually called a "black-oil" model, or also a β-model. According to Muskat [10] p.302, these equations were stated by Muskat and Meres as early as in 1936.

Other important examples of reservoirs exhibiting two-phase flow is gas condensate and volatile oil reservoirs where both hydrocarbon components can exist in both gas and oil phase. Generally, these systems are much more complicated than black-oil reservoirs, but for some reservoir processes the equilibrium ratios may be assumed to be independent of composition also in these cases. In 1973, Cook et al. [11] presented a generalized black oil model very similar to Eqs.(1.2.14) which accounted for compositional effects in volatile oil and gas condensate reservoirs. The fluid properties were then assumed to depend both on pressure and a compositional parameter. Spivak and Dixon [12] suggested that gas condensate reservoirs could be represented by a model which included a volatility-factor r_{sg}, but with $R_{so} \equiv 0$; and Fussell [13] presented a study showing that the K-values and phase densities could be considered unique functions of pressure for many single-well performance predictions for gas condensate reservoirs.

The boundary conditions imposed on the flow equations at wells produced with a surface volume rate of for instance gas component, $q_g(t)$, is found to be:

$$(1.2.15) \qquad \int_S \left\{ \left(\frac{k_{rG}}{\mu_G B_G} + R_{so} \frac{k_{rO}}{\mu_O B_O} \right) K \cdot \nabla p \right\} \cdot \underline{n} \, dS = -q_g(t)$$

or

$$(1.2.16) \qquad \left\{ \left(\frac{k_{rG}}{\mu_G B_G} + R_{so} \frac{k_{rO}}{\mu_O B_O} \right) K \cdot \nabla p \cdot \underline{n} \right\}_S = -\frac{q_g(t)}{2\pi r_w h}$$

S is the perforated part of the well, $\underline{n}$ is unit normal into the well, r_w is the well radius, and h the perforated height. The boundary conditions at the rest of the reservoir boundary can be a specified pressure or flux, or a combination of both. Usually in well test analysis only one well is considered, and the perforated interval is assumed to be equal to the reservoir height, which in turn is assumed

to be constant. The flow is assumed to be purely radial and K and φ to be independent of the radial distance from the well.

If only one single phase is flowing in the reservoir, the flow equations reduce to:

(1.2.17)
$$\frac{1}{r}\frac{\partial}{\partial r}\left\{ \frac{k}{\mu_j B_j} r \frac{\partial p}{\partial r} \right\} = \frac{\partial}{\partial t}\left\{\frac{\varphi}{B_j}\right\}$$

or

(1.2.18)
$$\frac{1}{r}\frac{\partial}{\partial r}\left\{ \frac{k\varrho_j}{\mu_j} r \frac{\partial p}{\partial r} \right\} = \frac{\partial}{\partial t}\left\{\varrho_j\varphi\right\}$$

where j = G or O, and k is the component of K in the direction of flow.

1.3 SOME QUALITATIVE CONSIDERATIONS

Before studying the nonlinear flow equations in detail, it may be useful to take a look at some of the well-known solutions of the linear diffusion equation. The term "liquid solution" will be used for these solutions, since they apply to flow of slightly compressible fluids, including oil.

If the permeability k and the porosity φ are constants, Eq.(1.2.18) may be written, with the subscripts omitted:

$$(1.3.1) \qquad (\frac{1}{\varrho}\frac{d\varrho}{dp} - \frac{1}{\mu}\frac{d\mu}{dp})(\frac{\partial p}{\partial r})^2 + \frac{1}{r}\frac{\partial}{\partial r}(r\frac{\partial p}{\partial r}) = \frac{\varphi\mu c}{k}\frac{\partial p}{\partial t}$$

For liquid flow, the first term in this equation is usually neglected based on the following assumptions (Dake [3]):

- The viscosity μ is practically independent of pressure and may be regarded as constant.

- The pressure gradient $\partial p/\partial r$ is small and therefore, terms of order $(\partial p/\partial r)^2$ can be neglected.

However, this simple linearization must be treated with caution, and Dake refers to a paper by Drauchuk and Quon (Ref. 2 p.39 in Ref [3]) who show that a necessary condition for linearization is that the product of pressure change and compressibility is small. It is here important to realize that it is the factor multiplying $(\partial p/\partial r)^2$ that makes the total term negligible, and not a small pressure gradient. As will be seen, the relative magnitude of the pressure gradient compared to the time derivative or Laplacian, will change considerably with time and space and depend on the type of flow considered.

To examplify this, we assume that Eq.(1.3.1) may be linearized and that $\mu c \approx$ constant. Assume further that the reservoir is circular with a closed outer boundary, that a single well at $r = 0$ is produced with constant rate q, and that the initial pressure is constant. This imply the following initial and boundary conditions:

$$(1.3.2) \qquad p(r,t=0) = p_i$$

$$(1.3.3) \qquad \lim_{r \to r_w} r\frac{\partial p}{\partial r} = \frac{qB\mu}{2\pi kh}$$

$$(1.3.4) \qquad \lim_{r \to r_e} \frac{\partial p}{\partial r} = 0$$

For early times, the reservoir may be assumed to be infinite in extent, and Eq.(1.3.4) is replaced by:

$$(1.3.5) \qquad \lim_{r \to \infty} p = p_i$$

As long as the reservoir is infinite-acting, the pressure is varying only over a single scale in r and t, respectively. Radius and time may then for instance both be scaled with the radius of the well, r_w as a basis. Dimensionless variables may be defined as:

$$(1.3.6) \qquad r_D = \frac{r}{r_w} \quad , \quad t_D = \frac{k\,t}{\varphi\mu c r_w^2}$$

The pressure drop depends on the production rate q, and a dimensionless pressure drop is therefore defined as:

$$(1.3.7) \qquad p_D = \frac{2\pi kh}{qB\mu}(p_i - p)$$

In the infinite-acting period, the well may be approximated by a line source, an approximation which gives a uniformly valid solution except for very small r and t.

The solution of the linearized form of Eq.(1.3.1) with the proper initial and boundary conditions, is then the well-known line-source solution, also named the Theis solution [14]:

(1.3.8)

$$p_D(r_D, t_D) = \frac{1}{2} E_1(y) = \frac{1}{2} E_1(\frac{r_D^2}{4t_D})$$

$$\approx - \frac{1}{2}(\ln y + \gamma) \qquad\qquad y \ll 1$$

where E_1 is the first order exponential integral function [15], and γ is Euler's constant.

Compute now $\dfrac{\partial p_D}{\partial r_D}$, $\dfrac{\partial p_D}{\partial t_D}$, and $\dfrac{1}{r_D}\dfrac{\partial}{\partial r_D} (r_D\dfrac{\partial p_D}{\partial r_D})$:

(1.3.9)

$$\frac{\partial p_D}{\partial r_D} = - \frac{1}{r_D} \exp\{- \frac{r_D^2}{4t_D} \}$$

(1.3.10)

$$\frac{\partial p_D}{\partial t_D} = \frac{1}{t_D} \exp\{- \frac{r_D^2}{4t_D} \}$$

(1.3.11)

$$\frac{1}{r_D}\frac{\partial}{\partial r_D} (r_D\frac{\partial p_D}{\partial r_D}) = \frac{1}{t_D} \exp\{- \frac{r_D^2}{4t_D} \}$$

At least in a region near the well, the gradient is not small compared to the other quantities. On the contrary, it is much larger except for very small times.

Now consider the effects of an outer boundary. In this case, there will be two scales for r; namely r_w and r_e, and correspondingly two scales for t. We may define r_{DA} and t_{DA} by:

$$(1.3.12) \qquad r_{DA} = \frac{r}{r_e} \quad , \quad t_{DA} = \frac{kt}{\varphi\mu cA} = \frac{kt}{\varphi\mu c\pi r_e^2}$$

If $r_w \ll r_e$, the difference between the two scales will be large, and if the small quantity $\varepsilon = r_w/r_e$ is introduced, we get:

$$(1.3.13) \qquad r_{DA} = \varepsilon r_D \quad , \qquad t_{DA} = \frac{\varepsilon^2}{\pi} t_D$$

The end of the infinite-acting period occurs approximately at $t_{DA} = 0.1$. Hence, we may say that we already are on the second time scale when the boundaries are felt.

The pseudosteady state (PSS) solution, which is obtained by assuming a constant pressure decline at every point in the reservoir, is [3]:

$$(1.3.14) \qquad p_D(r_D, t_{DA}) = 2\pi t_{DA} + \ln\frac{r_{eD}}{r_D} + \frac{r_D^2}{2r_{eD}^2} - \frac{3}{4}$$

Note that Eq.(1.3.14) is an exact solution of the linearized flow equation. The boundary conditions are almost exactly satisfied if $r_w \ll r_e$.

If now the derivatives are computed as in the infinite-acting case, it will be seen that the gradient near the well is still much larger than both the time derivative and the Laplacian.

As shown on Fig.1.1, the r-t plane may be divided into 4 different flow regions. Region 1 corresponds to the part of the infinite-acting period where $y \ll 1$, and Region 2 to the part where this assumption is invalid. Note that Region 1 corresponds to the region where the logarithmic approximation to $E_1(y)$ is valid. Somewhat loosely it may

be said that both in Region 1 and 2, r and t are on the r_w-scale. In
region 3, r_w defines the r-scale and r_e the t-scale, and in Region 4,
r_e defines both the r- and t-scales.

The linearized flow equation may then be written in Region 3 and 4,
respectively:

$$(1.3.15) \qquad \frac{1}{r_D}\frac{\partial}{\partial r_D}\left(r_D\frac{\partial p_D}{\partial r_D}\right) = \frac{\epsilon^2}{\pi}\frac{\partial p_D}{\partial t_{DA}} \qquad \text{Region 3}$$

$$(1.3.16) \qquad \frac{1}{r_{DA}}\frac{\partial}{\partial r_{DA}}\left(r_{DA}\frac{\partial p_D}{\partial r_{DA}}\right) = \frac{\partial p_D}{\partial t_{DA}} \qquad \text{Region 4}$$

In Region 4 the terms in the equation are of the same order, but in
Region 3 the right hand side is multiplied by ϵ^2, which usually is a
very small quantity.   The expansion term on the right hand side of
Eq.(1.3.15) may therefore be neglected in this region. Together with
the inner boundary condition this then yields an inner solution given
by:

$$(1.3.17) \qquad p_D(r_D,t_{DA}) = -\ln r_D + f(t_{DA})$$

f is a function of time that has to be determined by matching with an
outer solution valid in Region 4. Note that neglecting the term on
the right hand side of Eq.(1.3.15) is not the same as assuming steady
state flow, since the function f may have a general time dependence.

In principle, an estimate of the size of Region 3 could be found by
introducing a characteristic radius R and defining another
dimensionless radius $r_{DR} = r/R$. If this is inserted in Eq.(1.3.15),
neglection of the right hand side requires $R^2 \ll \pi r_e^2$. Numerical
results indicate that a reasonable estimate of R is about $r_e/3$. On a
logarithmic scale, this corresponds to Region 3 occupying a
significant part of the reservoir, confer Fig.1.1.

The same may be done with the gas flow equation, Eq.(2.2.1), implying
the condition:

(1.3.18) $$R^2 \ll \pi r_e^2 \frac{(\mu c)_i}{\mu c}$$

Hence, if the reservoir is not too small, Region 3 will still exist,
but the size is decreased because $\mu c \geqslant (\mu c)_i$. Since μc is varying
over the reservoir, it is difficult to estimate R from Eq.(1.3.18),
but it is useful as an illustration of the process.

Note that for steady state flow, Region 4 will not exist, and the
solution profile will be logarithmic for all r.

Now turn to the case of buildup where the well is shut in, and assume
that the reservoir is infinite with a logarithmic pressure profile for
all r at $\Delta t = 0$ (this is just a theoretical case that never will
occur in practice).   That is, we have the following problem for the
dimensionless pressure rise during buildup p_{Ds}:

(1.3.19) $$\left\{ \frac{1}{r_D} \frac{\partial}{\partial r_D} \left(r_D \frac{\partial}{\partial r_D} \right) - \frac{\partial}{\partial t_D} \right\} p_{Ds} = 0$$

(1.3.20) $$p_{Ds}(r_D, \Delta t_D = 0) = \frac{q\mu}{2\pi kh} \{ p(r, t_p) - p_w(t_p) \} = \ln r_D$$

(1.3.21) $$\lim_{r \to 0} \frac{\partial p_{Ds}}{\partial r_D} = 0$$

It is assumed that the presence of the well may be neglected. An
exact solution of Eqs.(1.3.19) - (1.3.21) is:

(1.3.22) $$p_{Ds}(r_D, \Delta t_D) = \frac{1}{2} E_1 \left(\frac{r_D^2}{4\Delta t_D} \right) + \ln r_D$$

and if the derivatives are calculated, it follows that in this case
the pressure gradient, except for very small Δt or large r, will be
smaller than the time derivative and the Laplacian, the difference
increasing with decreasing values of $r^2/\Delta t$.

Except for very small Δt, Eq.(1.3.22) for $r = r_w$ is equal to the
Miller-Dyes-Hutchinson (MDH) solution [16]:

$$(1.3.23) \qquad\qquad p_{wDs}(\Delta t) = \frac{1}{2} \{ \ln\Delta t_D + \ln 4 - \gamma \}$$

This shows that the logarithmic time dependence for the buildup
solution only depends on the drawdown solution profile in Region 3.
The deviation from the MDH straight line for large Δt is due to the
deviation from the logarithmic profile of the drawdown solution in
Region 4 in addition to the reservoir boundaries. That is, we may say
that the domain of dependence for the buildup solution for $\Delta t < \Delta t_{eMDH}$
(end MDH half-log straight line) is included in the part of the
drawdown solution at shut-in which lies in Region 3. This is
illustrated in Fig 1.1 where the curve between the points A and B is
drawn arbitrarily. Note that since the propagation speed is infinite
for a parabolic equation, this is rather a numerical and not a
strictly mathematical concept.

A consequence of this is that if we are mainly interested in obtaining
a buildup solution in the semilog straight line region, we do not have
to consider the drawdown solution in Region 4.

This discussion may be summarized as follows:

  i) It is misleading to say that the flow equation for liquid flow
     may be linearized because the pressure gradient is small. As
     demonstrated, the relative magnitude of the different terms in
     the flow equation will change considerably from point to point,
     and with the type of flow considered. The reason for the
     successful linearization is solely the factor multiplying the
     term involving $(\partial p/\partial r)^2$ in Eq.(1.3.1).

ii) For drawdown the r-t plane may be divided into two regions, each with two sub-regions: The first consisting of Region 1 and 3 where the expansion terms in the flow equation may be neglected, and the second which consists of Region 2 and 4 where all terms in the flow equation are of the same order.

iii) For buildup too, the r-t plane may be divided into two regions: One which is influenced only by the drawdown profile in Region 3 (or Region 1 if the well is closed in before the boundary is felt) and a second which is influenced both by the drawdown solution profile in Region 4 and the reservoir boundaries (or Region 2). The part of the line $r = r_w$ included in the first of these regions corresponds approximately to the time interval where the MDH-approximation is valid.

In this section only liquid flow has been considered. However, it is temptating to assume that the statements i) - iii) are generally valid also for gas flow and cases where oil and gas are flowing simultaneously, at least if the coefficients in the equations behave relatively "nice". In fact, it will be demonstrated in Part 2 and 3 that several of the commonly used methods for analysing gas well tests and two-phase tests are essentially based on these assumptions and the additional assumption that:

iv) Quadratic gradient terms may be neclected during buildup.

NOMENCLATURE

A	Drainage area
B_G, B_0	Formation volume factors for gas and oil
C_{iX}	Mass fraction of component i of the total mass of phase X
$c = \dfrac{1}{\varrho}\dfrac{d\varrho}{dp}$	Compressibility
$E_1(z) = \displaystyle\int_z^\infty \dfrac{e^{-t}}{t}dt$	Exponential integral function of order 1 [15]
$\underline{g}$	Gravity vector
h	Reservoir height
K, k	Absolute permeabilities
k_{rX}	Relative permeability of phase X
K_{iGO}, K_{iOW}, K_g, K_o	Phase equilibrium ratios (see Eqs.(1.2.9,11))
$\underline{n}$	Unit outer normal to reservoir boundary
p, p_X	Pressure, pressure of phase X
p_i	Initial pressure
p_w	Wellbore pressure
$p_D = \dfrac{2\pi kh}{qB\mu}(p_i - p(r,t))$	Dimensionless pressure fall
$p_{Ds} = \dfrac{2\pi kh}{qB\mu}(p(r,t_p+\Delta t) - p(r_w,t_p))$	Dimensionless pressure rise during buildup
p_{cGO}, p_{cOW}	Capillary pressure functions (see Eq.(1.2.8))

q, q_i	Production rate, production rate of component i
R	Characteristic radius of Region 3
r	Radius
r_w	Radius of well
r_e	Radius of outer boundary
$r_D = r/r_w$	Dimensionless radius based on r_w
$r_{DA} = r/r_e$	Dimensionless radius based on r_e
R_{so}	Solubility of gas component in oil phase
r_{sg}	Volatility of oil component
S	Surface of perforated part of well
S_X	Saturation of phase X
S_{iw}	Irreducible water saturation
T	Temperature
t	Time
t_p	Production time
$\Delta t = t - t_p$	Shut-in time
$t_D = \dfrac{kt}{\varphi\mu c r_w^2}$	Dimensionless time based on r_w
$t_{DA} = \dfrac{kt}{\varphi\mu cA}$	Dimensionless time based on drainage area
$\underline{u}_X$	Filtration velocity of phase X
$y = \dfrac{r_D^2}{4t_D}$	Boltzmann variable

$\gamma = 0.5772...$ Euler's constant

$\epsilon = r_w/r_e$

φ Porosity

μ_X Viscosity of phase X

ϱ_X Density of phase X

$\varrho_i^{\,s}$ Density of component i at standard conditions

Subscripts

D	Dimensionless
e	External
g,o,w	Gas, oil, or water component
i	Chemical component; in β-model i = g, o, or w
G,O,W	Gas, oil, or water phase
X	G, O, or W
sc	Standard conditions
w	Well

REFERENCES

[1] Matthews,C.S. and Russell,D.G.: "Pressure Buildup and Flow Tests
     in Wells," Monograph Series, Society of Petroleum
     Engineers of AIME, Vol.1, Dallas (1967).

[2] Earlougher,R.C.,Jr.: "Advances in Well Test Analysis,"
     Monograph Series, Society of Petroleum Engineers of AIME, Vol.5,
     Dallas (1977).

[3] Dake,L.P.: "Fundamentals of Reservoir Engineering," Elsevier
     Scientific Publishing Company, Amsterdam (1978).

[4] Lee,J.: "Well Testing," Textbook Series, Society of Petroleum
     Engineers of AIME, Vol.1, Dallas (1982).

[5] Peaceman,D.W.: "Fundamentals of Numerical Reservoir Simulation,"
     Elsevier Scientific Publishing Company, Amsterdam (1977).

[6] McCain,W.D.,Jr.: "The Properties of Petroleum Fluids,"
     PennWell Publishing Company, Tulsa (1973).

[7] Aziz,K. and Settari,A.: "Petroleum Reservoir Simulation,"
     Applied Science Publishers Ltd., London (1979).

[8] Marle,C.M.: "Multiphase Flow in Porous Media," Editions
     Technip, Paris (1981).

[9] Standing,M.B.: "Notes on Relative Permeability Relationships,"
     Division of Petroleum Engineering and Applied Geophysics,
     Norwegian Institute of Technology, University of Trondheim,
     Trondheim (1974).

[10] Muskat,M.: "Physical Principles of Oil Production," McCraw-
     Hill, New York (1949), Second Edition: IHRDC, Boston (1981).

[11] Cook,R.E., Jacoby,R.H., and Ramesh,A.B.: "A Beta-Type Reservoir
     Simulator for Approximating Compositional Effects During Gas
     Injection," Paper SPE 4272, Presented at the SPE-AIME 3rd
     Symposium on Numerical Simulation of Reservoir Performance,
     Houston, Texas, Jan. 10-12 (1973)
     Also: "Numerical Simulation," SPE Reprint Series No.11, Society
     of Petroleum Engineers of AIME, Dallas (1973) 246-257.

[12] Spivak,A. and Dixon,T.N.: "Simulation of Gas-Condensate
     Reservoirs," Paper SPE 4271, Presented at the SPE-AIME 3rd
     Symposium on Numerical Simulation of Reservoir Performance,
     Houston, Texas, Jan. 10-12 (1973).

[13] Fussell,D.D.: "Single-Well Performance Predictions for Gas
     Condensate Reservoirs," J.Pet.Tech. (July 1973) 860-870.

[14] Theis,C.V. "The Relation Between the Lowering of the Piezometric
     Surface and the Rate and Duration of Discharge of a Well Using
     Ground-Water Storage," Trans.Amer.Geophys.Union (1935) $\underline{16}$,
     519-524.
     Also: "Pressure Transient Testing Methods," SPE Reprint Series
     No. 14, Society of Petroleum Engineers of AIME, Dallas (1980),
     27-32.

[15] Abramowitz,M. and Stegun,I.A.: "Handbook of Mathematical
     Functions," Dover Publications, Inc., New York (1965).

[16] Miller,C.C., Dyes,A.B., and Hutchinson,C.A.,Jr.: "The
     Estimation of Permeability and Reservoir Pressure from
     Bottom Hole Pressure Build-Up Characteristics," Trans. AIME
     (1950) $\underline{189}$, 91-104
     Also: "Pressure Analysis Methods," SPE Reprint Series No.9,
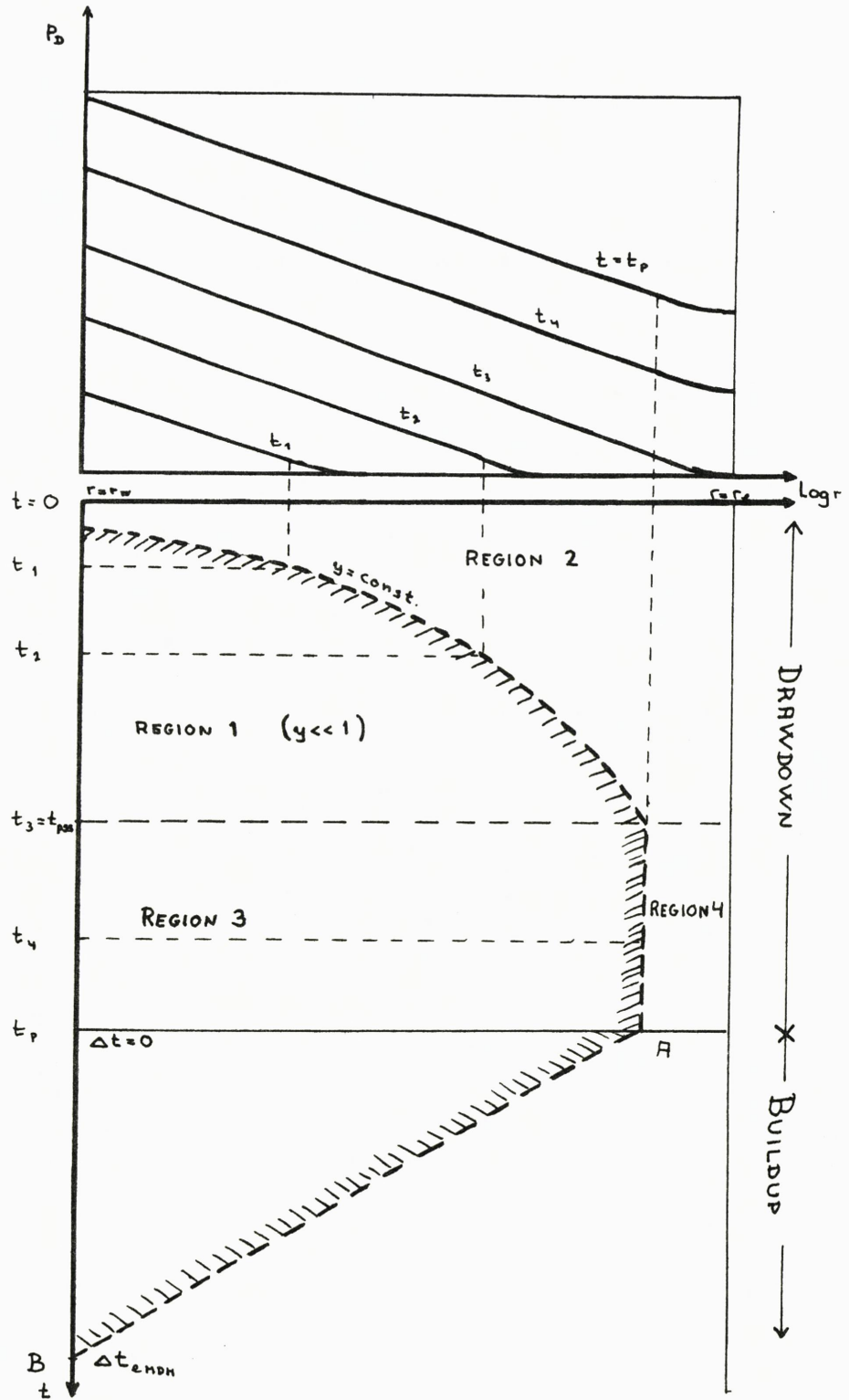   Society of Petroleum Engineers of AIME, Dallas (1967), 11-24.

<u>Fig. 1.1</u> Different flow regions for a drawdown/buildup process.

PART 2

REAL GAS FLOW

2.1 INTRODUCTION

In contrast to flow of a slightly compressible liquid, the equation
describing isothermal flow of real gases through porous media, is not
easily linearized. Several approaches have been used to generate
solutions of the nonlinear gas flow equation from the known liquid
solution. The work of Aronofsky and Jenkins[1] in 1954 lead to the
use of p^2 as the variable for analysing gas flow. Al-Hussainy et al.
[2] introduced in 1966 a Kirchhoff integral transformation of
pressure:

$$(2.1.1) \qquad m(p) = 2 \int_{p_0}^{p} \frac{p \ dp}{\mu(p)Z(p)}$$

Applying the equation of state for a real gas:

$$(2.1.2) \qquad \frac{p}{\varrho(p)Z(p)} = \frac{p_{sc} \ T}{\varrho_{sc} \ T_{sc}}$$

it is easily recognized that Eq.(1.2.18) together with Eq.(2.1.1)
transformes to an equation similar to the flow equation for a slightly
compressible fluid:

$$(2.1.3) \qquad \nabla^2 m = \frac{\varphi\mu c}{k} \frac{\partial m}{\partial t} \qquad m = m(p)$$

The new function m(p) was called "the real gas pseudopressure". In
Eq.(2.1.3) k and φ are assumed constant, but a variation in these
quantities with pressure can be accounted for in the definition of m
[3].

Since μc is not constant in Eq.(2.1.3), the equation is still not linearized. However, equally important may be that it linearizes the inner boundary condition when this is given as the surface production rate. We get the following boundary condition for m(p) corresponding to Eq.(1.3.3):

$$(2.1.4) \qquad \lim_{r \to r_w} \left(r \frac{\partial m}{\partial r} \right) = \frac{2Tp_{sc}}{T_{sc}} \frac{q(t)}{2\pi kh}$$

Al-Hussainy et al. [2] assumed μc to be constant, $\mu c = (\mu c)_i$, which gives an equation for m that is identical to the linear equation for liquid flow. A non-Darcy component is also often taken into account as a skin factor proportional to flow rate when analysing gas well tests (see Ref.[18] or [25], e.g.), but this effect will not be discussed here. However, the variations in μc with pressure, which are substantial for low pressures, may lead to serious errors and misinterpretation if the theory for liquid flow is used uncritically [4,5,6].

Agarwal[4] introduced in 1979 a transformation called "real gas pseudotime" to account for the variations in the μc-product when analysing buildup tests in massive hydraulic fractured (MHF) wells. However, this transformation still do not linearize the flow equation exact. Lee and Holditch [6] formulated in 1982 the correction terms that appear in the flow equation when pseudotime is used, but made no attempt to estimate their relative magnitude. In a recent paper, Finjord [7] gives an analytic study of the pseudo-time transformation, and shows that for drawdown in an infinite reservoir the correction terms will not be small. Hence, the transformation will not linearize the equation effectively in this case. The validity of pseudotime for buildup is not affected by this result, and pseudotime has been used to analyse buildup tests with good results [4,6,8,9]. However, a theoretical verification of pseudotime for the various cases is still missing.

Kale and Mattar [10] obtained in 1980 a solution of Eq.(2.1.3) that takes into account the variations in μc by using a regular

perturbation method. Only the case of drawdown in an infinite reservoir was studied, and the solution was given as an integral expression for the difference between the solution of the nonlinear equation and the liquid solution. They also showed that this correction term rapidly approaches a small constant value.

In Sec. 2.2 a similar solution is obtained by expanding μc in a Taylor series in the pseudopressure. We then get a correction term as an infinite sum involving the derivatives of μc with respect to pressure. This term approaches a slightly different value than the one obtained by Kale and Mattar [10] for large times. This is because they neglect a second order gradient term, which is not necessarily small (see Appendix 2.1). However, for the case of gas flow, the correction term, which can be seen as a constant negative skin, will usually be small and negligible.

The same procedure is used to find solutions for buildup, and it is shown that under certain conditions the wellbore pseudopressure will follow a straight line on a half-log plot with a slightly larger slope than the liquid solution. Hence, the superposition principle is not strictly valid. Analytic expressions are given for the slope if the μc-product can be approximated by a linear function of m.

The perturbation solution obtained for drawdown and buildup is in Sec. 2.3 compared with solutions based on Agarwal's pseudotime solution [4]. It is shown analytically that when the perturbation solution is valid, the pseudotime solution, to the leading order, is consistent with the perturbation solution for buildup, but not for drawdown. Thus the results of Finjord [7] for drawdown is verified.

The validity of the perturbation solution is studied in Sec. 2.4. Several functional dependences of $\mu c(m)$ was considered with good results. Problems arise, however, for buildup when the perturbation solution is applied to real gas flow. This is due to the extreme form of $\mu c(m)$ for low pressures.

In Secs. 2.5 and 2.6 a reservoir with finite size is considered. It is shown that an exact material balance equation may be used to

generate a solution valid in the whole reservoir after the boundaries are felt. A new method to estimate reservoir size and shape is proposed, and problems in connection with the estimation of average reservoir pressure in a gas reservoir are considered. Several methods have been proposed to account for the variation in μc when average pressure is estimated from a buildup test [5,11,12]. These methods are rather complicated, but it is shown in Sec. 2.6 that the standard methods for liquid flow may be used if shut-in time is replaced with pseudotime in the buildup plots.

The presented results are supported with several numerical simulations of drawdown/buildup in a gas reservoir. The simulations are, however, limited to the case of a single well producing from the center of a circular, homogeneous reservoir. Data for the simulations are given in Appendix 2.3.

2.2 SOLUTION OF FLOW EQUATION FOR AN INFINITE RESERVOIR BY A REGULAR PERTURBATION METHOD.

Assume that the initial pressure is constant and that one well in the center of an infinite reservoir is produced with a constant surface volum rate q for a time t_p before it is shut in. In terms of the dimensionless quantities defined in the nomenclature, the following system is then obtained:

(2.2.1)
$$\frac{1}{r_D} \frac{\partial}{\partial r_D} (r_D \frac{\partial m_D}{\partial r_D}) = \frac{\mu c}{(\mu c)_i} \frac{\partial m_D}{\partial t_{Di}} \qquad r_D > 0$$

(2.2.2)
$$m_D(r_D, 0) = 0 \qquad r_D > 0$$

(2.2.3)
$$\lim_{r_D \to \infty} m_D(r_D, t_D) = 0 \qquad t_D > 0$$

(2.2.4)
$$\lim_{r_D \to 1} (r \frac{\partial m_D}{\partial r_D}) = \begin{cases} -1 & 0 < t_D < t_{pD} \\ 0 & t_D > t_{pD} \end{cases}$$

The basic assumption is now that the nonlinear terms in μc are small. Solutions are then obtained by expanding μc in Taylor series about the initial and shut-in values respectively and assuming that all terms except for the constant term is of order ϵ in magnitude, where ϵ is a small parameter. At shut-in, the buildup solution is matched with the drawdown solution to every order in ϵ.

A solution of the dimensionless form of Eqs.(2.2.1) - (2.2.4) is then searched as an asymptotic series in ϵ:

(2.2.5)
$$m_D = m_D^{(0)} + \epsilon\, m_D^{(1)} + \ldots$$

For $t < t_p$ (drawdown) exact solutions may be obtained for $m_D^{(0)}$ and

$m_0^{(1)}$ if we assume the well to be a line source. μc is then expanded about the initial value:

$$\frac{\mu c}{(\mu c)_i} = 1 + [\frac{1}{\mu c}\frac{d(\mu c)}{dm_D}]_i \, m_D + \frac{1}{2}[\frac{1}{\mu c}\frac{d^2(\mu c)}{dm_D^2}]_i \, m_D^2 + \dots$$

(2.2.6)

$$= 1 + \varepsilon \sum_{n=1}^{\infty} a_n \, m_D^n$$

a_n, $n = 1\ 2\ \dots$ are similarity coefficients of order 1. ε may for instance be chosen equal to the first order derivative term implying $a_1 = 1$.

Substituting Eqs.(2.2.5) and (2.2.6) into Eq.(2.2.1), and identifying terms of the same order in ε, the result becomes for $m_D^{(0)}$ and $m_D^{(1)}$ (See Appendix 2.1):

(2.2.7) $m_D^{(0)}(y) = \frac{1}{2} E_1(y)$

(2.2.8) $m_D^{(1)}(y) = - \sum_{n=1}^{\infty} \frac{a_n}{2^{n+1}} \{ E_1(y) \int_0^y E_1^n(y)dy + \int_y^{\infty} E_1^{n+1}(y)dy \}$

where $y = r_D^2/4t_D$. Note that the zeroth order solution is the usual line source solution or Theis solution [14], and that the limit of $m_D^{(1)}$ as y approaches 0 gives the correction term to the line source solution at the well for large times:

$$\lim_{y \to 0} \varepsilon m_D^{(1)}(y) = - \sum_{n=1}^{\infty} \{ \frac{\varepsilon a_n}{2^{n+1}} \int_0^{\infty} E_1^{n+1}(y)dy \}$$

(2.2.9)

$$= - \sum_{n=1}^{\infty} \{ \frac{1}{2^{n+1}} [\frac{1}{\mu c}\frac{d^n(\mu c)}{dm_D^n}]_i \int_0^{\infty} E_1^{n+1}(y)dy \}$$

It can be shown that these integrals converge, and they are easily calculated numerically. We assume that the derivatives a_i behave

nicely enough for the infinite series to converge uniformly and absolute. If that is not the case, the nonlinear terms will not be small, and the perturbation solution will not be valid anyway.

Numerical calculations show that at the wellbore, $m_D^{(1)}$ approaches the asymptotic value given by Eq.(2.2.9) relatively quickly. The line source solution approaches a logaritmic dependence of time for large times. We have thus confirmed the well known fact that the wellbore pseudopressure follows the same straight line on a half-log plot as the solution of the linearized equation, only with a slight shift along the logt axis. This is also the conclusion of Kale and Mattar [10].

The fact that the first order correction term, $m_D^{(1)}$ quickly reaches a constant value implies that only the variations in μc near the initial value will affect the solution of Eq.(2.2.1). If the variations in μc with pseudopressure may be assumed to be linear in this region, we get a very simple expression for the perturbation solution at the well for large times:

$$m_{wD}(t_{Di}) = m_{wD}^{(0)} + \epsilon m_{wD}^{(1)}$$

(2.2.10)

$$= \frac{1}{2} \{ \ln t_{Di} + \ln 4 - \gamma \} - \frac{a}{2} \ln 2$$

where γ is Euler's constant, and $a = \epsilon a_1$.

Van Everdingen [19] introduced in 1953 the concept of a constant skin factor to describe the additional pressure drop due to formation damage around the well. In Eq.(2.2.10), $\epsilon m_D^{(1)}$ may be considered as an additional skin factor and may also be written in terms of the derivative of μc with respect to pressure:

$$S = - \ [\frac{1}{\mu c} \ \frac{d(\mu c)}{dm_D}]_i \cdot \frac{1}{2} \ \ln \ 2$$

(2.2.11)

$$= \frac{q}{2\pi kh} \ \frac{2Tp_{sc}}{T_{sc}} [\frac{1}{\mu c} \ \frac{d(\mu c)}{dm}]_i \cdot \frac{1}{2} \ \ln \ 2$$

$$= \frac{q}{2\pi kh} \ \frac{\varrho_{sc}}{\varrho_i c_i} [\frac{d(\mu c)}{dp}]_i \cdot \frac{1}{2} \ \ln \ 2$$

Note that S for a given initial pressure is proportional to production rate.

For buildup it is not evident what value μc should be expanded about. At the instant of shut-in μc varies from the initial value (at infinity) to the shut-in value at the well, $(\mu c)_s$. As could be expected, expansion about the shut-in value gives the best result shortly after shut-in, and expansion about the initial value the best result at late times when the pressure approaches the initial value. Which value that gives the best result will also depend on the form of μc, and generally the best point to choose would probably be a point between $(\mu c)_i$ and $(\mu c)_s$. However, since it is difficult to find such an optimal point, and since we intend to use asymptotic solutions for small $\Delta t / t_p$, the shut-in value is chosen (see also Sec. 2.4).

Another possibility would be to approximate μc with a straight line between $(\mu c)_i$ and $(\mu c)_s$, and still use an expansion about the shut-in value.

Define dimensionless pseudopressure rise during buildup as [23]:

$$m_{Ds} = \frac{2\pi kh}{q} \ \frac{T_{sc}}{2Tp_{sc}} \{ \ m(r,t_p+\Delta t) - m(r_w,\Delta t=0) \ \}$$

(2.2.12)

$$= m_D(r_w,\Delta t=0) - m_D(r,t_p+\Delta t)$$

The procedure for solving the equations for buildup is the same as for drawdown, and the buildup solution is matched with the drawdown solution to each order in ε. However, the use of the Boltzmann transformation is no longer valid, and the equations become much more complicated. The detailed calculations are shown in Appendix 2.1. The zeroth order solution becomes the usual liquid solution, and the first order solution can be shown to be a linear combination of the functions $U_{k,1}$ and $V_{k,1}$ defined in Appendix 2.2. This full solution is very complicated. However, as shown in Appendix 2.1, the solution can be simplified if μc can be approximated with a straight line. If in addition Δt_{Ds} satisfies the condition:

$$(2.2.13) \qquad \frac{\Delta t_{Ds}}{t_{pDi}} \ll 1 \ll \Delta t_{Ds}$$

the wellbore solution will be given by the analytic expression:

$$
\begin{aligned}
m_{wDs}(t_{Ds}) &= m_{wDs}^{(0)} + \epsilon m_{wDs}^{(1)} \\
&= \frac{1}{2}\left\{(1 + \frac{b}{2})\ln \Delta t_{Ds} + (\ln 4 - \gamma) + b(2\ln 2 - \frac{\gamma}{2} - 1)\right\}
\end{aligned}
$$

$(2.2.14)$

where b is the derivative of μc/(μc)$_s$ with respect to m_D at shut-in. Note that the condition, Eq.(2.2.13), is similar to the condition for the MDH-solution [15,20] to be valid in the oil reservoir case. Since μc is decreasing with increasing pressure, b will be positive. Hence, the wellbore solution will follow a straight line on a half-log plot, but with a slightly larger slope than the liquid soution, and the superposition prinsiple is not strictly valid. However, the deviation will not be very large for gas flow, and as will be demonstrated in the following sections, Eq.(2.2.14) will over-estimate the change in slope for low shut-in pressures.

If s is the slope of the m_{ws}-curve on a MDH or Horner plot, Eq.(2.2.14) gives for the permeability-thickness product:

$$kh = \frac{p_{sc}qTB/\pi T_{sc}}{1 - \sqrt{1 - 4Bs/\ln 10}} \qquad \text{Absolute units}$$

(2.2.15)

$$= \frac{1422qTB}{1 - \sqrt{1 - 1.737Bs}} \qquad \text{Field units}$$

where

(2.2.16) $$B = - \frac{T_{sc}}{2Tp_{sc}} \frac{2\pi kh}{q} \cdot b = [\frac{1}{\mu c} \frac{d(\mu c)}{dm}]_s = [\frac{1}{\mu c} \frac{dp}{dm} \frac{d(\mu c)}{dp}]_s$$

2.3 COMPARISON WITH PSEUDOTIME SOLUTION

Application of the pseudotime transformation introduced by Agarwal in 1979 [4] is based on the assumption that the solution of the nonlinear equation, when plotted against pseudotime, is identical to the solution of the linear equation. To investigate the validity of this assumption, the perturbation solution obtained in the previous section was compared with a solution based on this pseudotime approximation.

Agarwal defined the pseudotime transformation by the equation:

$$(2.3.1) \qquad t_a = \int_{t_0}^{t} \frac{dt}{\mu c(p(r,t))}$$

Since μc is a function of both r and t through pressure, this is not a pure time transformation. The transformed equation will consequently get additional terms containing the derivative of t_a with respect to r, as noted by Lee and Holditch [6]. The usefulness of the pseudotime transformation will then depend on the relative magnitude of these terms. Finjord [7] found that these terms are not small for drawdown, hence the pseudotime transformation will not linearize the equation in that case.

In practice the wellbore values of μc is used when t_a is calculated. The correspondence between t_{aD} and t_D may then be obtained to first order in ε retaining only two terms in the Taylor expansions for μc. The result is for drawdown:

$$t_{aD} = \int_{0}^{t_{Di}} \frac{d\tau}{1 + \varepsilon a_1 m_{wD}(\tau)}$$

$$= \int_{0}^{t_{Di}} [1 - \varepsilon a_1 m_{wD}^{(0)}(\tau)] d\tau + O(\varepsilon^2)$$

(2.3.2)

$$= t_{Di} - \varepsilon a_1 \int_{0}^{t_{Di}} [\frac{1}{2} E_1(1/4\tau)] d\tau + O(\varepsilon^2)$$

$$= t_{Di} - \varepsilon \frac{a_1}{8} \{E_1(1/4t_{Di})(1+4t_{Di}) - E_0(1/4t_{Di})\} + O(\varepsilon^2)$$

If terms of order ε^2 are neglected, and Eq.(2.3.2) is expanded for large times, we get:

(2.3.3) $$t_{aD} = t_{Di}\{ 1 - \varepsilon a_1(\frac{1}{2} \ln t_{Di} + \ln 2 - \frac{\gamma+1}{2}) \}$$

Assume now that the pseudotime transformation linearizes the equation, i.e., the correct solution of the nonlinear equation is found by replacing t_D with t_{aD} in the liquid solution. This implies that the solution of the nonlinear equation is (to first order in ε) of the form:

$$m_{wD}(t) = \frac{1}{2} \{\ln t_{aD} + \ln 4 - \gamma\}$$

$$= \frac{1}{2} \{\ln t_{Di} + \ln[1 - \varepsilon a_1(\frac{1}{2} \ln t_{Di} + \ln 2 - \frac{\gamma+1}{2})]$$

$$+ \ln 4 - \gamma\} + O(\varepsilon^2)$$

(2.3.4)

$$= \frac{1}{2} \{\ln t_{Di} + \ln 4 - \gamma - \varepsilon a_1[\frac{1}{2} \ln t_{Di} + \ln 2 - \frac{\gamma+1}{2}]\} + O(\varepsilon^2)$$

$$= m_{wD}^{(0)}(t_{Di}) + \varepsilon m_{wD}^{(1)}(t_{Di})$$

where terms of $O(\varepsilon^2)$ are neglected. It follows that the application of pseudotime for drawdown implies a correction term which increases

with time for large times. This result is in sharp contrast to the constant asymptotic correction term predicted by the perturbation method, an effect which also is verified by all numerical calculations. The conclusion must then be that the pseudotime solution is not valid for drawdown, at least not for large times. This is also in accordance with Finjord's result [7].

For buildup the definition of dimensionless pseudotime must be:

$$\Delta t_{aD} = \frac{k\Delta t_a}{\varphi r_w^2} = \frac{k}{\varphi r_w^2} \int_0^{\Delta t} \frac{d\tau}{\mu(p_{ws}(\tau))c(p_{ws}(\tau))}$$

$$(2.3.5) \qquad\qquad = (\mu c)_i \int_0^{\Delta t_{Di}} \frac{d\tau}{\mu(p_{ws}(\tau))c(p_{ws}(\tau))}$$

$$= (\mu c)_s \int_0^{\Delta t_{Ds}} \frac{d\tau}{\mu(p_{ws}(\tau))c(p_{ws}(\tau))}$$

which, under the condition given by Eq.(2.2.13), gives relations very similar to Eqs.(2.3.3) and (2.3.4):

$$(2.3.6) \qquad \Delta t_{aD} = \Delta t_{Ds}\{ 1 + \varepsilon b_1(\frac{1}{2}\ln\Delta t_{Ds} + \ln 2 - \frac{\gamma+1}{2}) \}$$

$$m_{wDs}(\Delta t) = m_{wDs}^{(0)}(\Delta t_{Ds}) + \varepsilon\, m_{wDs}^{(1)}(\Delta t_{Ds})$$

$$(2.3.7) \qquad = \frac{1}{2}\{\ln\Delta t_{Ds} + \ln 4 - \gamma + \varepsilon b_1(\frac{1}{2}\ln\Delta t_{Ds} + \ln 2 - \frac{\gamma+1}{2})\}$$

$$= \frac{1}{2}\{(1 + \frac{b}{2})\ln\Delta t_{Ds} + \ln 4 - \gamma + b(\ln 2 - \frac{\gamma+1}{2})\}$$

$b = \varepsilon b_1$ where b_1 is defined in Eq.(A2.1.14). If Eq.(2.3.7) is compared with the perturbation solution, Eq.(2.2.14), it is seen that except for the small quantity $b/2(\ln 2 - 1/2)$ the two methods give identical results to first order for buildup. The time dependence of $\varepsilon m_{Ds}^{(1)}$, which gives rise to the change in slope, is exactly equal. From this we draw the conclusion that, at least for the cases where

the perturbation solution is valid, pseudotime effectively linearizes the pseudopressure equation for buildup.

The reason for the slight shift between the perturbation solution and the pseudotime solution is not quite clear, but may be due to the use of the line source solution as the zeroth order solution in the calculation of the correction term, $m_{Ds}^{(1)}$ in Eq.(2.2.14) (see also Sec.2.4).

The validity of the pseudotime solution is based on an assumption of small gradients [6,7]. This assumption is independent of the assumptions on the variations in μc, and it is reasonable to believe that this is a characteristic feature of the buildup prosess itself. The fact that pseudotime produces the correct correction term to the liquid solution for small variations in μc, may therefore be taken as an indication that pseudotime gives good solutions also for stronger nonlinearity where the perturbation solution breaks down. This is also verified by all our numerical calculations.

Pseudotime has mainly been used to study problems concerning storage/afterflow and fractured wells [4,6,8,9]. These phenomena are not considered in this report, but generally the pseudotime approximation will be less good the more flow there is in the reservoir after shut in.

As stated by Finjord [7], not only the equation, but also the inner boundary condition will be changed when pseudotime is applied. However, the extra terms in the boundary condition will also involve the factor $\partial t_a/\partial r$.   Hence, if these terms can be neglected in the differential equation, it is reasonable to believe that they are negligible also in the boundary condition.

If the solution in terms of pseudotime is to follow the liquid solution for buildup, it is equally important that the initial condition for the buildup equation, i.e., the solution profile at the instant of shut-in, is equal to the liquid solution profile. We have shown that the correction term for drawdown in the well quickly approaches a constant value. Since the solution is given in terms of

the Boltzmann-variable, $y = r_0^2/4t_{0i}$, this implies that the correction term as a function of radius at shut in will also be constant, except for large (on a logarithmic scale) distances from the well. The initial condition for the pseudopressure rise during buildup will therefore be almost identical to the initial condition for the liquid solution. The discrepancy for large distances will only affect the solution for large shut in times, and for gas flow this deviation will usually be negligible.

2.4 DISCUSSION. VALIDITY OF PERTURBATION SOLUTION

To investigate the validity of the perturbation solution, Eqs.(2.2.1) - (2.2.4) was solved numerically using a routine for solving parabolic equations in the NAG library [17]. Several different functional dependences of $(\mu c)/(\mu c)_i$ on m_0 was used. The numerical solutions were then compared with the simplified perturbation solution; i.e., the solution obtained with only two terms retained in the Taylor series for μc (second order derivative terms and higher neglected). For buildup, expansion about shut-in value was compared with expansion about initial value.

Even if the perturbation solution is based on the assumption that the nonlinear terms are much less than unity, it was found that this solution was quite good even with $a = \epsilon a_1$ and $b = \epsilon b_1$ as high as about 0.5, provided the higher order derivatives were of the same order or smaller.

Fig.2.1 shows the first order correction term for drawdown, $m_{wD}^{(1)}$, calculated from Eq.(2.2.8) with only one term retained in the series and $\epsilon a_1 = 0.1$. Also shown is the asymptotic correction term, and it is seen that $m_{wD}^{(1)}$ reaches this constant value relatively quick (at about the same time as the liquid solution approaches the logarithmic time dependence). It is also seen that the asymptotic solution based on the pseudotime approximation is incorrect. However, since this "pseudotime correction term" is an asymptotic solution for large times, the pseudotime approximation may for small times be valid also for drawdown.

The correction term for buildup, $m_{wDs}^{(1)}$, calculated from Eq.(A2.1.45), is shown in Fig.2.2 as a function of dimensionless shut-in time based on $(\mu c)_s$ for different production times. This solution are compared with $m_{wDs}^{(1)}$ from Eq.(2.2.14) and Eq.(2.3.7). In these calculations the drawdown correction term, i.e., the initial condition for $m_{Ds}^{(1)}$ is set equal to zero, an approximation that only affects

the solution for large times. By looking at Fig.2.2 a rough estimate of the time interval where Eq.(2.2.14) is valid may be found to be:

$$(2.4.1) \qquad \frac{\Delta t}{t_p} \underset{\sim}{<} \frac{(\mu c)_s}{100(\mu c)_i} \quad , \quad t_{Ds} \underset{\sim}{>} 10$$

Shown in Figs. 2.3 and 2.4 are the solutions for two different functional forms of $(\mu c)/(\mu c)_i$, $1 + 0.5m_0$ and $\exp\{0.5m_0\}$. The drawdown solutions are compared with the solution obtained by Kale and Mattar[10], and it is seen that Eq.(2.2.9), even with only one term retained in the Taylor series, corresponds better to the numerical solution than the solution of Kale and Mattar.

The plots also show the difference between the solutions based on a Taylor expansion of μc about initial and shut-in value. For the linear case (Fig.2.3) the straight line used is the same whether μc is expanded about initial or shut in value, but the validity of the solution based on an expansion about shut in value depends on the factor b, which in that case is smaller than a. For the exponential case (Fig.2.4), a = b = 0.5, and the two solutions are of about the same overall quality, but an expansion about initial value gives best result for large Δt, and an expansion about shut-in value best result for small Δt.

Note also that the solution plotted against pseudotime almost perfectly follows the liquid solution in both cases, the discrepancy for large times being due to the drawdown correction term as mentioned in the previous section. The constant deviation between the perturbation solution and the pseudotime solution in Fig.2.2 seems to be due to an inaccuracy in the perturbation solution. The reason for this is not evident, but as mentioned in the previous section, one explanation can be that the line source solution is used as the zeroth order solution in the equation for $m_{Ds}^{(1)}$.

Even if the simplified perturbation solution, Eq.(2.2.14), seems to be reasonably good for quite large values of a and b, restrictions are imposed on the solution when applied to real gas flow because of the extreme form of μc. As mentioned by Dake [18], for high pressures μ ∝ p and c ∝ 1/p approximately. That is, the variations in μc are small for high pressures, and the liquid solution will in most cases be sufficiently accurate. When the pressure drops below about 1000 psia, however, μc increases very rapidly (see Fig.2.5). The higher order derivatives will be large, and more terms will have to be retained in the Taylor series if the perturbation solution is to be used. It can be shown that the next term in the Taylor series for buildup will give a negative correction term. The correct straight line (on a half-log plot) will lie between the liquid solution and the one predicted by the simplified perturbation solution. Hence, Eq.(2.2.15) and linear theory will give upper and lower bounds on the absolute permeability, respectively.

Note that the degree of nonlinearity is given by $\mu c/(\mu c)_i$ as a function of dimensionless pseudopressure and will depend both on initial pressure and production rate as shown in Fig. 2.6

Results from the simulated examples 1, 2, and 3 are shown in Figs. 2.7, 2.8, and 2.9. It is seen that the drawdown correction term is negligible in all cases. Since B given in Eq.(2.2.16) is less than zero, it follows that for buildup, absolute permeability estimated from linear theory will be too small. In the examples, the error varies from about 3 % to about 7 %. The perturbation solution gives best result in example 1, but is worse than the liquid solution in the other two examples.

A Horner[16] analysis of examples 1, 2, and 3 gave the following results (exact k-value is 1.5 mD):

	Measured slope, s: $(psi^2/cp-log\sim)$	k from linear theory: (mD)	k from Eq.(2.2.15): (mD)
Example 1:	$7.50 \cdot 10^7$	1.46	1.51
Example 2:	$15.63 \cdot 10^7$	1.40	1.94
Example 3:	$2.06 \cdot 10^7$	1.46	1.62

In some cases a better estimate of permeability from Eq.(2.2.15) may be obtained by approximating μc by a straight line from $(\mu c)_i$ to $(\mu c)_s$, but the general conclusion is that for real gas flow the liquid solution usually is equally good or better than the perturbation solution. In those cases where the perturbation solution gives better results, the error in the liquid solution is so small that it may be neglected in practice.

However, in all cases pseudotime will give the best result when analysing a buildup test, and if k has been determined from a standard procedure, the factor b in Eq.(2.2.14) may be calculated to check if the nonlinearity is significant and pseudotime should be applied.

The calculated skin factor will also be affected by the variation in μc. The error will depend on the value of μc and the point on the buildup curve used in the calculations, but the error will rarely be larger than about 1.

2.5 PSEUDOSTEADY STATE.   EXACT MATERIAL BALANCE EQUATIONS

The exact material balance equations for one-phase flow may be found by integrating the flow equation, Eq.(1.2.18) over the reservoir and applying the theorem of Gauss:

$$(2.5.1) \qquad \int_V \nabla \cdot \left\{ \frac{k\varrho}{\mu} \nabla p \right\} dV = \int_V \frac{\partial}{\partial t} (\varphi \varrho) dV$$

$$(2.5.2) \qquad \int_S \frac{k\varrho}{\mu} \nabla p \cdot \underline{n} dS = \frac{d}{dt} \int_V \varphi \varrho \, dV$$

S is the reservoir boundary, V the reservoir volume, and $\underline{n}$ unit outer normal to S. If k is constant, and the reservoir has a constant thickness h, the surface integral on the left hand side may be written as:

$$(2.5.3) \qquad \int_S \frac{k\varrho}{\mu} \nabla p \cdot \underline{n} dS = -2\pi k h \left\{ \left[\frac{\varrho}{\mu} r \frac{\partial p}{\partial r} \right]_{r_w} - \left[\frac{\varrho}{\mu} r \frac{\partial p}{\partial r} \right]_{r_e} \right\}$$
$$= \{\varrho_w q_w + \varrho_e q_e\}$$

q_w is the flow rate <u>into</u> the reservoir through the well and q_e is the flow rate into the reservoir through the outer boundary. If the flow in the well is assumed to be incompressible (storage neglected) we get:

$$(2.5.4) \qquad \varrho_w q_w = -\varrho_{sc} q$$

where ϱ_{sc} is density at standard conditions, and q is production rate at standard conditions.

If φ is constant, the right hand side of Eq.(2.5.2) becomes the change in volume-averaged density times the porosity. The result is then the material balance equation:

$$(2.5.5) \qquad \frac{d\bar{\varrho}}{dt} = -\frac{\varrho_{sc}q}{\varphi V} + \frac{\varrho_e q_e}{\varphi V}$$

or if q is constant and $q_e = 0$:

$$(2.5.6) \qquad \varrho_i - \bar{\varrho}(t) = \frac{\varrho_{sc}qt}{\varphi V}$$

Introduce now the pseudopressure corresponding to average density $\tilde{m}(t) = m(p(\bar{\varrho}(t)))$. If we use the equation of state to express pseudopressure in terms of density rather than pressure:

$$(2.5.7) \qquad m(\varrho) = \frac{2Tp_{sc}}{T_{sc}} \int\limits_{\varrho(p_0)}^{\varrho(p)} \frac{d\varrho}{\mu c}$$

it follows directly from Eq.(2.5.6) that

$$(2.5.8) \qquad m_i - \tilde{m}(t) = \frac{2Tp_{sc}}{T_{sc}} \frac{qt}{\varphi V (\mu c)_i} - \int\limits_{\tilde{m}(t)}^{m_i} \frac{\mu c - (\mu c)_i}{(\mu c)_i} dm$$

Correspondingly for the volume averaged pseudopressure:

$$(2.5.9) \qquad m_i - \bar{m}(t) = \frac{2Tp_{sc}}{T_{sc}} \frac{qt}{\varphi V (\mu c)_i} - \frac{1}{V} \int\limits_{V} \{ \int\limits_{m(r,t)}^{m_i} \frac{\mu c - (\mu c)_i}{(\mu c)_i} dm \} \, dV$$

It is seen that if μc is constant these expressions reduce to the usual linear material balance equations with decline of average pseudopressure being constant. Similar expressions may also be obtained for the pressure. Eqs.(2.5.8) and (2.5.9) may also be expressed in dimensionless forms:

$$(2.5.10) \qquad \tilde{m}_D(t_{DAi}) = 2\pi t_{DAi} - \int_0^{\tilde{m}_D} \frac{\mu c - (\mu c)_i}{(\mu c)_i} dm_D$$

and

$$(2.5.11) \qquad \bar{m}_D(t_{DAi}) = 2\pi t_{DAi} - \frac{1}{V} \int_V \left\{ \int_0^{m_D} \frac{\mu c - (\mu c)_i}{(\mu c)_i} dm_D \right\} dV$$

Al-Hussainy et al.[2] state without proof that the volume-averaged pseudopressure, $\bar{m}$, for all practical purposes will be approximately equal to the pseudopressure corresponding to average pressure $m(\bar{p})$. Our numerical results indicate that this will be the case also with $\bar{m}$ and $m(\bar{\varrho})$, although it is not evident how to show this analytically. The advantage of $\tilde{m}$ compared to $\bar{m}$ or $m(\bar{p})$ is that $\tilde{m}$, as long as μc is known as a function of m, can be calculated from Eq.(2.5.8) for all t without knowing the solution $m(r,t)$ in the reservoir. Eq.(2.5.8) is easily solved numerically if a table of $\mu c(m)$ is given.

If μc is approximated by an average value $\mu c \approx (\mu c)_{avg}$, the relation used by Al-Hussainy et al., with $m(\bar{p})$ replaced by $\tilde{m}$, is obtained:

$$(2.5.12) \qquad m_i - \tilde{m}(t) = \frac{2Tp_{sc}}{T_{sc}} \frac{q\ t}{\varphi V(\mu c)_{avg}}$$

or

$$(2.5.13) \qquad \tilde{m}_D(t_{DAi}) = \frac{(\mu c)_i}{(\mu c)_{avg}} 2\pi t_{DAi}$$

The problem now is how to calculate $(\mu c)_{avg}$. One way is to use the average between the initial and wellbore value. Another possibility is to use $(\mu c)(\tilde{m})$. These two methods yield the following expressions for $\tilde{m}_D$, respectively:

$$(2.5.14) \qquad \tilde{m}_D(t_{DAi}) = \frac{2}{1 + \dfrac{(\mu c)_{wf}}{(\mu c)_i}} \, 2\pi t_{DAi}$$

and

$$(2.5.15) \qquad \tilde{m}_D(t_{DAi}) = \frac{(\mu c)_i}{(\mu c)(\tilde{m}_D)} \, 2\pi t_{DAi}$$

Note that $(\mu c)_{wf}$ and $(\mu c)(\tilde{m}_D)$ will not be constant except for steady state flow, so these equations are still not linear. Fig. 2.10 shows $\tilde{m}_D(t_{DAi})$ for the simulated example 6. $\tilde{m}_D$ are calculated from Eqs.(2.5.14) and (2.5.15), respectively and compared with the solution of the exact equation, Eq.(2.5.10). The difference is significant for long producing times, and for this example a difference in m_D equal to one corresponds to a pressure difference of about 250 psi.

A closed reservoir with a slightly compressible fluid (liquid oil) that is produced at constant rate will eventually reach pseudosteady state or PSS. This state is characterized by a constant pressure decline at every point in the reservoir and will never be reached for gas flow. As shown by Al-Hussainy et al. [2] the solution of Eq.(2.2.1) for large times will deviate significantly from the solution of the linear equation. However, a gas well will reach a state that resembles PSS in the way that the pseudopressure profile will be approximately independent of time. The reason for this can be seen from the discussion in Sec. 1.3, and the form of the μc-curve: The variations in μc mainly occurs for large m_D, but the region where m_D is large is the region close to the well where the right hand side of the flow equation, Eq.(2.2.1), may be neglected (called Region 3 in Part 1). In Region 4, where the expansion terms must be taken into account, μc is essentially constant. Thus, the total solution profile becomes approximately equal to the solution profile of the linearized equation which is constant in time. (For an infinite reservoir this corresponds to Region 1 where the solution is parallel to the liquid solution.)

That is:

$$(2.5.16) \qquad m_D(r_D, t_D) = f(t) + \frac{r^2}{2r_e^2} - \ln\frac{r}{r_e}$$

which implies $f(t) = \overline{m}_D(t) - 3/4$ if we integrate over the reservoir and neglect terms of $O((r_w/r_e)^2)$. The result is then the well-known inflow equation:

$$(2.5.17) \qquad \frac{T_{sc}}{2T\,p_{sc}} \frac{2\pi kh}{q} \{\overline{m}(t) - m(r,t)\} = m_D(r_D, t_D) - \overline{m}_D(t_D)$$

$$= \frac{r^2}{2r_e^2} - \ln\frac{r}{r_e} - \frac{3}{4}$$

Inserting Eq.(2.5.17) on the left hand side of the flow equation yields $\partial\varrho/\partial t$ equal to $d\overline{\varrho}/dt$, which is constant. This is the usual way of deriving Eq.(2.5.17); starting with the assumption that $\partial\varrho/\partial t \approx d\overline{\varrho}/dt$ at all points in the reservoir. It is, however, important to realize that this is not correct, even if the result is very good. In fact, there may be a large difference in $\partial\varrho/\partial t$ from point to point. For instance, at $t = t_p$ in example 6, $\partial\varrho/\partial t$ at $r = r_w$ is more than 10 times $d\overline{\varrho}/dt$. The good result is solely due to the region of large variations in $\partial\varrho/\partial t$ being included in Region 3.

The right hand side of Eq.(2.5.17) may also be written in terms of the liquid solution p_{DLIN}:

$$(2.5.18) \qquad m_D(r_D, t_{DAi}) - \overline{m}_D(t_{DAi}) = p_{DLIN}(r_D, t_{DAi}) - 2\pi\, t_{DAi}$$

where $\overline{m}_D(t_{DAi})$ may be obtained by approximating $\overline{m}_D$ with $\widetilde{m}_D$ given by Eq.(2.5.10). Note that the value of μc used in the definition of dimensionless time in Eq.(2.5.18) is arbitrary as long as the same value is used in all terms.

Eq.(2.5.18) has only been verified for a circular reservoir with the well in its center, and its validity also for a general geometry should be investigated.

$m_D(r_D, t_{DAi})$ calculated from Eqs. (2.5.10) and (2.5.18) is plotted in Fig.2.11 and compared with the simulated example 6. The analytical solution is in perfect agreement with the simulated solution for all r and t except for very low pressures. The pressure will then become approximately constant because μc approaches infinity, and Eq.(2.5.18) will predict a negative pseudopressure. However, in practice other constraints on the pressure will probably imply a decrease in production rate before the pressure has reached this limit.

When approximating $\bar{m}$ with $\tilde{m}$ it follows from Eqs.(2.5.10) and (2.5.18) that:

$$(2.5.19) \qquad m_D(r_D, t_{DAi}) = p_{DLIN}(r_D, t_{DAi}) - \int_0^{\tilde{m}_D} \frac{\mu c - (\mu c)_i}{(\mu c)_i} \, dm_D$$

or

$$\frac{T_{sc}}{2Tp_{sc}} \frac{2\pi kh}{q}(m_i - m_w(t) + I(t)) = p_{wDLIN}(t_{DAi})$$

$(2.5.20)$

$$= 2\pi t_{DAi} + \frac{1}{2} \ln \frac{4A}{e^\gamma C_A r_w^2}$$

where C_A is the Dietz shape factor [21], and

$$(2.5.21) \qquad I(t) = \int_{\tilde{m}(t)}^{m_i} \frac{\mu c - (\mu c)_i}{(\mu c)_i} \, dm$$

That is, a plot of $m_{wf} - I$ v.s. time will give a straight line with slope s, given by:

$$s = \frac{2Tp_{sc}}{T_{sc}} \frac{q}{\varphi(\mu c)_i Ah} \qquad \text{Absolute units}$$

(2.5.22)

$$= 2.356 \frac{qT}{\varphi(\mu c)_i Ah} \qquad \text{Field units}$$

Reservoir limit tests for an oil reservoir is described in Refs. [18,20]. Generally, the usefulness of conducting such tests may be questionable due to the ideal conditions that the theory relies on. However, in some cases it may be possible to estimate drainage area using Eq.(2.5.20) provided the equation is valid also for a general geometry. Since the drainage area has to be known to calculate the integral in Eq.(2.5.21), an iterative procedure has to be used. A possible algorithm for this is then:

1) Make an initial guess on the drainage area.

2) Calculate $\widetilde{m}(t)$ and $I(t)$ from Eq.(2.5.8). Note that this requires an estimate of initial pressure.

3) Plot m_w - $I(t)$ v.s. time on a linear scale.

4) If this gives a straight line, control the result by calculating A from the slope using Eq.(2.5.22). If not, start again from 1). Note that if the plot curves upward, the guess was too large, and if it curves downward, it was too small.

As for an oil reservoir, C_A can be found by extrapolating the straight line to t = 0:

$$\ln C_A = \ln \frac{4A}{e^{\gamma} r_w^2} - \frac{T_{sc}}{T p_{sc}} \frac{2\pi kh}{q} (m_i - m_0) \qquad \text{Absolute units}$$

(2.5.23)

$$= 2.3 \log \frac{A}{r_w^2} - \frac{kh}{711qT} (m_i - m_0) + 0.81 \qquad \text{Field units}$$

where m_0 is the extrapolated value of $m_w - I$.

Fig. 2.12 shows plots of $m_w(t) - I(t)$ together with $m_w(t)$ for the simulated examples 6 and 7. One correct and two incorrect values of A are used in the calculation of I. Unfortunately, the drainage area used in the calculation of I has to be quite different from the correct value before the deviation from a straight line is clearly seen. Data for several time units measured with t_{DAi} is needed, and for example 6 this corresponds to several years of production with constant rate.

Straight lines were drawn through all 3 curves of $m_{wf} - I$ for the two examples, and A and $\ln C_A$ calculated from Eqs.(2.5.22) and (2.5.23). These estimates were then compared with the area used as input to Eq.(2.5.8). Correct values are $A = 21.9 \cdot 10^6$ sq.ft for example 6, and $1.37 \cdot 10^6$ sq.ft. for example 7. $\ln C_A = 3.45$ in both cases. The results are:

	Example 6			Example 7		
Curve	1	2	3	1	2	3
Slope, s ($\cdot 10^3 \text{psi}^2/\text{cp-hr}$)	75.83	86.80	96.04	247.9	286.7	369.7
m_0 ($\cdot 10^7 \text{psi}^2/\text{cp}$)	122	130	136	12.82	13.64	15.00
Area calculated from Eq.(2.5.22) ($\cdot 10^6$ sq.ft.)	25.0	21.8	19.7	1.58	1.37	0.989
$\ln C_A$	1.85	3.54	4.81	0.54	3.53	8.39
Area used in the calculation of I ($\cdot 10^6$ sq.ft.)	26.4	21.9	19.6	1.77	1.37	0.950

2.6 BUILDUP FROM PSEUDOSTEADY STATE. ESTIMATION OF AVERAGE RESERVOIR PRESSURE

For buildup the pressure behaviour is determined by the solution profile at shut-in. In the previous section we showed that the pseudopressure profile is approximately equal to the profile of the liquid solution in pseudosteady state. That is, the initial condition for the buildup solution is equal to the linear case, and the discrepancy between the pseudopressure rise and the corresponding liquid solution is only due to the variations in μc during buildup. Consequently, we may find a perturbation solution as for the infinite reservoir case. The procedure will be identical, except that the initial condition for $m_{Ds}^{(1)}$ will be zero for all r. Thus both the perturbation solution and the pseudotime solution will be as in Sec. 2.2 - 2.4. The only difference being that m_{Ds} will approach the liquid solution when $\Delta t \rightarrow \infty$, and the difference between $m_{Ds}(\Delta t_{aD})$ and $p_{DLIN}(\Delta t)$ for large Δt will disappear.

Dimensionless pseudopressure rise for example 4, 5, and 6 simulating buildup from PSS are shown in Fig. 2.13.

A standard MDH analysis [15,20] of pseudopressure for these examples gave k equal to 1.42, 1.42, and 1.41 mD, and an analysis using Eq.(2.2.15), 1.52, 1.69, and 2.99 mD, respectively. The perturbation method gave the best result in example 4, but as the pressure decreases, this solution becomes worse than the liquid solution, which gave a result within 6 % in all cases. Note that the pseudotime transformation gives excellent results in all cases (example 6 is also analysed in more detail on p.62).

Several methods have been proposed to correct for the variations in μc when average pressure is estimated from a buildup test in a gas well. Kazemi[5] presented a plot (his Fig.1) showing a dimensionless pseudopressure function, m_{DMBH}, corresponding to the liquid Matthews-

Brons-Hazebroek function, p_{DMBH} [22]. On the plot, $m_{DMBH}(t_{DAi})$, starts deviating from p_{DMBH} approximately at $t = t_{pss}$. Based on this, Kazemi presented an iterative algorithm to estimate average pressure by using t_{pss} instead of production time in the Horner plot. Ziauddin [11] and Toh et al. [12] used the perturbation solution of Kale and Mattar [10] to correct m_{DMBH} for variations in μc. This is done by first obtaining corrected dimensionless pseudopressure solutions for finite reservoirs.

In Sec 2.2, we showed that the pseudopressure profile very closely follows the solution profile of the liquid solution in the infinite-acting period. In Sec 2.5, it was demonstrated that this is the case also in pseudosteady state. A circular reservoir with the well in its center has a very short transition period between infinite-acting and PSS, and it is reasonable to assume that Eq.(2.5.18) is valid for all times (in the infinite-acting period $\bar{m}_D \approx 2\pi t_{DAi} \approx 0$). If this is the case also for a general geometry, Eq.(2.5.18) has the important implication that the error in estimated average pressure is only due to the inaccurate buildup solution and is independent of the foregoing drawdown. This may be the reason that the numerical results in Refs. [11], and [12] seems to be correct despite several questionable assumptions.

Note also that the validity of Eq.(2.5.18) for all times is equivalent to the validity of the drainage-radius concept introduced by Aronofsky and Jenkins [1] with pressure replaced by pseudopressure.

Eq.(2.5.18) may be written:

$$\frac{T_{sc}}{2Tp_{sc}}\frac{2\pi kh}{q}\{\bar{m} - m_{wfs}\} = p_{wDLIN}(t_{DAi}) - 2\pi t_{DAi}$$

(2.6.1)

$$= \frac{1}{2}\{\ln t_{DAi} + \ln \frac{A}{r_w^2} + \ln 4 - \gamma - p_{DMBH}(t_{DAi})\}$$

Replace now Δt by Δt_a in the liquid solution for buildup, and utilize the normal Horner approximation:

$$\frac{T_{sc}}{2Tp_{sc}} \frac{2\pi kh}{q}(m_{ws} - m_{wfs}) = \frac{1}{2} \{\ln \frac{\Delta t_{aD}}{t_{Di} + \Delta t_{aD}} + \ln t_{Di} + \ln 4 - \gamma\}$$

(2.6.2)

$$= \frac{1}{2} \{\ln \frac{\Delta t_a}{\frac{t_p}{(\mu c)_i} + \Delta t_a} + \ln t_{Di} + \ln 4 - \gamma\}$$

m^* is defined as the limit of m_{ws} when $\Delta t_{aD} \to \infty$ in Eq.(2.6.2), i.e.:

$$\frac{T_{sc}}{2Tp_{sc}} \frac{2\pi kh}{q}(m^* - m_{wfs}) = \frac{1}{2} \{\ln t_{Di} + \ln 4 - \gamma\}$$

(2.6.3)

$$= \frac{1}{2} \{\ln t_{DAi} + \ln \frac{A}{r_w^2} + \ln 4 - \gamma\}$$

It now follows directly from Eqs.(2.6.1) and (2.6.3) that:

(2.6.4) $$\frac{T_{sc}}{2Tp_{sc}} \frac{2\pi kh}{q}(m^* - \overline{m}) = \frac{1}{2} p_{DMBH}(t_{DAi})$$

Note that this result is independent of the difference between m_{wOfs} and $p_{wDLINfs}$. Hence, if the drainage area is known, and the correct MBH-function can be chosen, the standard MBH method [22] can be used to estimate average pseudopressure. No iteration procedure is then necessary. The only assmptions made in the derivation of Eq.(2.6.4) is that Eq.(2.5.18) is generally valid, and that the pseudotime transformation linearizes the flow equation for buildup. Similar arguments may also be used to show that other standard methods to estimate average pressure can be used as for an oil reservoir with Δt replaced by Δt_a.

All our simulation runs indicate that even when the perturbation solution is not valid, the buildup pseudopressure in a certain time interval will be of the form:

$$\frac{T_{sc}}{2Tp_{sc}} \frac{2\pi kh}{q} \{m_{ws} - m_{wfs}\} = \frac{1}{2}\{ (1+b')\ln\Delta t_{Ds} + \ln 4 - \gamma + a' \}$$

(2.6.5)
$$= \frac{1}{2}\{ (1+b')\ln\Delta t_{Di} + \ln 4 - \gamma + a' - (1+b')\ln\frac{(\mu c)_s}{(\mu c)_i} \}$$

$$= \frac{1}{2}\{(1+b')\ln\Delta t_{Di} + \ln 4 - \gamma + a'' \}$$

As seen from Fig. 2.13 , b' will, for low pressures be less than, and a' larger than the values predicted by the perturbation solution.

The same procedure that lead to Eq.(2.6.4) now gives:

$$\frac{T_{sc}}{2Tp_{sc}} \frac{2\pi kh}{q}(m'^* - \overline{m}) \equiv \frac{1}{2} m_{DMBH}$$

(2.6.6)
$$= \frac{1}{2} p_{DMBH}(t_{DAi}) - \frac{1}{2} a''$$

where m'^* is the extrapolated value from a plot of m_{ws} v.s. $\Delta t/(t_p +\Delta t)$, and m_{DMBH} is the quantity shown in Kazemi's Fig.1 [5]. a'' will generally be a complicated function of initial pressure, production rate and production time, but will be approximately equal to zero before the boundaries are felt.

Note that what one obtains from an analysis of a buildup test is the average pseudopressure. All our numerical results indicate that the three quantities $\overline{m}$, $m(\overline{p})$, and $\tilde{m} = m(\overline{\varrho})$ will be approximately equal. However, it still remains to show this analytically. An interesting implication if $\overline{m} \neq m(\overline{p}) \neq m(\overline{\varrho})$ when the well is shut-in, is that $\overline{m}$ and $\overline{p}$ will change during buildup. This is seen from the fact that $\overline{\varrho}$ has to be constant during buildup in a closed reservoir, and that in the limit when $\Delta t \rightarrow \infty$, $\overline{m} = m(\overline{p}) = m(\overline{\varrho})$ since all three values, m, p, and ϱ, then will be constant in space.

As mentioned in Sec 2.5 the validity of Eq.(2.5.18) has not been proven for a general geometry. It is also important to realize that the method proposed here will not be valid for very low pressures where Eq.(2.5.18) predicts a negative wellbore pressure. This may be checked by computing m_{wf} from Eqs.(2.5.18) and (2.5.8). However, it is doubtful that any of the other proposed methods will cover this case either.

Fig. 2.14 shows Horner plots for the simulated examples 6 and 7. Example 6 is similar to the example used in Refs. [5,11,12], but the production rate is constant in the whole production period. The results from an analysis of the Horner plots are (exact values are given in parenthesis):

1. Standard procedure:

	Example 6		Example 7	
s (psi^2/cp-log~)	$10.66 \cdot 10^7$		$0.618 \cdot 10^7$	
m_{ws} ($\Delta t=1hr$) (psi^2/cp)	$45.21 \cdot 10^7$		$4.217 \cdot 10^7$	
m^* (psi^2/cp)	$91.09 \cdot 10^7$		$5.921 \cdot 10^7$	

$==>$

	Example 6		Example 7	
k (mD)	1.41	(1.50)	97.6	(100)
S	-0.85	(0.00)	-0.42	(0.00)
t_{DAi}	3.36		4.67	
$\bar{m}$ (psi^2/cp)	$69.2 \cdot 10^7$	$(74.0 \cdot 10^7)$	$4.56 \cdot 10^7$	$(4.74 \cdot 10^7)$

2. Pseudotime procedure:

	Example 6	Example 7
s (psi^2/cp-log~)	$10.00 \cdot 10^7$	$0.5966 \cdot 10^7$
m^* (psi^2/cp)	$93.95 \cdot 10^7$	$6.0227 \cdot 10^7$

==>

k (mD)	1.51	(1.50)	101	(100)
S	-0.02	(0.00)	0.04	(0.00)
t_{DAi}	3.60		4.84	
$\overline{m}$ (psi^2/cp)	$73.11 \cdot 10^7$	$(74.0 \cdot 10^7)$	$4.70 \cdot 10^7$	$(4.74 \cdot 10^7)$

The error in average pseudopressure calculated with standard procedure corresponds to about 112 psi for example 6 and 12 psi for example 7. Relative errors about 5 % and 3 %, respectively. For example 6 this corresponds to the results of Kazemi [5].

The following expressions were used in the calculations (field units):

$$(2.6.7) \quad k = \frac{1637 \, qT}{hs}$$

$$(2.6.8) \quad S = 1.151\{\frac{m_{ws}(1hr) - m_{wfs}}{s} - \log\frac{k}{\varphi(\mu c)_i r_w^2} + 3.23\} \quad \text{Standard procedure}$$

$$(2.6.9) \quad S = 1.151\{\frac{m^* - m_{wfs}}{s} - \log\frac{kt_p}{\varphi(\mu c)_i r_w^2} + 3.23\} \quad \text{Pseudotime procedure}$$

$$(2.6.10) \quad t_{DAi} = \frac{0.0002637 \, kt}{\varphi(\mu c)_i A}$$

$$(2.6.11) \quad \bar{m} = m^* - \frac{s}{2.303} \, p_{DMBH}(t_{DAi})$$

Values for $p_{DMBH}(t_{DAi})$ were taken from Ref.[20].

2.7 CONCLUSIONS

1) Solutions of the nonlinear gas flow equation that takes into account the variations of the viscosity-compressibility product are obtained by using a regular perturbation method and expanding μc in Taylor series about the initial and shut in values, respectively.

2) If the variations in μc are relatively "nice", all but the two first terms in the Taylor series may be neglected. In this case, simple asymptotic expressions are found for the first order correction terms to the liquid solution.

3) For drawdown in an infinite reservoir, it is shown that the correction term relatively quickly approaches a constant value. That is, the solution of the nonlinear equation becomes parallel to the liquid solution.

4) If the production time is sufficiently large, the solution of the nonlinear equation for buildup is a linear function of $\log(\Delta t)$ in a certain time interval (conf. Eq.(2.4.1)). This interval is included in the time interval where the Miller-Dyes-Hutchinson (MDH) [15,20] solution is valid for an oil reservoir. However, this semi-log straight line will have a slightly larger slope than the liquid solution implying that the absolute permeability obtained from standard analysis of the buildup pseudopressure curve will be too low.

5) The solutions are applied to flow of real gases, and it is shown that for drawdown the nonlinear terms normally are negligible. Due to large variations in μc for low pressures, the simplified perturbation solution for buildup will estimate too large slope for the pseudopressure if the shut-in pressure is low. However, the slopes of the linear solution and the simplified perturbation

solution will give lower and upper bounds on the correct slope,
and hence the permeability-thickness product.

6) For buildup it is shown analytically that when the perturbation
   solution is valid, it is equivalent to a solution based on
   Agarwal's pseudotime transformation [4] in the semilog straight
   line interval, except for a very small constant term. This is not
   the case for drawdown where the pseudotime approximation implies a
   first order correction term that increases logarithmically with
   time for large times. The conclusion that pseudotime is not valid
   for drawdown, which is also the conclusion of Finjord [7], is
   reasonable since the validity of this approximation relies on an
   assumption of small gradients (Lee and Holditch [6]). Even if the
   pseudotime transformation effectively linearizes the flow equation
   for buildup, a necessary condition for the pseudopressure solution
   to follow the liquid solution is that the initial condition for
   buildup is the same as for liquid flow. We hawe shown that the
   pseudopressure profile is approximately equal to the profile of
   the liquid solution both for an infinite and finite reservoir.

7) The well-known result that the pseudopressure profile in
   pseudosteady state is independent of time and approximately equal
   to the liquid solution profile, may be explained by introducing
   different flow regions.

8) For a circular reservoir with the well in its center, the
   transition between the infinite acting period and PSS is very
   short. That is, the pseudopressure profile is approximately equal
   to the profile of the liquid solution for all t. This, in turn,
   implies that an application of Aronofsky and Jenkins' drainage
   radius correlation [1] to pseudopressure is valid.

9) Exact material balance equations can be used to find the time
   variation of the solution in pseudosteady state. The possibility
   of using this to estimate drainage area from a reservoir limit
   test is investigated, and it is demonstrated that a reasonable
   estimate of drainage area may be obtained under ideal conditions.
   However, this requires a test interval, with the production rate

being constant, of several time units measured with t_{DAi}

10) It is shown that the Matthews-Brons-Hazebroek (MBH) functions [22] may be used to estimate the average pseudopressure from a buildup test exactly as for an oil reservoir if pseudotime is used in the Horner plot. No iteration procedure is then needed.

NOMENCLATURE

A   Drainage area

$a = [\dfrac{1}{\mu c} \dfrac{d(\mu c)}{dm_D}]_i$ Dimensionless derivative of μc with respect to pseudopressure initially

a_n Similarity coefficients (see Eq.(2.2.6))

B   Defined by Eq.(2.2.16)

$b = [\dfrac{1}{\mu c} \dfrac{d(\mu c)}{dm_D}]_s$ Dimensionless derivative of μc with respect to pseudopressure for $r = r_w$ at shut in

b_n Similarity coefficients (see Eq.(A2.1.14))

C_A Dietz shape factor [21]

c   Compressibility

$E_0(z) = \dfrac{e^{-z}}{z}$ Exponential integral function of zeroth order [13]

$E_1(z) = \int\limits_{z}^{\infty} \dfrac{e^{-t}}{t} dt$ Exponential integral function of order 1 [13]

$E(r,t|r_0,t_0)$ Green's function for an infinite region defined by Eq.(A2.2.10)

$H(t-t_0) = \begin{cases} 0, & t < t_0 \\ 1, & t > t_0 \end{cases}$ Heaviside unit step function

I   Material balance correction term defined by Eq.(2.5.21)

I_n, K_n Modified Bessel functions [13]

k   Absolute permeability

h   Reservoir height

m   Pseudopressure (see Eq.(2))

$m_D = \dfrac{T_{sc}}{2T\, p_{sc}} \dfrac{2\pi kh}{q} (m_i - m(r,t))$ Dimensionless pseudo-pressure fall

$m_{Ds} = \dfrac{T_{sc}}{2T\, p_{sc}} \dfrac{2\pi kh}{q} (m(r,t_p+\Delta t) - m(r_w,t_p))$ Dimensionless pseudo-pressure rise during buildup

$\bar{m}$ Volume averaged pseudopressure

$\tilde{m} = m(\bar{\varrho})$ Pseudopressure corresponding to average density

m^*, m'^* Extrapolated values on Horner plots (pp.60-61)

m_0 Extrapolated value on linear plot (p. 57)

$m^{(n)}$ N'th term in asymptotic expansion (see Eq.(2.2.5))

$\underline{n}$ Unit outer normal to reservoir boundary

p Pressure

p_{DLIN} Dimensionless solution of the linear heat equation (liquid solution)

$\bar{p}$ Volume averaged pressure

q Surface production rate

r Radius

r_w Radius of well

r_e Outer radius of reservoir

$r_D = r/r_w$ Dimensionless radius

S Skin factor (except in Eqs.(2.5.2) and (2.5.3))

s Slope

T Temperature

t Time

t_p Production time

$\Delta t = t - t_p$ Shut-in time

$t_{Di} = \dfrac{kt}{\varphi(\mu c)_i r_w^2}$ Dimensionless time based on initial value of μc

$\Delta t_{Ds} = \dfrac{k(t-t_p)}{\varphi(\mu c)_s r_w^2}$ Dimensionless shut-in time based on μc at shut-in

t_a Pseudotime, defined by Eq.(2.3.1)

$t_{aD} = \dfrac{kt_a}{\varphi r_w^2}$ Dimensionless pseudotime

Δt_a, Δt_{aD} Shut-in pseudotime, dimensionless shut-in pseudotime (see Eq.(2.3.5)

$$t_{DAi} = \frac{kt}{\varphi(\mu c)_i A}$$ Dimensionless time based on drainage area

$U_{k,1}$, $V_{k,1}$ Functions defined in Appendix 2.2

V Reservoir volume

$$y = \frac{r_D^2}{4t_{Di}}$$ Boltzmann variable

Z Gas law deviation factor

$\gamma = 0.5772...$ Euler's constant

ε Small parameter (see Eqs.(2.2.5) and (2.2.6))

φ Porosity

μ Viscosity

ϱ Density

$\bar{\varrho}$ Volume averaged density

$(\mu c)_i$ Initial value of μc

$(\mu c)_s$ Wellbore value of μc at the instant of shut-in

Subscripts

D Dimensionless

e External

f Flowing

i Initial

s Shut-in

sc Standard conditions

w Well

wfs Wellbore value at shut-in

REFERENCES

[1]   Aronofsky,J.S. and Jenkins,R.: "A Simplified Analysis of Unsteady
       Radial Gas Flow," Trans., AIME (1954) 201, 149-154.

[2]   Al-Hussainy,R., Ramey,H.J.Jr., and Crawford,P.B.: "The Flow
       of Real Gases Through Porous Media,"
       Trans., AIME (1966) 237, 624-636.

[3]   Raghavan,R., Scorer,J.D.T., and Miller,F.G.: "An Investigation by
       Numerical Methods of the Effect of Pressure-Dependent Rock and
       Fluid Properties on Well Flow Tests," Soc.Pet.Eng.J. (June 1972)
       267-275, Trans., AIME 253.

[4]   Agarwal,R.G.: "'Real Gas Pseudo-Time' - A New Function for
       Pressure Buildup Analysis of MHF Gas Wells," Paper SPE 8279,
       Presented at the SPE-AIME 54th Annual Fall Meeting,
       Las Vegas, Nev., Sept. 23-26, 1979.

[5]   Kazemi,H.: "Determining Average Reservoir Pressure From Pressure
       Buildup Tests," Trans., AIME (1974) 255, 55-62.

[6]   Lee,W.J. and Holditch,S.A.: "Application of Pseudotime to Buildup
       Test Analysis of Low-Permeability Gas Wells With Long-Duration
       Wellbore Storage Distortion," J.Pet.Tech. (December 1982)
       2877-2887.

[7]   Finjord,J.: "A Study of Pseudotime," Paper SPE 12577 (1984),
       Submitted to Soc.Pet.Eng.J.

[8]   Bostic,J.N., Agarwal,R.G., and Carter,R.D.: "Combined Analysis
       of Postfracturing Performance and Pressure Buildup Data for
       Evaluating an MHF Gas Well," J.Pet.Tech. (October 1980),
       1711-1719.

[9]   Verbeek,C.M.J.: "Analysis of Production Tests of Hydraulically
       Fractured Wells in a Tight Solution Gas-Drive Reservoir,"
       Paper SPE 11084, Presented at the SPE-AIME 57th Annual Fall
       Meeting, New Orleans, LA, Sept. 26-29, 1982.

[10] Kale,D. and Mattar,L.: "Solution of a Non-Linear Gas Flow
     Equation by the Perturbation Technique," J.Can.Pet.Tech.
     (October-December 1980), 63-67.

[11] Ziauddin,Z.: "Determination of Average Pressure in Gas
     Reservoirs From Pressure Buildup Tests," Paper SPE 11222,
     Presented at the SPE-AIME 57th Annual Fall Meeting,
     New Orleans, LA, Sept. 26-29, 1982.

[12] Toh,C.H., Farshad,F.F., and LeBlanc, J.L.: "A New Iterative
     Technique With Updated Curves for Estimating Average Reservoir
     Pressure of Gas Wells From Buildup Tests," Paper SPE 13235,
     Presented at the SPE-AIME 59th Annual Fall Meeting, Houston, TX,
     Sept. 16-19, 1984.

[13] Abramowitz,M. and Stegun,I.A.: "Handbook of Mathematical
     Functions," Dover Publications, Inc., New York (1965).

[14] Theis,C.V. "The Relation Between the Lowering of the Piezometric
     Surface and the Rate and Duration of Discharge of a Well Using
     Ground Water Storage," Trans.Amer.Geophys.Union (1935) 16,
     519-524. Also:
     "Pressure Transient Testing Methods," SPE Reprint Series No. 14,
     Society of Petroleum Engineers of AIME, Dallas (1980), 27-32.

[15] Matthews,C.S. and Russell,D.G.: "Pressure Buildup and Flow Tests
     in Wells," Monograph Series, Society of Petroleum Engineers of
     AIME, Vol.1, Dallas (1967).

[16] Horner,D.R.: "Pressure Build-Up in Wells," Proc.,Third World Pet.
     Cong., The Hague (1951) Sec II, 503-523. Also:
     "Pressure Analysis Methods," SPE reprint series No. 9,
     Society of Petroleum Engineers of AIME, Dallas (1967), 25-43.

[17] NAG FORTRAN Library Mark 9, Numerical Algorithms Group, Oxford
     (1983).

[18] Dake,L.P.: "Fundamentals of Reservoir Engineering," Elsevier
     Scientific Publishing Company, Amsterdam, (1978).

[19] Van Everdingen, A.F.: "The Skin Effect and Its Influence on The
     Productive Capacity of a Well," Trans., AIME (1953), 198,
     171-176.

[20] Earlougher,R.C.,Jr.: "Advances in Well Test Analysis," Monograph
     Series, Society of Petroleum Engineers of AIME, Vol.5,
     Dallas (1977).

[21] Dietz,D.N.: "Determination of Average Reservoir Pressure From
     Build-Up Surveys,"
     J.Pet.Tech. (Aug., 1965), 955-959, Trans.AIME, 234.

[22] Matthews,C.S., Brons,F., and Hazebroek,P.: "A Method for
     Determination of Average Pressure in a Bounded Reservoir,"
     Trans., AIME (1954) 201, 182-191.

[23] Raghavan,R.: "The effect of Producing Time on Type Curve
     Analysis," J.Pet.Tech. (June, 1980), 1053-1064.

[24] Luke,Y.L.: "Integrals of Bessel Functions," McCraw-Hill, New York
     (1962).

[25] Lee,J.: "Well Testing," Textbook Series, Society of
     Petroleum Engineers of AIME, Vol. 1, Dallas (1982).

[26] Doetsch,G.: "Handbuch der Laplace-transformation," Vol.II,
     Verlag Birkhauser, Basel (1950).

APPENDIX 2.1   SOLUTION OF A NONLINEAR FLOW EQUATION BY REGULAR PERTURBATION

The non-linear problem given by Eqs.(2.2.1) - (2.2.4) is studied. In this appendix all variables will be dimensionless. The subscript D is therefore omitted for simplicity.

1. Drawdown, $t < t_p$:

Assume now that μc can be expanded in a Taylor series about the initial value as shown in Eq.(2.2.6), and that the well may be approximated by a line source. If we in addition assume that the solution is a function only of the Boltzmann variable $y = r^2/4t_i$, the problem is transformed to a boundary value problem for an ordinary differential equation:

$$(A2.1.1) \qquad \frac{1}{y}\frac{d}{dy}(y\frac{dm}{dy}) = -(1 + \epsilon \sum_{n=1}^{\infty} a_n m^n)\frac{dm}{dy}$$

$$(A2.1.2) \qquad \lim_{y \to \infty} m = 0$$

$$(A2.1.3) \qquad \lim_{y \to 0} y\frac{dm}{dy} = -\frac{1}{2}$$

Insert now in Eq.(A2.1.2) a trial solution written as an asymptotic series in ϵ, Eq.(2.2.5), and identify terms to each power in ϵ. The result is then to the two lowest orders:

$$(A2.1.4) \qquad [\frac{d^2}{dy^2} + (1+\frac{1}{y})\frac{d}{dy}]\, m^{(0)} = 0 \qquad\qquad O(\epsilon^0)$$

and

$$(A2.1.5) \qquad [\frac{d^2}{dy^2} + (1+\frac{1}{y})\frac{d}{dy}]\, m^{(1)} = -\sum_{n=1}^{\infty} a_n (m^{(0)})^n \frac{dm^{(0)}}{dy} \qquad O(\epsilon^1)$$

The standard procedure is to let the zeroth order solution satisfy the boundary conditions if possible, thus getting homogeneous boundary conditions to higher orders. Eq.(A2.1.5) together with the boundary conditions Eqs.(A2.1.3) and (A2.1.4) have the well-known solution:

$$(A2.1.6) \qquad m^{(0)}(y) = \frac{1}{2} E_1(y) = \frac{1}{2} \int_y^\infty \frac{e^{-t}}{t} \, dt$$

If the second derivative of $m^{(1)}$ is neglected in Eq.(A2.1.5), as done by Kale and Mattar [10], Eq.(A2.1.5) may now be directly integrated to give their Eq.(9):

$$(A2.1.7) \qquad \varepsilon m^{(1)} = \frac{1}{2} \int_\infty^y \frac{\alpha e^{-y}}{1 + y} \, dy$$

where $\alpha = (\mu c - (\mu c)_i)/(\mu c)_i$.

However, a general solution of Eq.(A2.1.5) may be found by the method of variation of parameters. The result is then:

$$(A2.1.8) \quad m^{(1)} = A E_1(y) + B + \sum_{n=1}^\infty \frac{a_n}{2^{n+1}} \{ E_1(y) \int_y^\infty E_1^n(y) dy - \int_y^\infty E_1^{n+1}(y) dy \}$$

A and B are arbitrary constants, which may be determined from the boundary conditions:

$$(A2.1.9) \qquad 0 = \lim_{y \to \infty} m^{(1)}(y) = B$$

$$(A2.1.10) \qquad 0 = \lim_{y \to 0} y \frac{dm^{(1)}}{dy} = -A - \sum_{n=1}^\infty \frac{a_n}{2^{n+1}} \int_0^\infty E_1^n(y) dy$$

Here it is assumed that the series converges uniformly and absolute and hence may be derived term by term. This gives for $m^{(1)}$:

$$(A2.1.11) \quad m^{(1)}(y) = - \sum_{n=1}^{\infty} \frac{a_n}{2^{n+1}} \{ E_1(y) \int_0^y E_1^{\,n}(y)dy + \int_y^{\infty} E_1^{\,n+1}(y)dy \}$$

By using properties of the exponential-integral functions, it can be shown that the integrals in Eq.(A2.1.11) exists for all $y \in [0,\infty)$.

Note that in the variables r and t_i the equation for $m^{(1)}$ becomes:

$$(A2.1.12) \quad [\frac{1}{r} \frac{\partial}{\partial r} (r \frac{\partial}{\partial r}) - \frac{\partial}{\partial t_i}] \, m^{(1)} = \sum_{n=1}^{\infty} a_n \, (m^{(0)})^n \frac{\partial m^{(0)}}{\partial t_i}$$

$$= \sum_{n=1}^{\infty} \frac{a_n}{2^{n-1}} \{\frac{e^{-y}}{4t_i} E_1^{\,n}(y)\}$$

It follows that in terms of the functions $U_{k,l}$ and $V_{k,l}$ defined in Appendix 2.2, the drawdown correction term may be written as:

$$(A2.1.13) \quad m^{(1)}(r,t_i) = \sum_{n=1}^{\infty} \frac{a_n}{2^{n-1}} V_{n,0}(r,t_i)$$

It may be shown that the limit of $\partial m^{(1)}/\partial r$ when $r \rightarrow 0$ is zero with $m^{(1)}$ given by Eq.(A2.1.11), even if $dm^{(1)}/dy$ approaches infinity when $y \rightarrow 0$. Thus, the boundary condition, Eq.(A2.2.5), used in the definition of $U_{k,l}$ and $V_{k,l}$ is consistent with the solution obtained with the Boltzmann transformation.

2. Buildup, $t > t_p$:

The procedure for buildup is quite similar irrespectively of the chosen value for expansion of µc is expanded about. The presentation will consequently be restricted to the case where the shut in value is chosen (µ and c is here dimensional variables):

$$\mu c = \mu c[m(1,t_p)] + \frac{d}{dm}(\mu c)[m(1,t_p)]\{m(r,t) - m(1,t_p)\} + \ldots$$

$$(A2.1.14) \quad = \mu c[m(1,t_p)]\{ 1 + \frac{\frac{d}{dm}(\mu c)[m(1,t_p)]}{\mu c[m(1,t_p)]}\{m(r,t) - m(1,t_p)\} + \ldots\}$$

$$= (\mu c)_s\{ 1 + \varepsilon \sum_{n=1}^{\infty} (-1)^n b_n\, m_s{}^n\}$$

where $m_s = (m(1,t_p) - m(r,t))$ is pseudopressure rise during buildup as defined by Raghavan[23], and b_n, $n=1,2,\ldots$, are similarity coefficients.

In terms of m_s, the flow equation, Eq.(2.2.1) then becomes:

$$\frac{1}{r}\frac{\partial}{\partial r}(r\frac{\partial m_s}{\partial r}) = \frac{(\mu c)_s}{(\mu c)_i}\{1 + \varepsilon \sum_{n=1}^{\infty} (-1)^n b_n m_s{}^n\}\frac{\partial m_s}{\partial(\Delta t_i)}$$

$$(A2.1.15)$$

$$= \{1 + \varepsilon \sum_{n=1}^{\infty} (-1)^n b_n m_s{}^n\}\frac{\partial m_s}{\partial(\Delta t_s)} \qquad r > 0,\ \Delta t > 0$$

with initial and boundary conditions:

$$(A2.1.16) \qquad m_s(r,\Delta t=0) = m(1,t_p) - m(r,t_p) \qquad\qquad r > 0$$

$$(A2.1.17) \qquad \lim_{r \to \infty} m_s = m(1,t_p) \qquad\qquad \Delta t > 0$$

$$(A2.1.18) \qquad \lim_{r \to 0} \frac{\partial m_s}{\partial r} = 0 \qquad\qquad \Delta t > 0$$

$\Delta t_s = [(\mu c)_i/(\mu c)_s]\Delta t_i$ is dimensionless shut-in time based on the value of μc at $r = r_w$ and $t = t_p$. The boundary condition, Eq.(A2.1.18) corresponds to the line source condition for drawdown, and expresses the assumption that the well may be neglected after shut-in.

As for drawdown a solution written as an asymptotic series in ε is tried:

$$m_s = m_s^{(0)} + \varepsilon\, m_s^{(1)} + \ldots$$

(A2.1.19)
$$= \{m^{(0)}(1,t_p) - m^{(0)}(r,t)\} + \varepsilon\{m^{(1)}(1,t_p) - m^{(1)}(r,t)\} + \ldots$$

This gives to $O(\varepsilon^0)$:

(A2.1.20)
$$\left[\frac{1}{r}\frac{\partial}{\partial r}\left(r\frac{\partial}{\partial r}\right) - \frac{\partial}{\partial(\Delta t)_s}\right] m_s^{(0)} = 0$$

$$m_s^{(0)}(r,\Delta t=0) = m^{(0)}(1,t_p) - m^{(0)}(r,t_p)$$

(A2.1.21)
$$= \frac{1}{2} E_1(1/4t_p) - \frac{1}{2} E_1(r^2/4t_p)$$

(A2.1.22)
$$\lim_{r \to \infty} m_s^{(0)} = m^{(0)}(1,t_p), \qquad \lim_{r \to 0} \frac{\partial m_s^{(0)}}{\partial r} = 0$$

with solution:

(A2.1.23)
$$m_s^{(0)} = \frac{1}{2} E_1(y_p) - \frac{1}{2} E_1(y) + \frac{1}{2} E_1(\Delta y)$$

$y_p = 1/4t_p = $ constant, $y = r^2/4(t_p+\Delta t_s)$, and $\Delta y = r^2/4\Delta t_s$.

To the next order:

$$\left[\frac{1}{r}\frac{\partial}{\partial r}\left(r\frac{\partial}{\partial r}\right) - \frac{\partial}{\partial(\Delta t)_s}\right] m_s^{(1)} = \sum_{n=1}^{\infty} (-1)^n b_n (m_s^{(0)})^n \frac{\partial m_s^{(0)}}{\partial(\Delta t)_s}$$

$$= \sum_{n=1}^{\infty} (-1)^n \frac{b_n}{2^n} \{E_1(y_p) - E_1(y) + E_1(\Delta y)\}^n \left\{\frac{e^{-\Delta y}}{2\Delta t_s} - \frac{e^{-y}}{2(t_p+\Delta t_s)}\right\}$$

(A2.1.24)
$$= \sum_{n=1}^{\infty} \sum_{i=0}^{n} \sum_{j=0}^{i} (-1)^{n+i-j}\frac{b_n}{2^{n-1}} \binom{n}{i}\binom{i}{j} E_1^{n-i}(y_p) E_1^{i-j}(y) E_1^{j}(\Delta y)$$

$$\cdot \left\{\frac{e^{-\Delta y}}{4\Delta t_s} - \frac{e^{-y}}{4(t_p+\Delta t_s)}\right\}$$

$$m_s^{(1)}(r, \Delta t = 0) = m^{(1)}(1, t_p) - m^{(1)}(r, t_p)$$

(A2.1.25)

$$= \sum_{n=1}^{\infty} \frac{a_n}{2^{n-1}} \{ V_{n,0}(1, t_p) - V_{n,0}(r, t_p) \}$$

(A2.1.26) $$\lim_{r \to \infty} m_s^{(1)} = m^{(1)}(1, t_p) \, , \qquad \lim_{r \to 0} \frac{\partial m^{(1)}}{\partial r} = 0$$

A particular solution of Eq.(A2.1.24) that satisfies homogeneous initial and boundary conditions is:

$$m_{sp}^{(1)} = \sum_{n=1}^{\infty} \sum_{i=0}^{n} \sum_{j=0}^{i} (-1)^{n+i-j} \frac{b_n}{2^{n-1}} \binom{n}{i}\binom{i}{j} E_1^{n-i}(y_p)$$

(A2.1.27)

$$\cdot \{ V_{j,i-j}(r, \Delta t_s) - U_{i-j,j}(r, \Delta t_s) \}$$

Define now $f(r, \Delta t_s)$ by:

(A2.1.28) $$f(r, \Delta t_s) \equiv \sum_{n=1}^{\infty} \frac{a_n}{2^{n-1}} \{ V_{n,0}(1, t_p) - V_{n,0}(r, t_p + \Delta t_s) \}$$

It is seen that $f(r, \Delta t_s)$ satisfies the initial and boundary conditions, Eqs.(A2.1.25) and (A2.1.26), and that:

(A2.1.29) $$[\frac{1}{r} \frac{\partial}{\partial r}(r \frac{\partial}{\partial r}) - \frac{\partial}{\partial(\Delta t_s)}][\ f(r, \Delta t_s) + \sum_{n=1}^{\infty} \frac{a_n}{2^{n-1}} U_{n,0}(r, \Delta t_s)\ ] = 0$$

Hence, a solution of the homogeneous equation corresponding to Eq.(A2.1.24) satisfying the initial and boundary conditions is:

(A2.1.30) $$m_{sh}^{(1)} = \sum_{n=1}^{\infty} \frac{a_n}{2^{n-1}} \{ V_{n,0}(1, t_p) - V_{n,0}(r, t_p + \Delta t_s) + U_{n,0}(r, \Delta t_s) \}$$

The complete solution of Eqs.(A2.1.24) - (A2.1.26) then becomes:

$$m_s^{(1)} = m_{sh}^{(1)} + m_{sp}^{(1)}$$

$$\text{(A2.1.31)} \quad = \sum_{n=1}^{\infty} \frac{1}{2^{n-1}} \{ a_n \{ V_{n,0}(1,t_p) - V_{n,0}(r,t_p+\Delta t_s) + U_{n,0}(r,\Delta t_s) \}$$

$$+ b_n \sum_{i=0}^{n} \sum_{j=0}^{i} (-1)^{n+i-j} \binom{n}{i}\binom{i}{j} E_1^{n-i}(y_p)$$

$$\cdot \{ V_{j,i-j}(r,\Delta t_s) - U_{i-j,j}(r,\Delta t_s) \} \}$$

One disadvantage with Eq.(A2.1.31) is that the production time is given implicitly through the functions $U_{k,l}$ and $V_{k,l}$. However, if the shut-in time is much shorter than the production time, the solution may be simplified considerably. For simplicity, the calculations will be performed with only one term retained in the Taylor series. Eq.(A2.1.24) then becomes:

$$\text{(A2.1.32)} \quad [\frac{1}{r}\frac{\partial}{\partial r}(r\frac{\partial}{\partial r}) - \frac{\partial}{\partial (\Delta t)_s}] \, m_s^{(1)} = -b_1 \, m_s^{(0)} \frac{\partial m_s^{(0)}}{\partial (\Delta t)_s}$$

$$= -b_1 \{ \frac{e^{-\Delta y}}{4\Delta t_s} - \frac{e^{-y}}{4(t_p+\Delta t_s)} \}\{ E_1(y_p) - E_1(y) + E_1(\Delta y) \}$$

$$\equiv g$$

Assume now that $\Delta t_s \ll t_p$. For small values of Δt_s the disturbance caused by the closing of the well will not have reached far out in the reservoir. We may therefore also assume $\max\{1/4t_p, \, r^2/4t_p\} \ll 1$, and the right hand side of Eq.(A2.1.32) may be approximated by:

$$\text{(A2.1.33)} \quad g = - b_1 \frac{e^{-\Delta y}}{4\Delta t} \{ E_1(\Delta y) + 2 \ln r \}$$

When $\Delta t_s \ll t_p$ and $r^2 \ll 4t_p$ we may assume that only the constant part

of the drawdown correction term, $m^{(1)}$, will affect the solution. Hence, we assume both the initial and boundary conditions for Eq.(A2.1.32) to be homogeneous.

The first term in Eq.(A2.1.33) is identical to the first term in the drawdown equation, Eq.(A2.1.12) with t_i and a_1 replaced by Δt_s and $-b_1$, respectively. The solution of Eq.(A2.1.33) will then be equal to $b_1\{u - V_1\}$ where $u(r,\Delta t_s)$ is the solution of:

$$(A2.1.34) \qquad [-\frac{1}{r}\frac{\partial}{\partial r}(r\frac{\partial}{\partial r}) - \frac{\partial}{\partial (\Delta t)_s}]\, u = -\ln r \,\frac{\exp\{-r^2/4\Delta t_s\}}{2\Delta t_s}$$

with homogenous initial and boundary conditions.

For the Laplace-transformed of u, $U(r;s)$, we get the following problem:

$$(A2.1.35) \qquad \frac{1}{r}\frac{d}{dr}(r\frac{dU}{dr}) - sU = -\ln r \cdot K_0(r\sqrt{s}) \quad , \quad r > 0$$

$$(A2.1.36) \qquad \lim_{r \to \infty} U(r;s) = 0$$

$$(A2.1.37) \qquad \lim_{r \to 0} U'(r;s) = 0$$

The general solution of Eq.(A2.1.35) is:

$$U(r;s) = AI_0(z) + BK_0(z) + \frac{1}{s} I_0(z) \int_z^\infty \tau\ln\frac{\tau}{\sqrt{s}} K_0^2(\tau)\, d\tau$$

$$- \frac{1}{s} K_0(z) \int_z^\infty \tau\ln\frac{\tau}{\sqrt{s}} K_0(\tau)I_0(\tau)\, d\tau$$

$$(A2.1.38) \qquad = AI_0 + BK_0$$

$$- \frac{z^2}{2s} I_0\{ (\ln\frac{z}{\sqrt{s}} - 1)(K_0^2 - K_1^2) - \frac{1}{z} K_0K_1 \}$$

$$+ \frac{z^2}{2s} K_0\{ (\ln\frac{z}{\sqrt{s}} - 1)(K_0I_0 + K_1I_1) + \frac{1}{2z}(K_0I_1 - K_1I_0) \}$$

Here K_0, I_0, K_1, and I_1 are modified Bessels functions of zeroth and first order, all with argument $z = r\sqrt{s}$. The integrals are found from formulas given by Luke [24] together with partial integration. The boundary conditions imply $A = 0$ and $B = 1/4s$, and the complete solution of Eqs.(A2.1.35) - (A2.1.37) becomes:

$$U(r;s) = \frac{1}{4s} K_0(r\sqrt{s})$$

(A2.1.39)
$$+ \frac{r^2}{2}\{\ln r - 1\}\{K_0(r\sqrt{s})K_1(r\sqrt{s})I_1(r\sqrt{s}) + K_1^2(r\sqrt{s})I_0(r\sqrt{s})\}$$

$$+ \frac{r}{4\sqrt{s}}\{K_0^2(r\sqrt{s})I_1(r\sqrt{s}) + K_0(r\sqrt{s})K_1(r\sqrt{s})I_0(r\sqrt{s})\}$$

From asymptotic properties of the Laplace transformation found in Ref.[26], e.g., it follows that a solution valid for large t and small r may be obtained by expanding Eq.(A2.1.39) for small $r\sqrt{s}$ before it is inverted. The result is:

(A2.1.40) $\qquad U(r;s) \approx -\frac{1}{2s}\{\frac{1}{2}\ln s - \ln 2 + \gamma + 1\} \qquad\qquad r\sqrt{s} \ll 1$

i.e.

(A2.1.41) $\qquad u(r,t) \approx \frac{1}{2}\{\frac{1}{2}\ln\Delta t_s + \ln 2 - \frac{\gamma}{2} - 1\} \qquad\qquad \Delta t \gg 1$

From Eqs.(A2.1.11) and (A2.1.13) it follows that:

(A2.1.42) $\qquad V_{1,0}(r,\Delta t_s) \approx -\frac{1}{4}\int_0^\infty E_1^2(\Delta y)d\Delta y = -\frac{1}{2}\ln 2 \qquad \frac{\Delta t_s}{r^2} \gg 1$

A solution for $m_s^{(1)}$ valid for small r and $1 \ll \Delta t_s \ll t_{pi}$ is then:

(A2.1.43) $m_s^{(1)} = \frac{b_1}{2}\{ \frac{1}{2} \ln\Delta t_s + 2 \ln 2 - \frac{\gamma}{2} - 1 \}$

Note that the solution is independent of r.

The convergence of the various integrals and limits used in developing
this solution may be shown using properties of Bessel functions found
in Ref. [13], e.g., and will not be presented here.

For reference, the solution corresponding to Eq.(A2.1.31) when μc is
expanded about the initial value, and only one term retained in the
Taylor series, is:

$$m_s^{(1)} = a_1 \{ V_{1,0}(1,t_p) - V_{1,0}(r,t_p+\Delta t_i) - V_{1,0}(r,\Delta t_i)$$

(A2.1.44)

$$+ U_{0,1}(r,\Delta t_i) + V_{0,1}(r,\Delta t_i) \}$$

When only one term is retained on the right hand side, Eq.(A2.1.31)
becomes:

$$m_s^{(1)} = a_1 \{ V_{1,0}(1,t_p) - V_{1,0}(r,t_p+\Delta t_s) + U_{1,0}(r,\Delta t_s) \}$$

$$+ b_1 \{ E_1(y_p)\{ U_{0,0}(r,\Delta t_s) - V_{0,0}(r,\Delta t_s) \}$$

(A2.1.45)

$$+ \{ V_{0,1}(r,\Delta t_s) - U_{1,0}(r,\Delta t_s) \}$$

$$- \{ V_{1,0}(r,\Delta t_s) - U_{0,1}(r,\Delta t_s) \} \}$$

APPENDIX 2.2 DEFINITIONS OF THE FUNCTIONS $U_{k,1}$ AND $V_{k,1}$

The functions $U_{k,1}$ and $V_{k,1}$ are defined as the solutions of the following linear, nonhomogeneous problems:

(A2.2.1)
$$\left[\frac{1}{r}\frac{\partial}{\partial r}\left(r\frac{\partial}{\partial r}\right) - \frac{\partial}{\partial t}\right] U_{k,1}(r,t) = u_{k,1}(r,t)$$

(A2.2.2)
$$\left[\frac{1}{r}\frac{\partial}{\partial r}\left(r\frac{\partial}{\partial r}\right) - \frac{\partial}{\partial t}\right] V_{k,1}(r,t) = v_{k,1}(r,t)$$

$$r > 0 \qquad t > 0$$

(A2.2.3)
$$U_{k,1}(r,0) = V_{k,1}(r,0) = 0$$

(A2.2.4)
$$\lim_{r \to \infty} U_{k,1} = \lim_{r \to \infty} V_{k,1} = 0$$

(A2.2.5)
$$\lim_{r \to 0} \frac{\partial U_{k,1}}{\partial r} = \lim_{r \to 0} \frac{\partial V_{k,1}}{\partial r} = 0$$

$$k,1 = 0,1,2,\ldots$$

where

(A2.2.6)
$$u_{k,1}(r,t) \equiv \frac{\exp[-r^2/4(t_p+t)]}{4(t_p + t)} E_1^{\ k}\left\{\frac{r^2}{4(t_p+t)}\right\} E_1^{\ 1}\left\{\frac{r^2}{4t}\right\}$$

(A2.2.7)
$$v_{k,1}(r,t) \equiv \frac{\exp[-r^2/4t]}{4t} E_1^{\ k}\left\{\frac{r^2}{4t}\right\} E_1^{\ 1}\left\{\frac{r^2}{4(t_p+t)}\right\}$$

Solutions of these equations may be found on integral form in terms of the Green's function for an infinite region corresponding to the radial heat equation:

(A2.2.8)
$$U_{k,1} = \int_0^t \int_0^\infty 2\pi r_0\, u_{k,1}(r_0,t_0) E(r,t|r_0,t_0)\, dr_0\, dt_0$$

(A2.2.9)

$$V_{k,1} = \int_0^t \int_0^\infty 2\pi r_0 \, v_{k,1}(r_0,t_0) E(r,t|r_0,t_0) dr_0 dt_0$$

where $E(r,t|r_0,t_0)$ is defined by:

(A2.2.10)

$$E(r,t|r_0,t_0) \equiv \frac{H(t-t_0) I_0(rr_0/2(t-t_0))}{4\pi(t-t_0)} \exp\left\{-\frac{r^2+r_0^2}{4(t-t_0)}\right\}$$

$H(t-t_0)$ is the Unit step function.

Numerically, $U_{k,1}$ and $V_{k,1}$ may be found either by solving the defining equations directly, or from the integral forms given in Eqs.(A2.2.8) – (A2.2.10).

APPENDIX 2.3 SIMULATION EXAMPLES

To examplify the theory presented in this part, 7 examples of drawdown and buildup in a gas reservoir were simulated. Except for example 7, reservoir and fluid properties are as in the example of Ziauddin [11] and are presented in Table 2.1 and 2.3. μc as a function of pressure is shown in Fig. 2.5, and to illustrate the effect of different initial pressures and rates, $\mu c/(\mu c)_i$ v.s. m_0 is plotted in Fig. 2.6 for the simulated examples 1, 2, and 3.

The simulations were performed by transforming the problem to the dimensionless form given by Eqs. (2.2.1) - (2.2.4). This system was then solved numerically using a routine for solving parabolic partial differential equations from the NAG-library [17].

Data for the different simulations is:

Example 1:

p_i = 4000 psi, q = 4000 Mscf/d, t_p = 27 hrs, p_{wfs} = 2698 psi
$(\mu c)_i$ = $4.47 \cdot 10^{-6}$ cp/psi, $(\mu c)_s$ = $6.72 \cdot 10^{-6}$ cp/psi,
m_i = $95.3 \cdot 10^7$ psi^2/cp, m_{wfs} = $50.6 \cdot 10^7$ psi^2/cp,
t_{pDi} = $6.3 \cdot 10^5$.

Example 2:

p_i = 4000 psi, q = 8000 Mscf/d, t_p = 27 hrs, p_{wfs} = 876 psi
$(\mu c)_i$ = $4.47 \cdot 10^{-6}$ cp/psi, $(\mu c)_s$ = $1.72 \cdot 10^{-5}$ cp/psi,
m_i = $95.3 \cdot 10^7$ psi^2/cp, m_{wfs} = $6.13 \cdot 10^7$ psi^2/cp,
t_{pDi} = $6.3 \cdot 10^5$.

Example 3:

p_i = 1500 psi, q = 1100 Mscf/d, t_p = 240 hrs, p_{wfs} = 691 psi
$(\mu c)_i$ = $1.11 \cdot 10^{-5}$ cp/psi, $(\mu c)_s$ = $2.11 \cdot 10^{-5}$ cp/psi,
m_i = $17.3 \cdot 10^7$ psi^2/cp, m_{wfs} = $3.89 \cdot 10^7$ psi^2/cp,
t_{pDi} = $2.3 \cdot 10^6$.

Example 4:

p_i = 7000 psi, q = 5500 Mscf/d, t_p = 16000 hrs, p_{wfs} = 1943 psi
$(\mu c)_i$ = $2.29 \cdot 10^{-6}$ cp/psi, $(\mu c)_s$ = $8.94 \cdot 10^{-6}$ cp/psi,
m_i = $203 \cdot 10^7$ psi^2/cp, m_{wfs} = $28.2 \cdot 10^7$ psi^2/cp,
t_{pDAi} = 2.52.

Example 5:

p_i = 7000 psi, q = 5500 Mscf/d, t_p = 20200 hrs, p_{wfs} = 1127 psi
$(\mu c)_i$ = $2.29 \cdot 10^{-6}$ cp/psi, $(\mu c)_s$ = $1.39 \cdot 10^{-5}$ cp/psi,
m_i = $203 \cdot 10^7$ psi^2/cp, m_{wfs} = $10.0 \cdot 10^7$ psi^2/cp,
t_{pDAi} = 3.19.

Example 6:

p_i = 7000 psi, q = 5500 Mscf/d, t_p = 22700 hrs, p_{wfs} = 202 psi
$(\mu c)_i$ = $2.29 \cdot 10^{-6}$ cp/psi, $(\mu c)_s$ = $5.87 \cdot 10^{-5}$ cp/psi,
m_i = $203 \cdot 10^7$ psi^2/cp, m_{wfs} = $0.502 \cdot 10^7$ psi^2/cp,
t_{pDAi} = 3.58.

For example 1, 2, and 3, the reservoir may be considered infinite in
extent. Example 4, 5, and 6 demonstrate depletion of a closed
reservoir and buildup from PSS.

In addition an example with a small reservoir and high permeability
was run to simulate a reservoir limit test. The reservoir parameters
are shown in table 2.2. The fluid properties were as in the other
examples and are shown in Table 2.3.

Example 7:

p_i = 1500 psi, q = 5500 Mscf/d, t_p = 550 hrs, p_{wfs} = 352 psi
$(\mu c)_i$ = $1.11 \cdot 10^{-5}$ cp/psi, $(\mu c)_s$ = $4.10 \cdot 10^{-5}$ cp/psi,
m_i = $17.3 \cdot 10^7$ psi^2/cp, m_{wfs} = $1.05 \cdot 10^7$ psi^2/cp,
t_{pDAi} = 4.82.

PART 2   91

Well radius	0.276 ft
Radius of reservoir	2640 ft
Reservoir height	40 ft
Absolute permeability	1.5 mD
Porosity	0.05
Temperature	670^0 R

<u>Table 2.1</u> Reservoir properties. Examples 1 - 6.

Well radius	0.276 ft
Radius of reservoir	660 ft
Reservoir height	10 ft
Absolute permeability	100 mD
Porosity	0.2
Temperature	670^0 R

<u>Table 2.2</u> Reservoir properties. Example 7.

p(psi)	m(psi^2/cp)	μ(cp)	c(1/psi)
200	.32233E7	.01265	.50944E-2
400	.12865E8	.01295	.25914E-2
600	.28808E8	.01333	.17539E-2
800	.50834E8	.01377	.13316E-2
1000	.78731E8	.01419	.10744E-2
1200	.11229E9	.01464	.89907E-3
1400	.15118E9	.01514	.76989E-3
1600	.19507E9	.01565	.66927E-3
1800	.24361E9	.01619	.58766E-3
2000	.29635E9	.01677	.51954E-3
2200	.35174E9	.01743	.46158E-3
2400	.41223E9	.01813	.41168E-3
2600	.47434E9	.01887	.36842E-3
2800	.53862E9	.01961	.33077E-3
3000	.60477E9	.02035	.29790E-3
3200	.67245E9	.02110	.26917E-3
3400	.74140E9	.02185	.24400E-3
3600	.81134E9	.02260	.22191E-3
3800	.88206E9	.02336	.20247E-3
4000	.95336E9	.02412	.18533E-3
4200	.10251E10	.02485	.17017E-3
4400	.10972E10	.02558	.15672E-3
4600	.11695E10	.02629	.14476E-3
4800	.12419E10	.02700	.13409E-3
5000	.13144E10	.02770	.12455E-3
5200	.13869E10	.02839	.11599E-3
5400	.14593E10	.02906	.10828E-3
5600	.15317E10	.02970	.10134E-3
5800	.16040E10	.03033	.95050E-4
6000	.16762E10	.03095	.89351E-4
6200	.17482E10	.03155	.84170E-4
6400	.18201E10	.03214	.79449E-4
6600	.18918E10	.03273	.75136E-4
6800	.19633E10	.03332	.71188E-4
7000	.20346E10	.03389	.67565E-4
7200	.21056E10	.03447	.64234E-4

Table 2.3   Gas properties corresponding to a natural gas with
            gravity γ = 0.7   (from Ziauddin [11]).
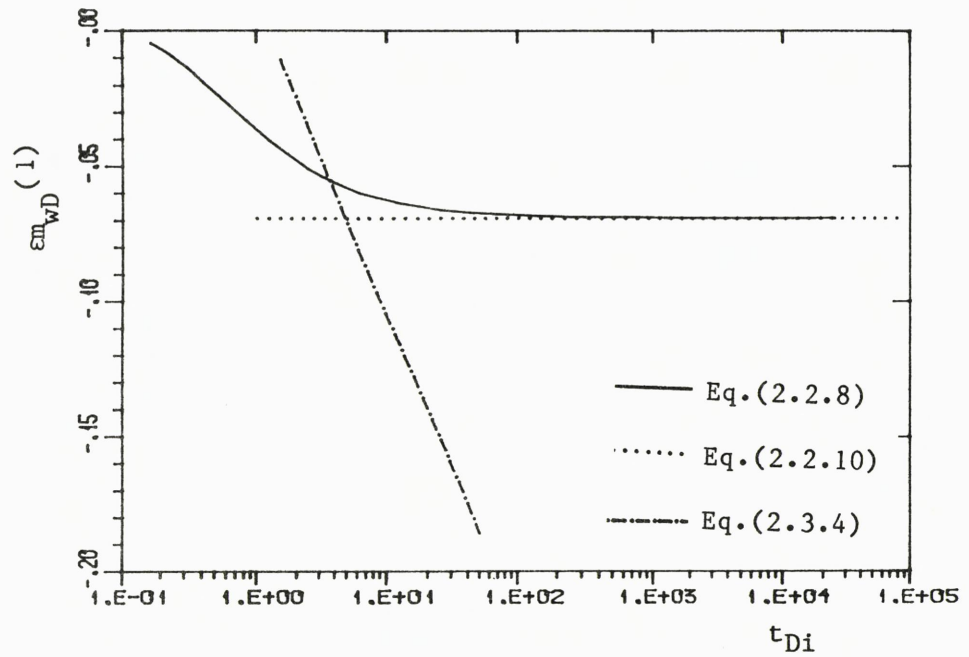
Fig. 2.1 Drawdown correction terms; $\varepsilon a_1 = 0.1$, $a_n = 0$, $n \geqslant 2$.
$r = r_w$.
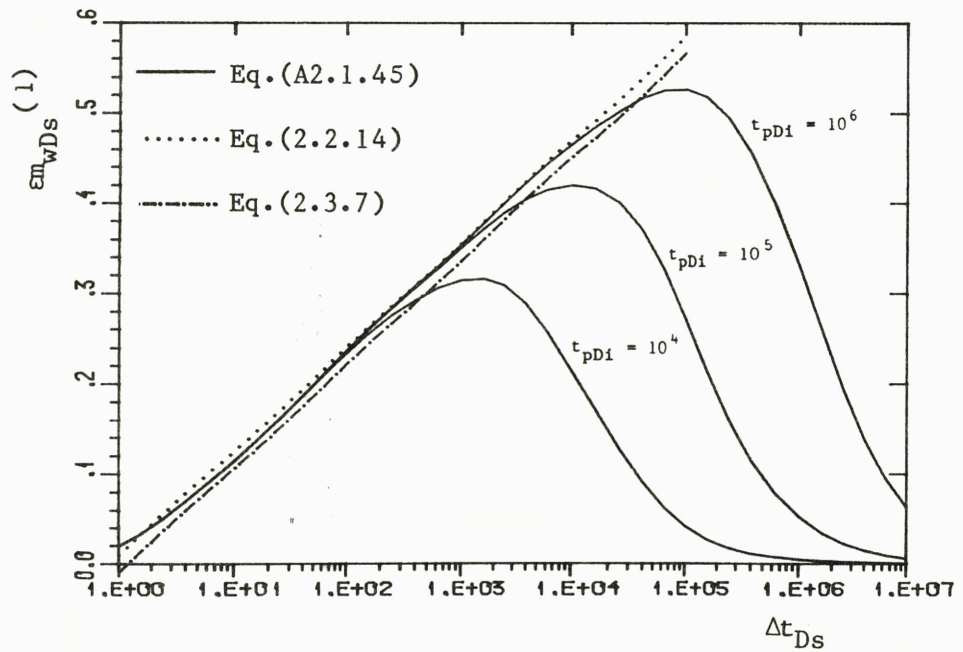
Fig. 2.2 Buildup correction terms: $a_n = 0$, $n = 1,2,\ldots$
$\varepsilon b_1 = 0.1$, $b_n = 0$, $n \geqslant 2$. $r = r_w$

DRAWDOWN CORRECTION TERMS
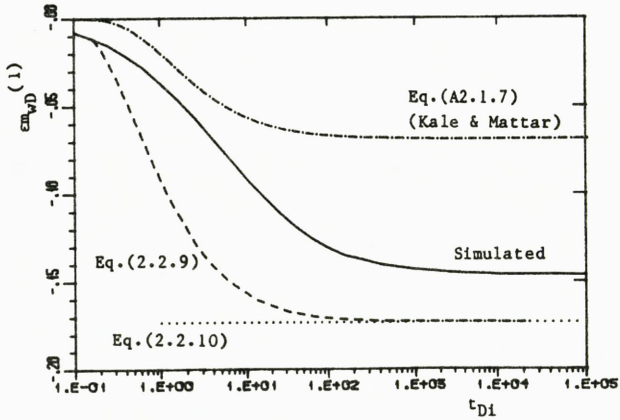
DRAWDOWN SOLUTIONS
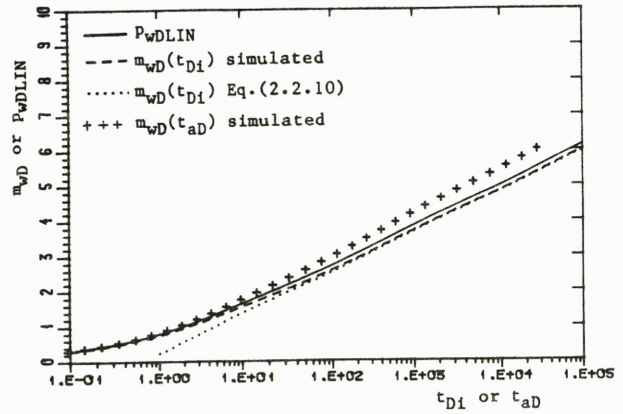
BUILDUP CORRECTION TERMS
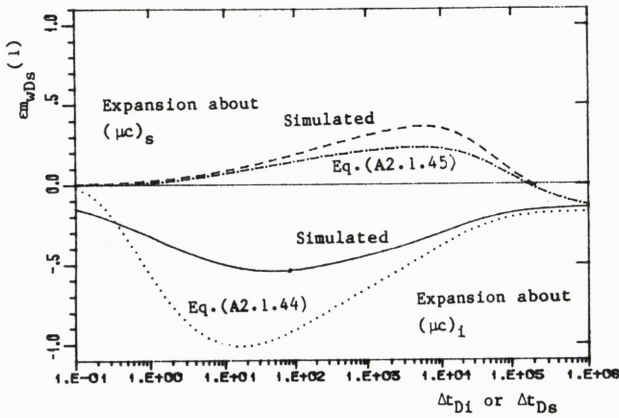
BUILDUP SOLUTIONS
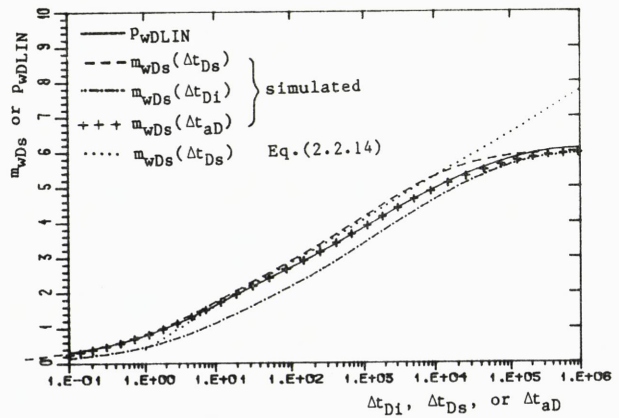
Fig. 2.3 Numerical and analytical solutions for $r = r_w$ of
Eqs.(2.2.1)-(2.2.4) with $\mu c / (\mu c)_i = 1 + 0.5 m_D$, $t_{pDi} = 10^5$.

DRAWDOWN CORRECTION TERMS

DRAWDOWN SOLUTIONS

BUILDUP CORRECTION TERMS

BUILDUP SOLUTIONS
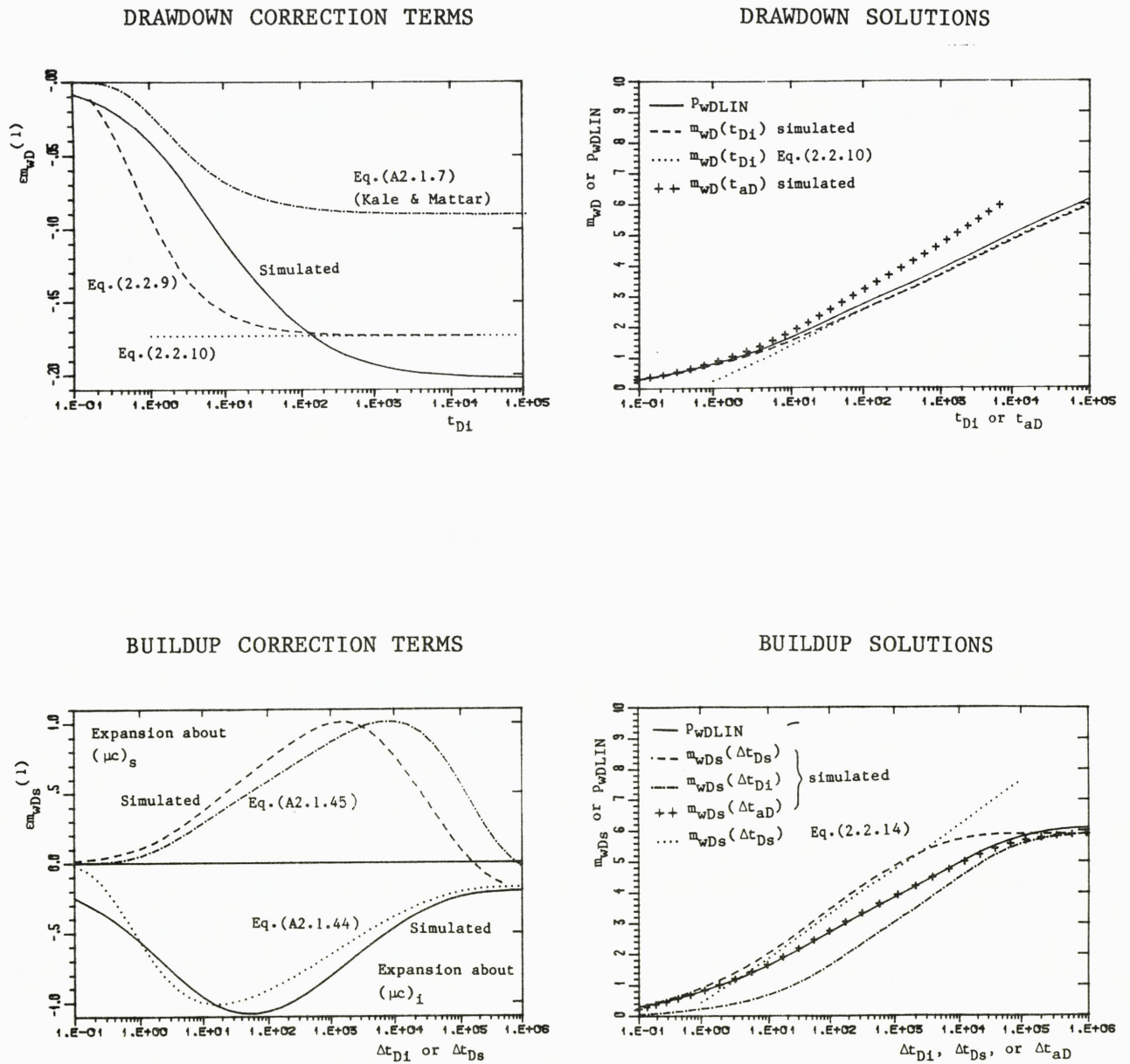
Fig. 2.4 Numerical and analytical solutions for $r = r_w$ of
Eqs.(2.2.1) - (2.2.4) with $\mu c/(\mu c)_i = \exp\{0.5 m_D\}$. In the
perturbation solutions only two terms are retained in the
Taylor expansion of $\mu c/(\mu c)_i$, i.e., $\varepsilon a_1 = \varepsilon b_1 = 0.5$,
$a_n = b_n = 0$ for $n \geqslant 2$. $t_{pDi} = 10^5$.
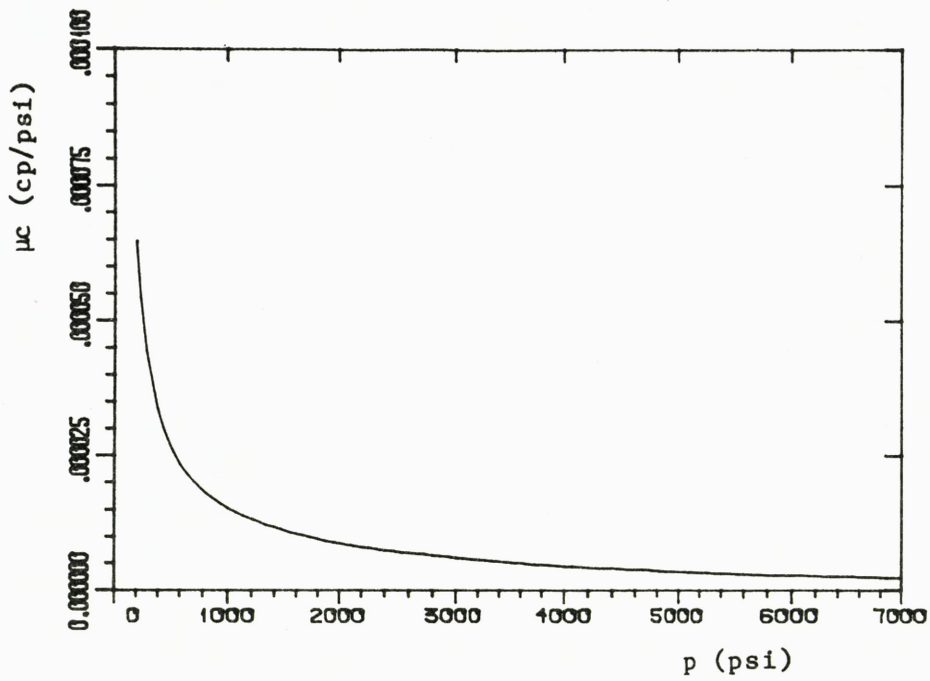
Fig. 2.5 μc vs. pressure.
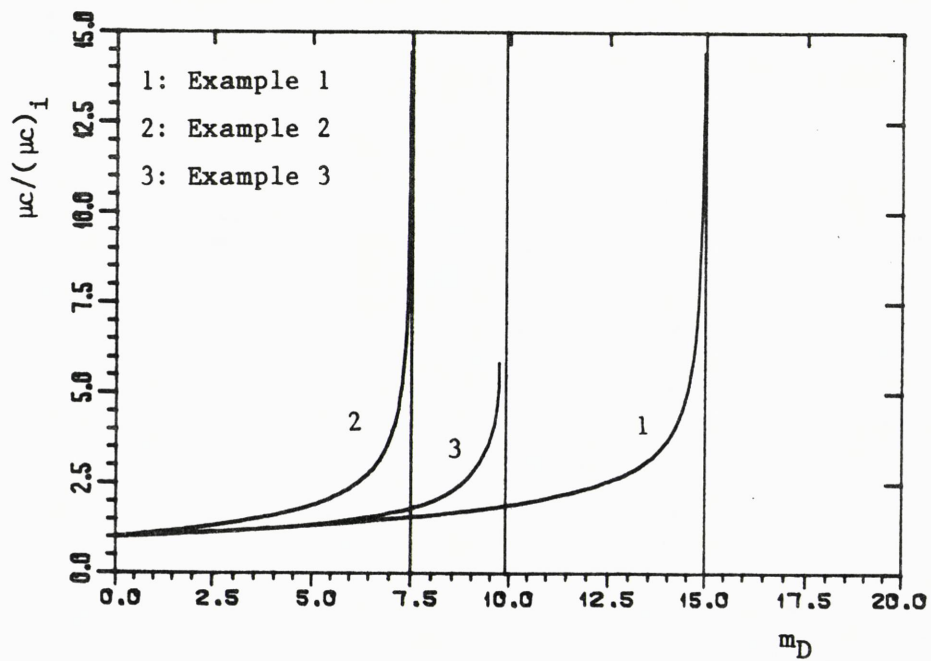
Fig. 2.6 $\mu c/(\mu c)_i$ vs. dimensionless pseudopressure fall, example 1, 2, and 3. The vertical lines corresponds to zero pressure for the respective examples.
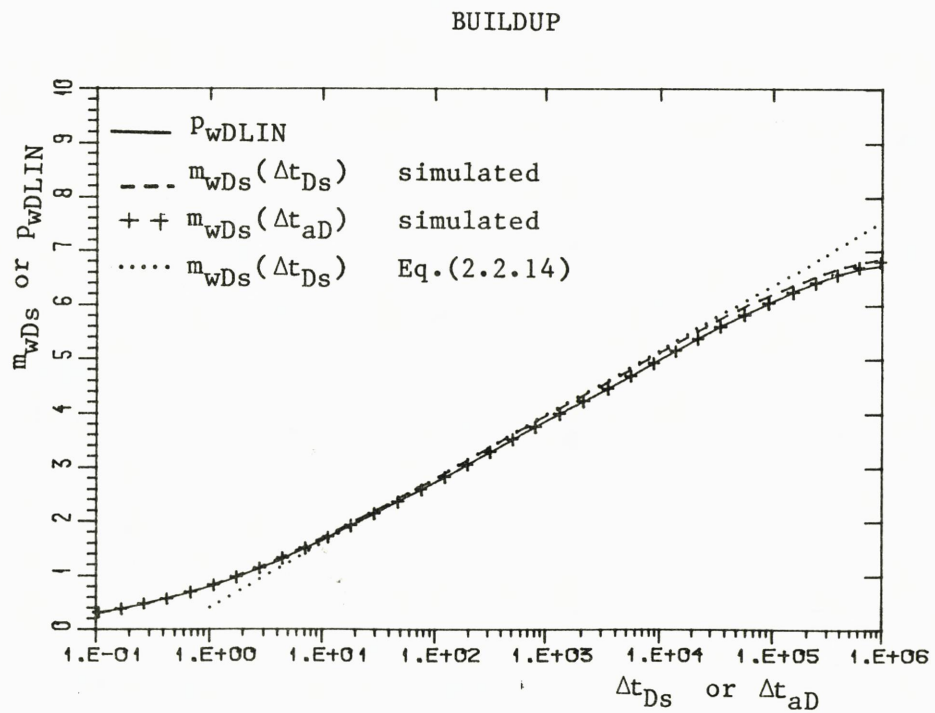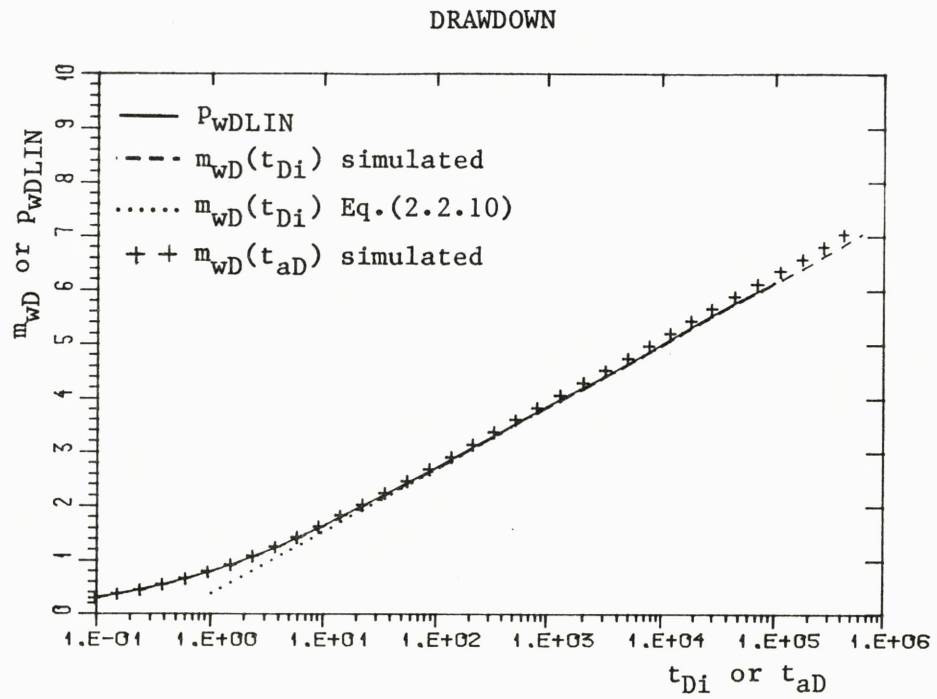
DRAWDOWN

BUILDUP

Fig. 2.7 Example 1.

Perturbation solution and pseudotime solution, compared
with simulated pseudopressure and liquid solution
respectively. $r = r_w$.
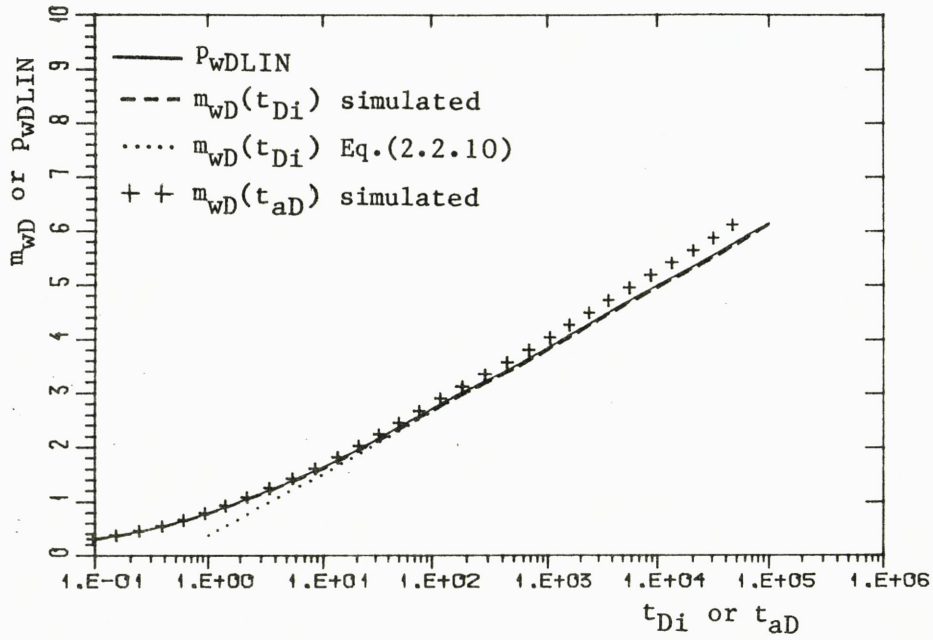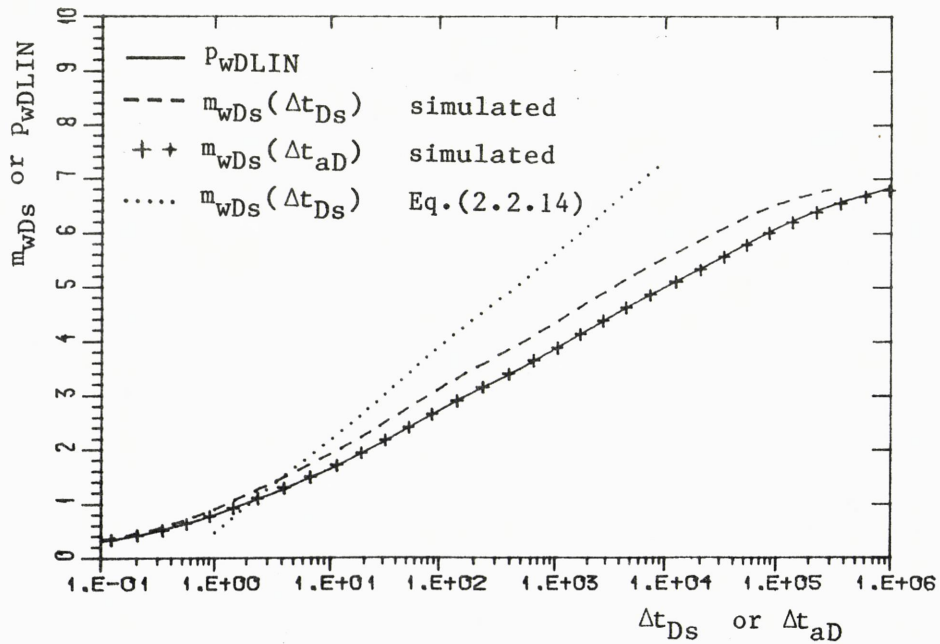
DRAWDOWN

BUILDUP

Fig. 2.8 Example 2.

Perturbation solution and pseudotime solution, compared
with simulated pseudopressure and liquid solution
respectively. $r = r_w$.

DRAWDOWN
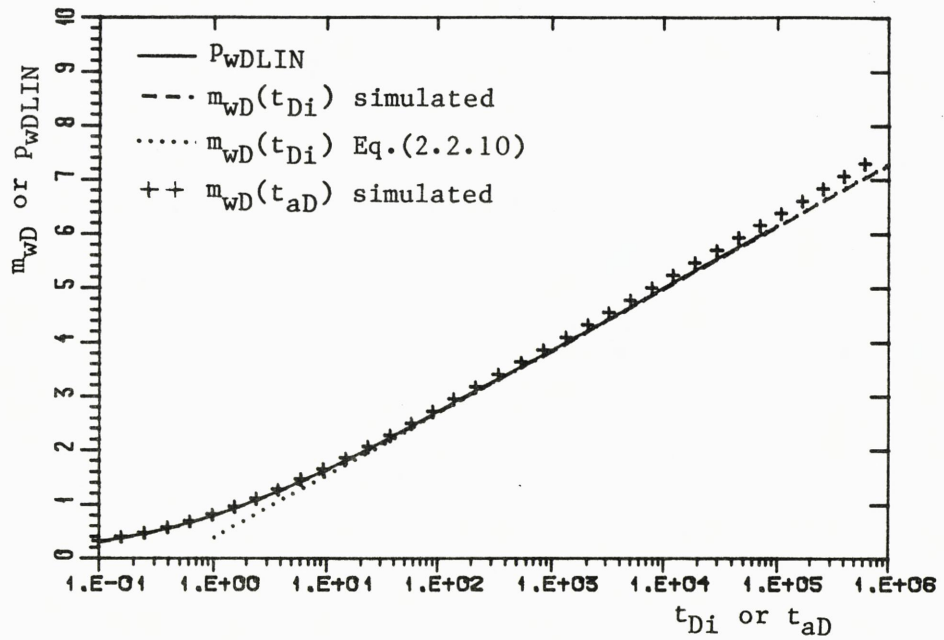
BUILDUP
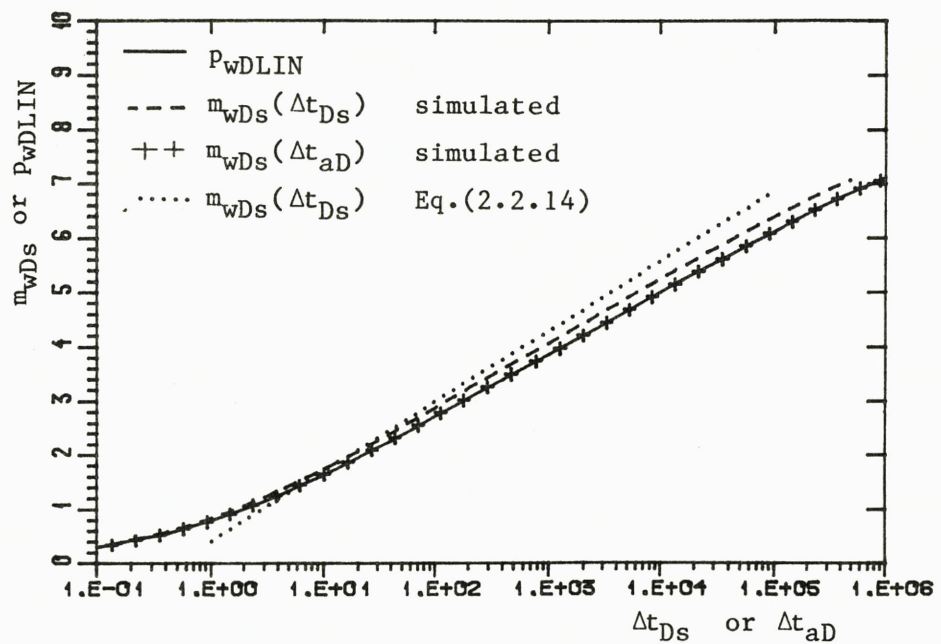
Fig. 2.9 Example 3.

Perturbation solution and pseudotime solution, compared
with simulated pseudopressure and liquid solution
respectively. $r = r_w$.
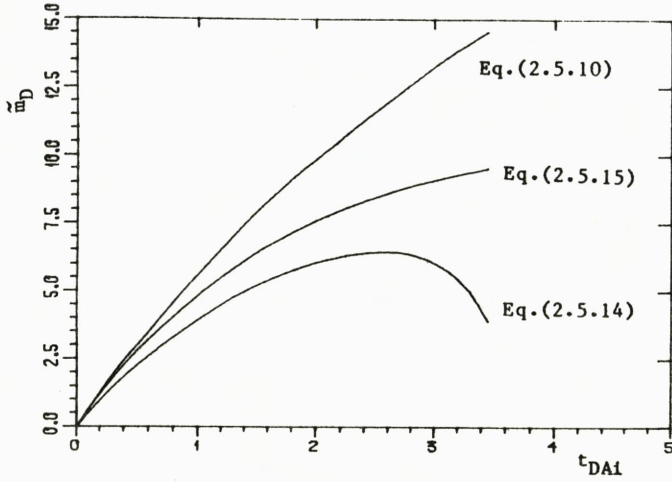
Fig. 2.10 Pseudopressure corresponding to average density for the simulated example 6.
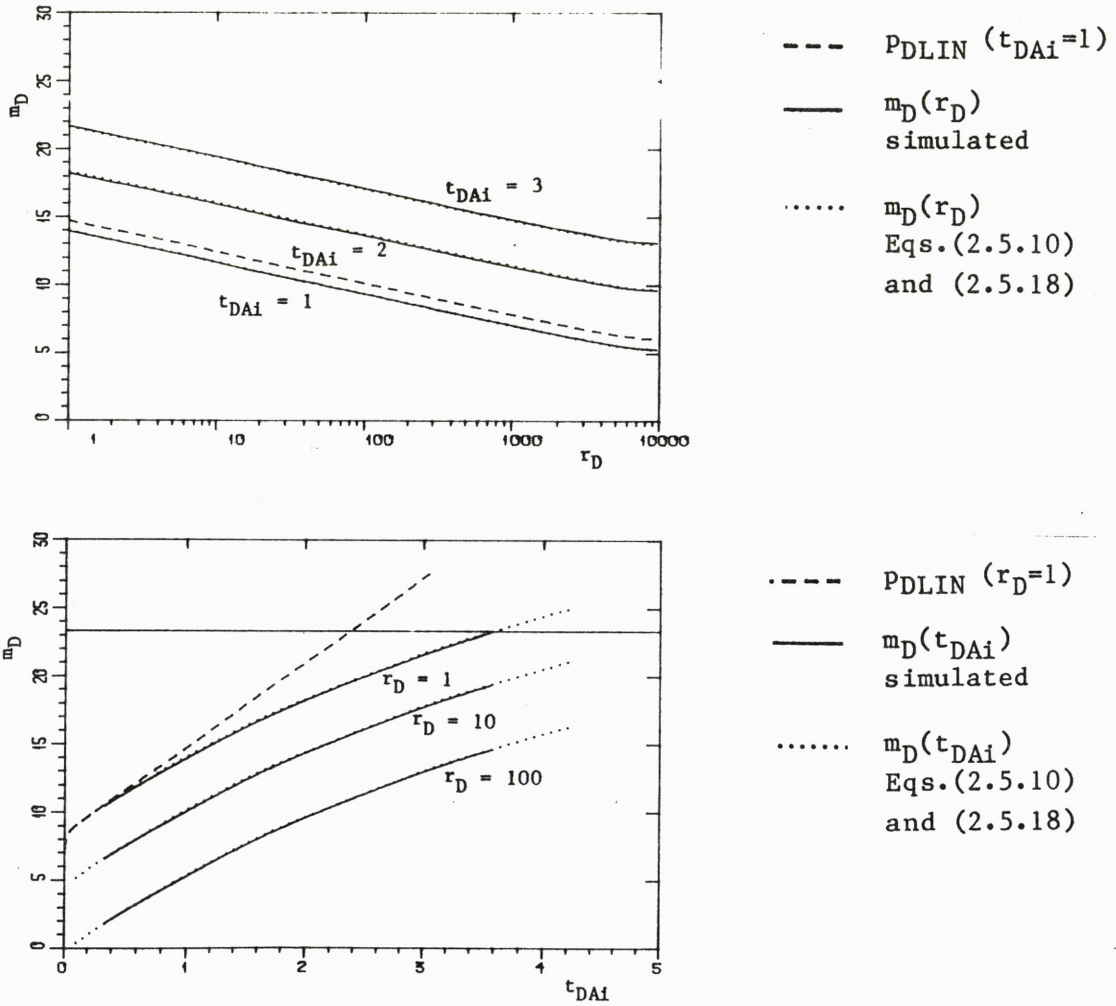
Fig. 2.11 Simulated pseudopressure compared with analytical solution and liquid solution for example 6. The horizontal line at $m_D = 23.3$ corresponds to zero pressure.

EXAMPLE 6
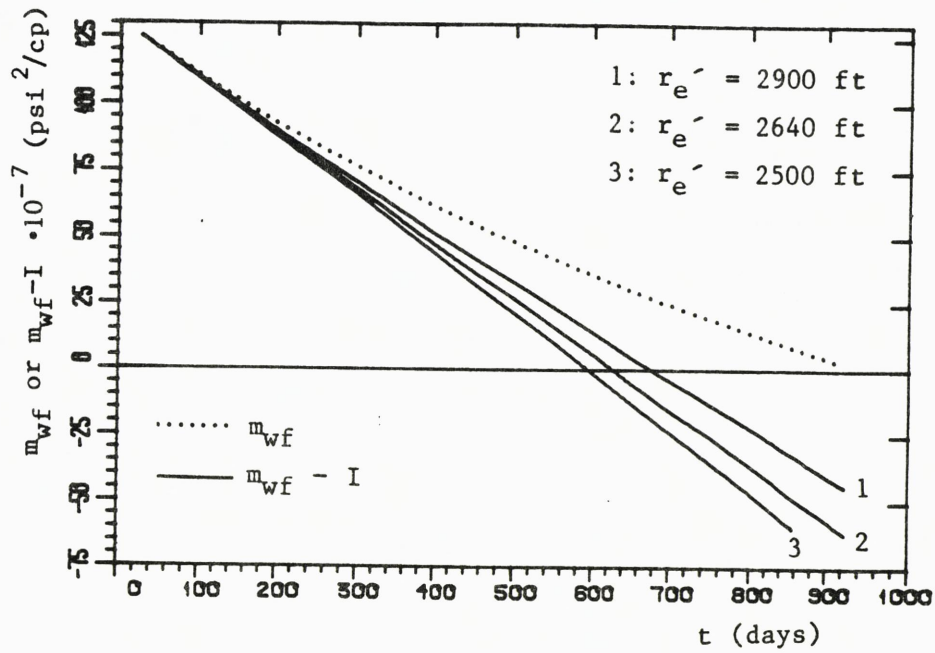
EXAMPLE 7
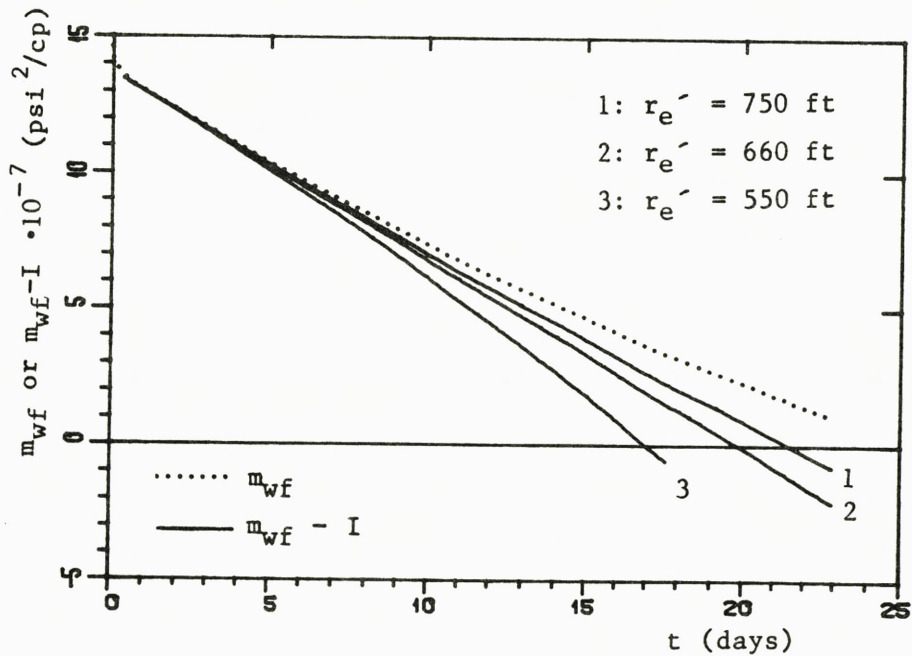
Fig. 2.12 Reservoir limit tests example 6 and 7.

r_e' is value of external radius used in the

calculation of I(t).

EXAMPLE 4

EXAMPLE 5

EXAMPLE 6

Legend (right side):

p_{wDLIN} (solid line)
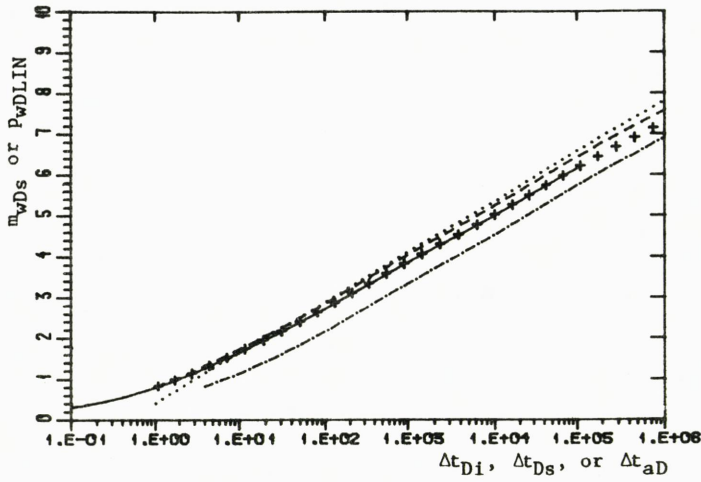
$m_{wDs}(\Delta t_{Ds})$ simulated (dashed line)

$m_{wDs}(\Delta t_{Di})$ simulated (dash-dot line)

$m_{wDs}(\Delta t_{aD})$ simulated (+ + +)

$m_{wDs}(\Delta t_{Ds})$ Eq.(2.2.14) (dotted line)
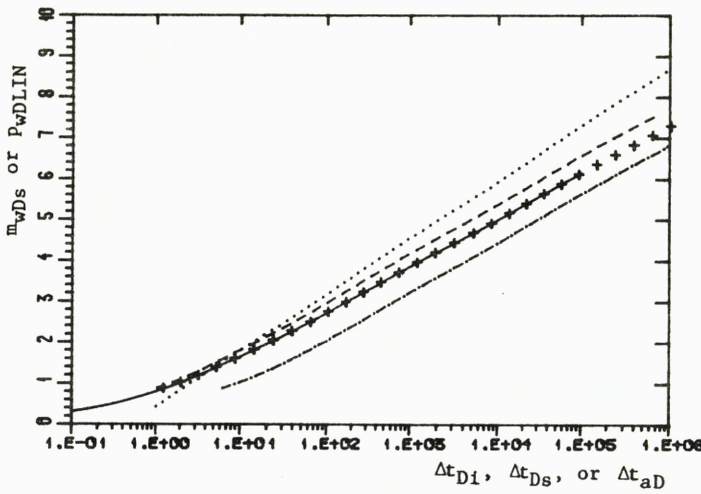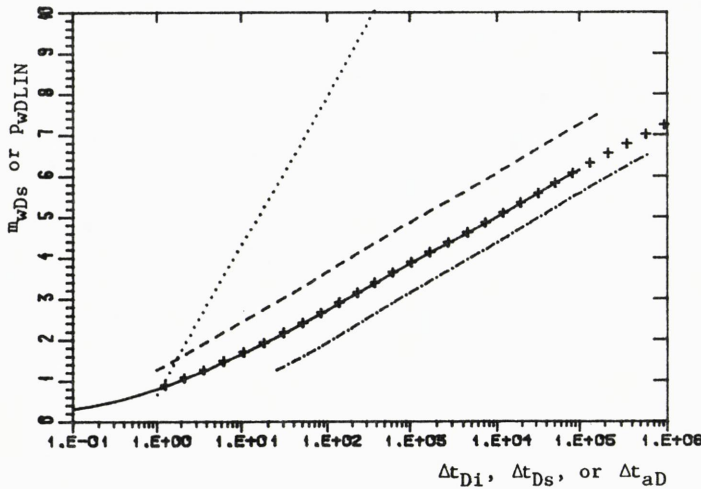
Fig. 2.13 Dimensionless pseudopressure rise during buildup. Perturbation solution and pseudotime solution, compared with simulated pseudopressure and liquid solution respectively. $r = r_w$.

EXAMPLE 6
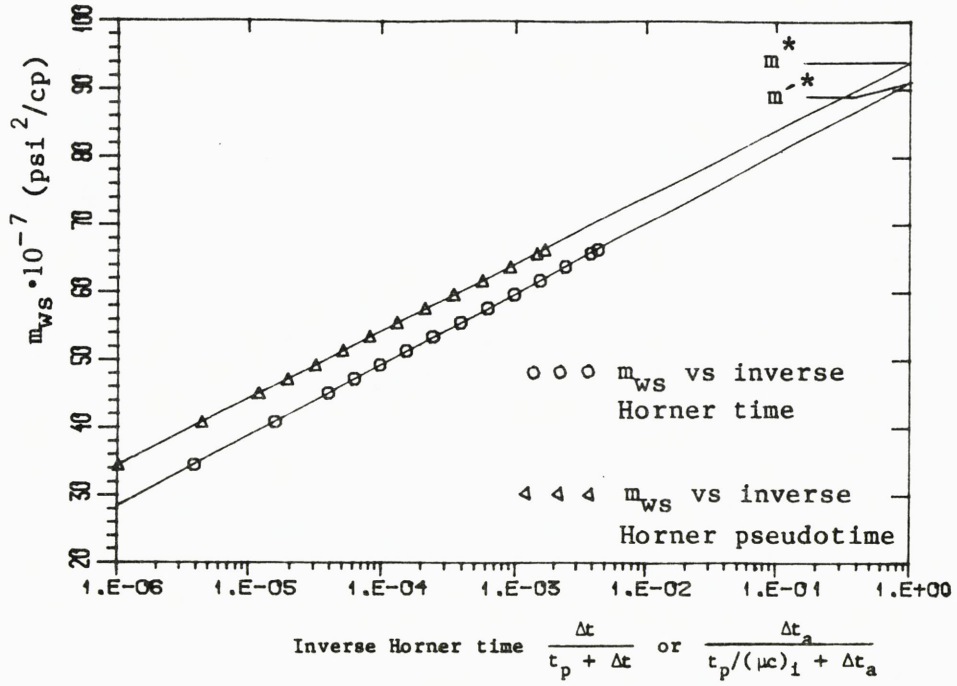
EXAMPLE 7
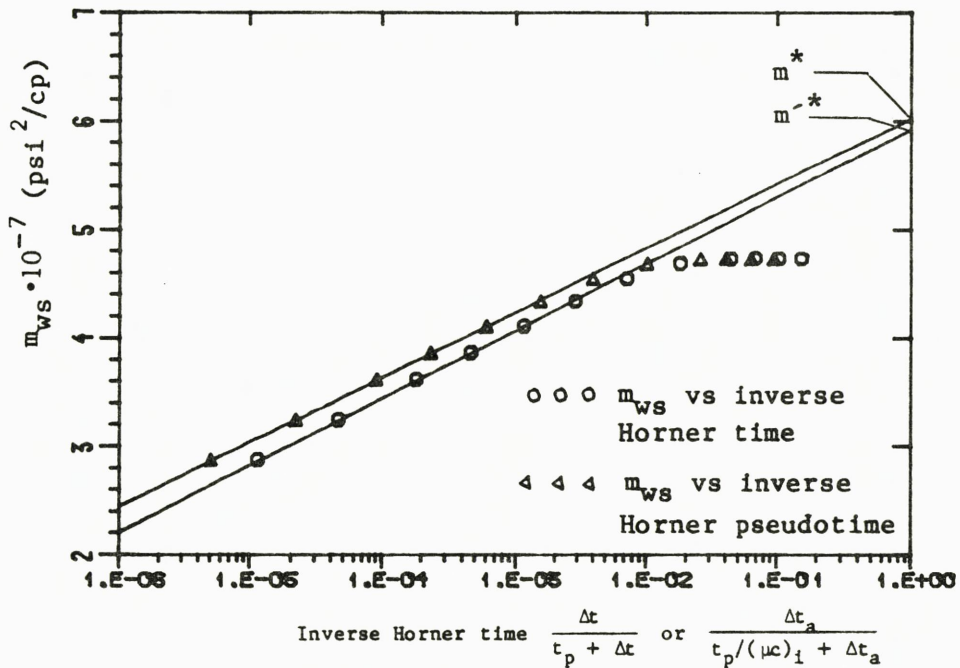
Fig. 2.14 Horner plots example 6 and 7.

PART 3

TWO-PHASE FLOW

3.1 INTRODUCTION

Undoubtedly, one of the most important tools in well test analysis has been solutions of the linear diffusion equation. This also apply to two-phase pressure tests. Muskat [1] solves the model equations for two-phase flow in a few special cases, but most of the work so far has been concentrated on how these complicated equations can be transformed to the familiar diffusion equation, and how the well-known solutions of this equation can be used to analyse well tests where both oil and gas are flowing simultaneously in the reservoir. This approach will form the basis also for this report.

Perrine [2] suggested in 1956 that the mobility term in the diffusion equation should be replaced by adding the mobilities of the individual phases, and the total system compressibility by weighting the individual compressibilities by the average saturation of that phase. Martin [3] gave Perrine's empirical approach a theoretical basis by showing that these modifications could be justified if quadratic terms in ∇p were negligible. Later Perrine's approach was studied numerically by Weller [4] and Earlougher et al. [5] who demonstrated its validity for small gas saturations. However, Weller showed that the analysis becomes less accurate with increasing gas saturation.

In 1961, Levine and Prats [6] made numerical studies of the performance of solution-gas-drive reservoirs and compared the numerical solutions with a semisteady-state solution. This approximate solution was based on the assumption that the decline rate of the oil component (stock tank oil in place) at a given time is the same at every point in the reservoir. The saturation profile was calculated from the gas-oil ratio (GOR), which was assumed to be constant for all r and correspond to the pressure and saturation at the outer boundary.

The concept of pseudopressure was introduced to two-phase flow by
Fetkovich in 1973 [7], and Raghavan [8] presented in 1976 methods to
obtain the pressure-saturation relation needed in the calculation of
the pseudopressure function for drawdown and buildup. For drawdown
the producing GOR as a function of time was used, and for buildup the
producing GOR at the instant of shut-in. The method was also applied
to fractured wells [9]. In Ref.[10], Raghavan's method was used
together with Agarwal's [12] pseudotime transformation.

In 1981, another approach to pseudopressure was presented by
Bøe et al.[11]. An analytical expression relating pressure and
saturation was developed, assuming that saturation is a uniquely
defined function of pressure. This relation, which is valid for
infinite reservoirs, was used to calculate the pseudopressure
function. The wellbore S(p) relation was used both for drawdown and
buildup. Bøe et al. claime that when pseudopressure is calculated
with their method a good adaption to the liquid model is achieved both
for drawdown and buildup. However, later results show that the
buildup solution is highly rate sensitive and not as good as may be
inferred from the results in Ref.[11] (Skjæveland[13] and Whitson[14]
p.123). This is also confirmed by our simulation runs.

As noted by Whitson [14], most of the contributions involving a
pseudopressure function are closely related to an approach suggested
by Evinger and Muskat as early as 1942 [15](or Ref.[1] p.336 ff.)
based on steady state flow. Whitson concludes that most of the work
done after 1942 could have been saved if the work of Evinger and
Muskat had been considered more seriously, and that it is questionable
trying to solve the fully diffusion equations given the uncertainties
associated with the definition of realistic relative permeabilities.
However, even if it turns out that the Evinger/Muskat method is
satisfactory from an engineering point of view, one has to start with
the exact equations to explain why a method based on steady state flow
seems to work also for semisteady and transient flow included buildup.
Hopefully, the validity and connections between the different theories
are made more clear through this report.

In Sec. 3.2 the model equations are discussed and presented on forms suitable for studying. Then the special cases of drawdown and buildup in solution gas drive reservoirs - both infinite and finite - are studied in Sec.3.3 and 3.4. For buildup the applicability of the pseudotime transformation is considered.

One of the main problems concerning two-phase flow is the relative permeability curves. Models exist for relative permeability based on the characterization of the porous media and the flowing fluids, and in Ref.[16], Standing has developed correlations both for drainage and imbibition processes. Very often, however, the relative permeability relationships in the reservoir is not well known. Based on the pressure-saturation relation developed in Ref.[11], attempts have been made to estimate relative permeabilities from drawdown tests with varying success [17]. To investigate the possibility of estimating the parameters used in Standing's correlations, one of the simulated examples was analysed using several incorrect relative permeability relations to see the effect on the drawdown and buildup pseudopressure curves. The results are presented in Sec. 3.6.

The theory is examplified by several simulated drawdown and buildup tests, and seven simulation runs are presented. Example 1-6 simulate a solution gas drive reservoir, and one simulation of a gas condensate reservoir is presented to demonstrate the general applicability of the theory. The results from this simulation are presented in Sec. 3.5. Reservoir and fluid properties are the same for all solution gas drive examples, only initial pressure, production rate, and production time are varying. Initial bubble point pressure is assumed to be 4000 psi, and initial pressure is equal to initial bubble point pressure except for example 1, which demonstrate the case where bubble point pressure is passed during production. Example 2, 3, and 4 show the effect of different production rate in an infinite-acting reservoir (q_o = 50, 100, and 200 stb/d, respectively), while example 5 and 6 demonstrate effects of a closed boundary and buildup from pseudosteady state. Production rate is 100 stb/d for example 5 and 200 stb/d for example 6.

All simulation runs were performed with a 2-dimensional, 3-phase reservoir simulator capable of handling both variable bubble point and variable dew point pressure[18]. The data for all simulation runs are presented in Appendix 3.1.

3.2 THEORY AND GENERAL CONSIDERATIONS

We assume that the fluid flow can be described by the β-model described in Sec. 1.2. The flow is then given by Eq.(1.2.14), which in the notation of Bøe et al. [11] may be written:

$$(3.2.1) \qquad \nabla \cdot \{ \, a(p,S)\nabla p \, \} = \frac{\varphi}{k} \frac{\partial}{\partial t} b(p,S) \qquad \text{gas component}$$

$$(3.2.2) \qquad \nabla \cdot \{ \, \alpha(p,S)\nabla p \, \} = \frac{\varphi}{k} \frac{\partial}{\partial t} \beta(p,S) \qquad \text{oil component}$$

$$(3.2.3) \qquad S \equiv S_o = 1 - S_{iw} - S_g$$

where a, b, α, and β are functions of pressure and saturation defined by:

$$(3.2.4) \qquad a = \frac{k_{rg}}{\mu_g B_g} + R_{so} \frac{k_{ro}}{\mu_o B_o}$$

$$(3.2.5) \qquad \alpha = \frac{k_{ro}}{\mu_o B_o} + r_{sg} \frac{k_{rg}}{\mu_g B_g}$$

$$(3.2.6) \qquad b = \frac{S_g}{B_g} + R_{so} \frac{S_o}{B_o}$$

$$(3.2.7) \qquad \beta = \frac{S_o}{B_o} + r_{sg} \frac{S_g}{B_g}$$

One main question now is whether it is possible to reduce the system of equations, Eqs.(3.2.1) and (3.2.2) to one single diffusion equation of the same form as the real gas equation, Eq.(2.1.3); and eventually, how should it be done? Further, will the results from Part 2 be applicable to account for the nonlinearities in this equation?

Based on the results in Refs.[7-11], a pressure transformation seems to be a reasonable approach to the problem. However, since different methods of calculating this transformation have been presented, a general integral transformation of pressure is considered:

$$(3.2.8) \qquad m(p) \equiv \int_{p_i}^{p} f(p')dp'$$

f is a function of pressure not yet defined. The choise of reference pressure is arbitrary, and p_i is chosen for practical computational reasons. Note that this choise results in a negative pseudopressure when applied to a drawdown/buildup process.

For constant rate drawdown, pressure will be a strictly monotone function of radius and time. This will not be the case for buildup since the pressure, except for points close to the well, will continue to drop for some time after shut-in. This pressure drop will be very small, however, and it should be a reasonable approximation to assume that pressure will be a strictly monotone function of r and t both for drawdown and buildup separately. Saturation may then be written as a function of pressure and time or pressure and radius, respectively:

$$(3.2.9) \qquad \begin{aligned} S &= S(r,t) \\ &= S(r,t(p,r)) = S(p,r) \\ &= S(r(p,t),r) = S(p,t) \end{aligned}$$

Note that this relation may be different for drawdown and buildup. Note also that for a general rate history this approximation will not be valid, and each case then has to be considered separately.

Using Eq.(3.2.9), Eq.(3.2.8) inserted in Eqs.(3.2.1) and (3.2.2) then yields the following equations:

$$(3.2.10) \qquad \nabla^2 m = \frac{\varphi}{k} \frac{[\frac{\partial b}{\partial S}\{\frac{\partial S}{\partial p}\}_r + \frac{\partial b}{\partial p}]}{a} \frac{\partial m}{\partial t} - \frac{f}{a} \nabla(\frac{a}{f}) \cdot \nabla m$$

$$(3.2.11) \qquad \nabla^2 m = \frac{\varphi}{k} \frac{[\frac{\partial \beta}{\partial S}\{\frac{\partial S}{\partial p}\}_r + \frac{\partial \beta}{\partial p}]}{\alpha} \frac{\partial m}{\partial t} - \frac{f}{\alpha} \nabla(\frac{\alpha}{f}) \cdot \nabla m$$

or by introducing the generalized compressibility-mobility ratios $(c/\lambda)^*$ (defined in Ref.[11]) and $(c/\lambda)^{**}$:

$$(3.2.12) \qquad \nabla^2 m = \frac{\varphi}{k}(\frac{c}{\lambda})^{**} \frac{\partial m}{\partial t} - \frac{f}{a} \nabla(\frac{a}{f}) \cdot \nabla m$$

$$(3.2.13) \qquad \nabla^2 m = \frac{\varphi}{k}(\frac{c}{\lambda})^* \frac{\partial m}{\partial t} - \frac{f}{\alpha} \nabla(\frac{\alpha}{f}) \cdot \nabla m$$

$\{\partial S/\partial p\}_r$ is defined as the derivative of S with respect to pressure when written as a function of pressure and radius, i.e., along a line parallel to the time axis in the r-t plane for radial flow.

As pointed out in Part 2, one of the most important objects of the pseudopressure transformation is to linearize the inner boundary condition, which in this case may be a specified surface oil or gas production rate or a specified linear combination of both. If the well is located at r = 0, we get, respectively:

$$(3.2.14) \qquad \lim_{r \to r_w} \{a\, r\frac{\partial p}{\partial r}\} = \frac{q_g}{2\pi k h}$$

or

$$(3.2.15) \qquad \lim_{r \to r_w} \{\alpha\, r\frac{\partial p}{\partial r}\} = \frac{q_o}{2\pi k h}$$

Hence, if an oil production different from zero is given, f must be chosen so that:

(3.2.16) $f(p_w(t)) = \alpha(p_w(t), S_w(t))$

This is possible as long as pressure is a strictly monotone function of time at $r = r_w$.

The boundary condition for m then becomes:

(3.2.17) $\lim_{r \to r_w} \left\{ r\frac{\partial m}{\partial r} \right\} = \frac{q_o}{2\pi kh}$

Note that if the well is closed in and both q_o and q_g are equal to zero, the boundary condition is linearized irrespectively of f.

In the rest of this report, except for Sec 3.5, it will be assumed that the reservoir is an oil reservoir with a given oil production rate, but as noted by Bøe et al. [11] any linear combination of a and α corresponding to a given linear combination of q_o and q_g can be used in Eq. (3.2.16).

Equations similar to Eqs.(3.2.10) and (3.2.11) may also be obtained for pressure, and if quadratic gradient terms can be neglected both equations reduce to the equation (12) of Martin [3] with c_t/λ_t replaced by $(c/\lambda)^*$ and $(c/\lambda)^{**}$, respectively. In this case the quantities are identical and reduce to:

$$\left(\frac{c}{\lambda}\right)^* = \left(\frac{c}{\lambda}\right)^{**} = \frac{c_t}{\lambda_t}$$

(3.2.18)

$$- \frac{S_o r_{sg}(1 - \frac{B_g}{B_o}R_{so})\frac{dR_{so}}{dp} + S_g R_{so}(1 - \frac{B_o}{B_g}r_{sg})\frac{dr_{sg}}{dp}}{\lambda_t (1 - R_{so}r_{sg})}$$

where

$$(3.2.19) \quad \frac{c_t}{\lambda_t} \equiv \left\{ \frac{S_o}{B_o}\left(B_g\frac{dR_{so}}{dp} - \frac{dB_o}{dp}\right) + \frac{S_g}{B_g}\left(B_o\frac{dr_{sg}}{dp} - \frac{dB_g}{dp}\right) \right\} / \left\{ \frac{k_{ro}}{\mu_o} + \frac{k_{rg}}{\mu_g} \right\}$$

Note that $(c/\lambda)^*$ simplifies to c_t/λ_t if R_{so} or r_{sg} are identically zero.

Since α too may be written as a function of pressure and radius or pressure and time when Eq.(3.2.9) is valid, two natural possibilities of defining the pseudopressure function is:

$$(3.2.20) \quad m_r(p) \equiv \int_{p_i}^{p} \alpha(p';r)\,dp'$$

or

$$(3.2.21) \quad m_t(p) \equiv \int_{p_i}^{p} \alpha(p';t)\,dp'$$

That is, we may integrate over time at a given point or over radius for a fixed time. A combination of these two definitions may also be used, and one choise which linearizes the inner boundary condition for all t is:

$$m(r,t) \equiv m_{r_w}(p_w(t)) + m_t(p(r,t))$$

$$(3.2.22)$$

$$= \int_{p_i}^{p_w(t)} \alpha(p';r_w)\,dp' + \int_{p_w(t)}^{p(r,t)} \alpha(p';t)\,dp'$$

Note that Eq.(3.2.22) combines both the pseudopressure as defined by Fetkovich [7] for pseudosteady and steady state flow and the pseudopressure as calculated by Raghavan [8].

Since α generally will be a different function of pressure at different times $m_t(r)$ will be a function of both r and t, and the equation for m (when defined by Eq.(3.2.22)) becomes:

$$(3.2.23) \qquad \nabla^2 m = \frac{\varphi}{k}\frac{c}{\lambda}(\frac{c}{\lambda})^* \frac{\partial m}{\partial t} - \frac{\varphi}{k}\frac{c}{\lambda}(\frac{c}{\lambda})^* \int_{p_w(t)}^{p(r,t)} \{\frac{\partial \alpha}{\partial t}(p';t)\} \, dp'$$

If saturation is uniquely defined by pressure, all these definitions of pseudopressure are equivalent. In that case, a and α will also be uniquely defined by pressure, and the last term in Eqs.(3.2.13) and (3.2.23) dissappears by choosing $f(p) = \alpha(p)$. If, in addition, saturation and pressure are functions of the Bolzmann-variable $y = \varphi r^2/4kt$, Eqs.(3.2.13) and (3.2.23) reduce to the single equation presented by Bøe et al. [11] (their (Eq.(10)). Following the procedure of Bøe et al., it is in this case easily shown that the relation between pressure and saturation is:

$$(3.2.24) \qquad \frac{dS}{dp} = \frac{(\alpha\frac{\partial a}{\partial p} - a\frac{\partial \alpha}{\partial p})(\frac{\partial p}{\partial r})^2 - (\alpha\frac{\partial b}{\partial p} - a\frac{\partial \beta}{\partial p})\frac{\varphi}{k}\frac{\partial p}{\partial t}}{(a\frac{\partial \alpha}{\partial S} - \alpha\frac{\partial a}{\partial S})(\frac{\partial p}{\partial r})^2 - (a\frac{\partial \beta}{\partial S} - \alpha\frac{\partial b}{\partial S})\frac{\varphi}{k}\frac{\partial p}{\partial t}}$$

Eq.(3.2.24) reduces to the equation of Bøe et al. (their Eq.(17)) if the Bolzmann-variable is introduced.

Based on the fact that both the pseudopressure function presented by Raghavan and by Bøe et al. behave very similar to the real gas pseudopressure function, one could be tempted to seek a perturbation solution of Eq.(3.2.13) by neglecting the last term to zeroth order. If the magnitude of ∇m is of the same order as the time derivative and the Laplacian, f then have to be equal to α to zeroth order. This in turn requires that saturation to zeroth order is a function of pressure only. It is possible to show that a perturbation procedure, where p and S are expanded in asymptotic series with $S = S(p)$ to zeroth order, will produce a sequence of linear diffusion equations

for pressure under certain conditions on the coefficients a, b, α, and β. The saturation is then determined from conditions on the coefficients in the corresponding pressure equation. To zeroth order, the relation between pressure and saturation reduces to Eq.(3.2.24). However, since the equations quickly become very complicated and the application to well test analysis is not evident, this idea will not be pursued here.

Due to the nonlinearities of the flow equations, it is not possible to generate solutions corresponding to a general rate history directly from the constant terminal rate solution for two-phase flow as for flow of a slightly compressible liquid where the flow equation is linear and the superposition principle is valid. Hence, if we want to make use of the well-known liquid solution, it is necessary to study each situation separately, and hopefully be able to utilize the characteristics of flow in each case.

Based on Eqs.(3.2.13) and (3.2.23), together with the assumptions stated at the end of Sec. 1.3, the possibilities of reducing the flow equations to the familiar diffusion equation for drawdown and buildup will be investigated in the following sections. However, note that even if the flow equations are reduced to an equation similar to Eq.(2.1.3) with μc replaced by $(c/\lambda)^*$, we are still left with the problem that $(c/\lambda)^*$ is not uniquely defined by pressure or pseudopressure, but rather is a function of two independent variables:

$$(3.2.25) \qquad \left(\frac{c}{\lambda}\right)^* = \left(\frac{c}{\lambda}\right)^* (\ p,S\ ) = \left(\frac{c}{\lambda}\right)^* (\ r,t\ )$$

or if pressure is a strictly monotone function of time or space, respectively:

$$(3.2.26) \qquad \left(\frac{c}{\lambda}\right)^* = \left(\frac{c}{\lambda}\right)^* (\ p(r,t),r\ )$$

$$(3.2.27) \qquad \left(\frac{c}{\lambda}\right)^* = \left(\frac{c}{\lambda}\right)^* (\ p(r,t),t\ )$$

This additional problem, which was not present for gas flow, will be discussed for each case separately.

When passing pubble point pressure or dew point pressure, the derivatives of pressure and saturation may be discontinuous, thus introducing further difficulties. One of the simulated examples has initial pressure above the bubble point pressure, and for most of the examples, parts of the reservoir become single-phased shortly after shut-in. However, this does not seem to seriously affect the calculated pseudopressure.

Most plots show dimensionless pseudopressure as a function of dimensionless time. The dimensionless variables are defined similarly to the corresponding quantities for gas flow, confer the list of symbols on p.143.

3.3 DRAWDOWN

In this section production with constant surface oil rate is studied. Pressure and saturation are assumed to be uniformly distributed initially. First, the reservoir is assumed to be infinite in extent, then the effect of a closed outer boundary is considered.

3.3.1 INFINITE ACTING RESERVOIRS

If saturation is uniquely defined by pressure at all points, α and $(c/\lambda)^*$ will be functions only of pressure. As mentioned previously, the undetermined function $f(p)$ in Eq.(3.2.8) may then be chosen equal to $\alpha(p)$, and it follows that Eq.(3.2.13) becomes identical to Eq.(2.1.3) with μc replaced by $(c/\lambda)^*$. Hence, the results in Part 2 concerning the variations in μc will be valid also for two-phase flow.

Bøe et al.[11] argued that saturation is a unique function of pressure in the infinite acting drawdown period because both saturation and pressure are strictly monotone functions of the Boltzmann-variable $y = \varphi r^2/4kt$. This statement would be correct if the flow equations were linear, but for a system like Eqs.(3.2.1) - (3.2.2) one cannot be sure that all solutions are found when one solution being a function of y is found. However, it may also be argued from a physical point of view that saturation is a unique function of pressure as long as the resevoir is homogeneous and infinite, and both pressure and saturation are uniformly distributed initially:

A given pressure drop in a saturated oil will result in a change in saturation. Since the permeability of free gas is different from the permeability of the oil phase, this may also result in a change in composition, but as long as there are no constraints on this process

and the initial oil saturation and composition are the same at all points, there is no reason to believe that the process should be different from point to point. However, if there is a no-flow boundary present, the composition is forced to be constant along this boundary. At $r = r_e$, the saturation corresponding to a given pressure will therefore be given by the pressure-saturation relation of the initial fluid composition, and may be different from the saturation at other points having the same pressure, but a different composition.

This is clearly demonstrated in Fig. 3.2 where saturation is plotted as a function of pressure at different points, and in Fig. 3.3 where lines of constant pressure and saturation are drawn for the simulated example 5. Before the boundary is felt the pressure and saturation lines coincide and are straight lines with slope 1/2 on a log-log plot. This corresponds to both pressure and saturation being functions of r^2/t. After the boundary is felt, however, the curves immediately start departing.

Based on this, we conclude that in the infinite acting period saturation is a unique function of pressure, at least to a very good approximation. As pointed out by Bøe et al. [11], the pseudopressure function can then be evaluated simply by using the correct pressure-saturation relation at wellbore. This relation may be found from the producing gas-oil ratio (GOR) as suggested by Raghavan [8], or from the relation of Bøe et al. (Eq.(3.2.24)).

GOR can be defined at any point in the reservoir by:

$$(3.3.1) \qquad GOR \equiv \frac{a}{\alpha} = \frac{k_{rg} / \mu_g B_g + R_{so} k_{ro} / \mu_o B_o}{k_{ro} / \mu_o B_o + r_{sg} k_{rg} / \mu_g B_g}$$

i.e.

$$(3.3.2) \qquad \frac{k_{rg}}{k_{ro}} = \frac{\mu_g B_g}{\mu_o B_o} \cdot \frac{GOR - R_{so}}{1 - GOR \, r_{sg}}$$

Eq.(3.3.2) simplifies to the usual GOR-relation for a solution gas drive reservoir if $r_{sg} \equiv 0$. The producing GOR is given by a/α at wellbore, and if k_{rg}/k_{ro} is a known function of saturation, Eq.(3.3.2) can be used to calculate $S(p)$.

Theoretically, both Raghavan's method and the method proposed by Bøe et al. will give the correct $S(p)$. However, Raghavan's method is simpler and also more stable numerically since the method of Bøe et al. implies solving a differential equation. Note, however, that when $S_g < S_{gc}$, GOR $= R_{so}$, and S_g cannot be determined from Eq.(3.3.2). Saturation will then be given by the relative permeability of oil and may be found from the relation of Bøe et al.

Whitson [14] mentions as a problem that k_{rg}/k_{ro} may become negative for early times when calculated from Eq.(3.3.2). A negative permeability is of course not possible physically, and if this situation occurs in practice the explanation has to be either that the measured GOR is different from a/α or the PVT data is incorrect. Another possibility can be that the β-model is invalid. In our calculations of saturation using the gas-oil ratio, the gas saturation is set equal to zero if the ratio k_{rg}/k_{ro} becomes less than or equal to zero, and any occurence of large negative values for the right hand side of Eq.(3.3.2) is not checked. In addition, this results in an error in calculated saturation when $S_g < S_{gc}$, but for drawdown the only effect on pseudopressure will be a constant difference for late times as demonstrated in Fig.3.10.

The problem with $k_{rg}/k_{ro} < 0$ may also occur for buildup, when saturation is calculated from Raghavan's method. This case will be discussed in Sec. 3.4.

One important result of Bøe et al. is that GOR relatively quickly stabilizes at a constant value. The region of stabilized GOR corresponds to Region 1 on Fig. 1.1. and is also identical to the "half-log straight line region" when no well effects are present. That is, the constant GOR-method, refered to as the Evinger-Muskat method by Whitson[14], will also give the correct wellbore pseudopressure for late times, except for a constant term. Whitson analyses example 1 of

Bøe et al. using this method and GOR equal to the initial gas-solubility, R_{soi}. He obtains an estimate of absolute permeability about 18 % larger than the model input permeability. A better result is obtained if the stabilized GOR is used.

The variations in $(c/\lambda)^*$ with m will, as shown in Part 2, result in a slight shift in wellbore pseudopressure on a half-log plot. To estimate the magnitude of this shift, $(c/\lambda)^*$ may be calculated as a function of pseudopressure when saturation and pseudopressure are known as functions of pressure. However, $(c/\lambda)^*$ has, for the solution gas drive case, the characteristic form shown in Figs. 3.7 and 3.8, and it would probably be better to assume a quadratic form initially instead of a linear form as done in Part 2. Note also that the variations in $(c/\lambda)^*$ with rate in this case are much more complicated than for gas flow. The irregularities in Figs. 3.7 - 3.9 corresponds to the pressure points in the PVT table, and show how sensitive $(c/\lambda)^*$ and c_t/λ_t are to the calculated derivatives of b and β.

Another interesting feature with the $(c/\lambda)^*$-function is that it becomes negative after some time. Since $\partial m/\partial t$ always is negative, this implies that the pseudopressure profile must change from being concave to convex. However, this always occurs in Region 1 where the expansion terms are small, and the effect will usually be negligible.

Fig. 3.11 shows dimensionless pseudopressure and pressure compared with the liquid solution for 5 of the simulated examples. Pseudo-pressure is in all cases calculated from the simulated pressure-saturation relation in block 1. Note especially that the pseudopressure follows the liquid solution almost exactly in example 1 despite the discontinuity in compressibility when passing bubble point. Note also that due to the different relative permeabilities used, dimensionless pressure in example 3 and 4 is different from example 5 and 6, respectively, but that the pseudopressure functions are almost identical.

3.3.2 PSEUDOSTEADY STATE

Like a gas reservoir, a reservoir with simultaneous flow of both oil and gas will not achieve a condition where the pressure drop is proportional to flowing time. With "pseudosteady state" we will understand a stabilized condition in a closed reservoir where the effects of all boundaries have reached the well.

The most common pseudosteady state assumption is that the decline rate of stock tank oil is the same for all r when the reservoir is produced with constant surface oil rate, i.e., $\partial\beta/\partial t \approx d\bar\beta/dt$ [6]. However, the discussion in Sec. 2.5 concerning gas flow will apply also for this case. That is, the assumption of constant $\partial\beta/\partial t$ will not be correct near the well, but in that region (Region 3 on Fig.1.1) the expansion terms will be negligible, and a solution may be found as for steady state flow. In addition, most of the variations in pressure and saturation occur in that region, and the effect of errors in the calculated Region 4-solution will be limited. As for gas flow, the final conclusion is that a good approximation to the solution in pseudosteady state may be found by setting the right hand side of Eq.(3.2.2) equal to $d\bar\beta/dt$. $d\bar\beta/dt$ and $d\bar b/dt$ are given by the material balance equations for the oil and gas component, respectively, and may be found by integrating the flow equations, Eqs.(3.2.1) and (3.2.2) over the reservoir:

(3.3.3)
$$\frac{d\bar b}{dt} = -\frac{q_g}{\varphi Ah}$$

(3.3.4)
$$\frac{d\bar\beta}{dt} = -\frac{q_o}{\varphi Ah}$$

Define now pseudopressure by Eq.(3.2.22) and approximate the right hand side of Eq.(3.2.2) by Eq.(3.3.4). When terms of $O(r_w^2/r_e^2)$ are neglected, the result is then the equations given by Fetkovich [7], which is identical to the equations for real gas pseudopressure and pressure in a slightly compressible fluid:

(3.3.5) $\qquad \dfrac{2\pi kh}{q_o} \{m(r,t) - m_w(t)\} = \ln\dfrac{r}{r_w} - \dfrac{r^2}{2r_e^2}$

and

(3.3.6) $\qquad \dfrac{2\pi kh}{q_o} \{\bar{m}(t) - m(r,t)\} = \dfrac{r^2}{2r_e^2} - \ln\dfrac{r}{r_w} - \dfrac{3}{4}$

If these equations can be generalized to an arbitrary geometry and to $t_{eia} < t < t_{pss}$, Eq.(3.3.6) may be written in a form corresponding to Eq.(2.5.18):

(3.3.7) $\qquad \dfrac{2\pi kh}{q_o} \{\bar{m}(t) - m(r,t)\} = p_{DLIN}(r_D, t_{Di}) - 2\pi t_{DAi}$

The saturation profile has to be known to calculate the pseudopressure profile as defined by Eq.(3.2.22). However, in Region 3 the flow is approximately steady state, and the expansion terms may be neglected. It follows that:

(3.3.8) $\qquad a \approx \dfrac{C_1(t)}{r\,\dfrac{\partial p}{\partial r}}$

and

(3.3.9) $\qquad \alpha \approx \dfrac{C_2(t)}{r\,\dfrac{\partial p}{\partial r}}$

where $C_i(t)$ are arbitrary functions of time. That is:

(3.3.10) $\qquad GOR = \dfrac{a}{\alpha} \approx \dfrac{C_1(t)}{C_2(t)}$

Consequently, in Region 3 the gas-oil ratio is independent of position and hence equal to the producing GOR. This is also verified for the simulated examples, and simulated drawdown GOR for example 5 is shown in Fig. 3.5. Levine and Prats [6] assume that GOR is the same at all points and corresponds to the pressure and saturation at the outer boundary. However, an overall better saturation profile will probably be obtained by using the wellbore value, i.e., the producing GOR.

Fig. 3.12 shows dimensionless pseudopressure profiles for example 5 and 6 obtained by integrating the simulated pressure and saturation over wellbore and over radius, respectively. Pseudopressure is also calculated from the saturation profile obtained by assuming GOR equal to the producing GOR for all r, and it is seen that this corresponds very closely to the result when the simulated saturation profile is used. In addition, both these curves are good approximations to the liquid solution. At the beginning of pseudosteady state, also the pseudopressure profile calculated from wellbore $S(p)$ is approximately equal to the liquid solution, as expected. For late times, however, there is a significant difference.

Note that when the expansion terms on the right hand side of Eqs.(3.2.1) and (3.2.2) are neglected, $S(p;t)$ may be found from Eq.(3.2.24) neglecting terms involving $\partial p/\partial t$. Eq.(3.2.24) then reduces to the asymptotic relation for large t presented by Bøe et al. (their Eq.(21)). The connection between Eq.(3.2.24) and the constant GOR method also appears on Fig.3.4 by comparing drawdown $S(p)$ calculated from Eq.(3.2.24) with buildup $S(p)$ calculated with Raghavan's method for example 5 and 6.

For gas flow, the material balance equation combined with the relation between pseudopressure and density was used to calculate $\overline{m}(t)$. The density now corresponds to β, but there is in this case no one to one correspondence between m and β. We have, with m defined by Eq.(3.2.22):

$$(3.3.11) \qquad \frac{\partial \beta}{\partial t} = \left(\frac{c}{\lambda}\right)^{*} \frac{\partial m}{\partial t} - \left(\frac{c}{\lambda}\right)^{*} \int_{p_w(t)}^{p(r,t)} \left\{ \frac{\partial \alpha}{\partial t}(p';t) \right\} \ dp'$$

Hence, if the last term in this equation can be neglected and $(c/\lambda)^{*}(m;r)$ approximated with a kind of average function of m, $\overline{(c/\lambda)}^{*}(m)$, an equation corresponding to Eq.(2.5.8) may be used to calculate the time variation. If $(c/\lambda)^{*}$ from Fig. 3.8 is compared with the corresponding plots of c_t/λ_t (Fig. 3.9), it is seen that $c_t/\lambda_t(p)$ seems to be relatively independent of position for drawdown, and, in addition, this curve seems to be a reasonable average for $(c/\lambda)^{*}$. With μc replaced by drawdown c_t/λ_t, $\overline{m}(t)$ and $m_w(t)$ was calculated from Eqs.(2.5.8) and (3.3.6) for example 5 and 6 with the results shown in Fig 3.13. The calculated m_w is much closer to the simulated solution than the liquid solution is, but still a significant difference makes it difficult to interpret a reservoir limit test.

The results presented in this section are essentially well known aspects of well performance. However, with pseudopressure defined by Eq.(3.2.22), the different theories are combined in a compact form. Using this definition, the pseudopressure profile will be approximately constant in the pseudosteady state period, and the continuous changes in well performance is taken care of by the time variation in $\alpha(p;t)$. It is shown that a good estimate of saturation, and hence pseudopressure profile, may be obtained from an assumption of constant GOR, and the connection to the Evinger-Muskat theory [15], based on steady state flow, is thus established. We have tried to show that these results follow from the exact model equations together with basic assumptions about flow regions.

Application of these results to well testing is thoroughly described for instance in Ref.[7] or Appendix A.8 of Ref.[14] and will not be discussed here. In these papers good results is reported from multirate testing of oil wells. However, the superposition principle is a priori not valid for the nonlinear equations describing two-phase flow. If pseudosteady state has been reached between every change in

rate, it is reasonable to believe that the pseudopressure profile is given by equations corresponding to Eqs. (3.3.5) and (3.3.6), but care should be taken to apply these results to multirate testing if this is not the case.

3.4 BUILDUP

3.4.1 BUILDUP PSEUDOPRESSURE FUNCTION

As mentioned in Sec. 3.1, several methods have been proposed to analyse two-phase buildup tests. Perrine [2] suggested a simple modification of the standard tests for liquid flow. Raghavan [8] introduced the pseudopressure transformation, and to calculate the pressure-saturation needed, the gas oil ratio was assumed to be constant during buildup. Bøe et al. [11] used pseudopressure too, but based on the fact that the pressure gradient during buildup is zero at the well, wellbore saturation calculated from Martin's [3] pressure-saturation relation was used to calculate buildup pseudopressure. For all the simulated examples, this relation gives a good approximation to the correct saturation at all points in the reservoir during buildup. Saturation calculated from Raghavan's constant GOR assumption, however, does not correspond to the simulated saturation in this period (see Fig. 3.4). Despite this, buildup pseudopressure calculated by the method of Bøe et al. is highly rate dependent, and this method seems to be inferior to the one proposed by Raghavan.

One of the fundamental assumptions stated in Sec 1.3 was that quadratic gradient terms can be neglected during buildup. The validity of the pseudotime transformation discussed in Sec.2.3 depends on an assumption of small gradients, and as will be shown also the applicability of Raghavan's method of calculating buildup pseudopressure follows from this assumption. The reason for this can be seen by looking at Eq.(3.2.13). If the pressure gradient is small enough and the coefficients in the flow equation behave reasonably "nice", it follows that the pseudopressure function will satisfy a diffusion equation of the desired type <u>almost independent of the function f(p) chosen in Eq.(3.2.8)</u>. The inner and outer boundary conditions are homogeneous and hence independent of f. The important factor is therefore <u>the initial condition, i.e., the solution profile</u>

at shut in. Since pseudopressure calculated from the saturation profile at shut-in is a good approximation to the liquid solution profile, and this saturation profile may be obtained from the producing GOR, it follows that pseudopressure calculated from Raghavan's method, approximately satisfies both the desired equation as well as initial and boundary conditions; the only remaining problem being the variations in $(c/\lambda)^*$. Note that pseudopressure as defined by Bøe et al. will satisfy the same diffusion equation approximately, but not the desired initial condition. The difference in solution profiles at shut in will increase with production rate and the stage of depletion, and in turn affect the buildup solution. For infinite reservoirs, Raghavan's method corresponds to using drawdown $S(p)$-relation, and the method of Bøe et al. corresponds to using buildup $S(p)$-relation at wellbore. The difference is clearly demonstrated in Fig.3.16. It is, however, important to realize that the reason for the validity of Raghavan's approach is not that the GOR is constant during buildup. On the contrary, the GOR varies considerably during the buildup period (see Fig. 3.6). From the plots of saturation vs. pressure, there is no evidence that pressure changes occur much faster than changes in saturation either. In addition, $f(p)$ as defined is quite different from α for buildup. Hence, the determining factor is the assumption of negligible quadratic gradient terms.

The accuracy of the constant-GOR method to calculate the saturation profile will depend on the relative size of Region 1 or 3 compared with Region 2 or 4, and the variations in GOR in the two latter regions, but for all the simulated solution gas drive examples the pseudopressure seems to be relatively insensitive to these variations. Note also that the applicability of Raghavan's method for buildup is increased by the fact that the buildup solution in the semilog straight line period only depends on the solution profile in Region 3 (or 1), where GOR $\approx$ constant is a very good approximation. Still, of course, we are left with the problem that nonlinearity is decreasing the size of Region 3 (or 1), and hence the length of the semilog straight line, and it is possible that the straight line will disappear completely, especially if well effects are present. However, if the remaining part is sufficient for analysis, it may be concluded that Raghavan's method gives the "correct" pseudopressure function in

this period.

The problem with negative k_{rg}/k_{ro} when calculated from Eq.(3.3.2) may in this case be due to GOR in Region 2 or 4 being larger than the producing GOR. However, as mentioned by Whitson [14], this will only happen at early stages of depletion, and the drawdown pressure-saturation relation of Bøe et al. may then be used. Another possibility is to extrapolate the $S(p)$ or $k_{ro}(p)$ relations.

Note that the procedure for calculating buildup $m(p)$ outlined here is equivalent to use the pseudopressure function defined by Eq.(3.2.22) with t equal to the production time and $p_w(\Delta t)$ inserted as the upper integration limit in the last term:

(3.4.1) $$m_w(\Delta t) = m_{r_w}(p_w(t_p)) + m_{t_p}(p_w(\Delta t))$$

However, in this case the equation for m will not be Eq.(3.2.23), but rather Eq.(3.2.13) with $f(p) = \alpha(p;t_p)$.

Provided that pressure can be assumed to be a strictly monotone function of radius and time both for drawdown and buildup, we have thus shown that the pseudopressure function can be uniquely defined for all r and t by Eq.(3.2.22). For a given r and $t \leqslant t_p$, pseudopressure is then obtained by integrating first over time for $r = r_w$ and then over radius for the given time. For a given buildup pressure, the pseudopressure is equal to the pseudopressure corresponding to the given pressure at the instant of shut-in. The integration paths are shown on Fig.3.1.

3.4.2 EFFECT OF VARIATIONS IN $(c/\lambda)^*$. PSEUDOTIME

We have argued that buildup pseudopressure, when defined by Eq.(2.2.22) and calculated as suggested by Raghavan [8], will approximately satisfy an equation of the form:

$$(3.4.2) \qquad \nabla^2 m = \left(\frac{c}{\lambda}\right)^* \frac{\partial m}{\partial \Delta t}$$

together with initial and boundary conditions as for liquid flow. $(c/\lambda)^*$ is defined by Eqs.(3.2.11) and (3.2.13), but will be given by Eq.(3.2.18) when quadratic gradient terms can be neglected. For solution gas drive reservoirs with $r_{sg} \equiv 0$, $(c/\lambda)^*$ then reduces to c_t/λ_t. When free gas is present, this is a rapidly changing factor like for gas flow. In addition, it will not be a unique function of pressure or pseudopressure, but rather a function of two independent variables as indicated in Eqs.(3.2.25) - (3.2.27).

From Fig. 3.8 it is seen that there can be a significant difference between the curves for different values of r. For example 4, 5, and 6, the gas saturation near the well quickly drops to zero, and $(c/\lambda)^*$ becomes approximately constant, given by the oil parameters. However, farther out in the reservoir free gas is present during the whole buildup period.

If the variations in $(c/\lambda)^*$ could be accounted for by a kind of average function of pressure, the results of Part 2 could possibly be extended. The problem is to obtain such an average $\overline{(c/\lambda)}^*(p)$-curve. Verbeek reports excellent results when using an average of c_t/λ_t between initial and wellbore values [10]. For the case of buildup from PSS, however, it is doubtful that this will be a good solution. A possible method could then be to use an average between $c_t/\lambda_t(\overline{p})$ and $c_t/\lambda_t(p_w)$, but this requires that $\overline{p}$ and a corresponding saturation are known. Refering to the plots of $(c/\lambda)^*$ and c_t/λ_t, a better solution

seems to be to use the drawdown c_t/λ_t as a reasonable average also for the buildup $(c/\lambda)^*$-curve. Δt_a and Δt_{aD} are then defined by:

$$(3.4.3) \qquad \Delta t_a = \int_{p_{wfs}}^{p_{ws}(\Delta t)} \frac{dp_{ws}}{(c_t/\lambda_t)\,(dp_{ws}/dt)}$$

$$(3.4.4) \qquad \Delta t_{aD} = \frac{k\Delta t_a}{\varphi r_w^2}$$

The $(c_t/\lambda_t)(p)$ function used is __drawdown__ c_t/λ_t as a function of wellbore flowing pressure.

Pseudotime was calculated by Eq.(3.4.3) for all the simulated examples, and the results are shown in Fig. 3.15. In all cases, m_{wDs}, when plotted against pseudotime, very closely follows the liquid reference curve as opposed to $m_{wDs}(\Delta t_{Di})$ and $m_{wDs}(\Delta t_{Ds})$.

Note that since integration over radius is equivalent to integration over time in the infinite acting period, drawdown $(c_t/\lambda_t)(p)$ then will be approximately equal to $(c_t/\lambda_t)(p)$ for buildup if the pressure-saturation relation calculated from Raghavan's method is used.

By examining the buildup $(c/\lambda)^*$-curves, it seems that a straight-line approximation to $(c/\lambda)^*(m)$ should give better results than for gas flow. The simplified perturbation solution, Eq.(2.2.14), was therefore calculated from estimates of the derivative of $(d/dm)(c/\lambda)^*$ at shut-in, and, although not shown on the plots, this solution corresponds very closely to the simulated solution except for example 1. In example 1 the "S-shape" of $m_{ws}(\Delta t)$ is very pronounced, and no portion of the buildup curve can be said to follow a straight line.

3.4.3 ESTIMATION OF AVERAGE RESERVOIR PRESSURE

According to the previous section, when pseudopressure is combined with pseudotime, a good adaption to the liquid model is obtained for buildup. As long as Eq.(3.3.7) is valid and the correct MBH-function [19] can be chosen, average pseudopressure may therefore be estimated from buildup tests in solution-gas-drive reservoirs using pseudotime, just as for gas reservoirs (confer Sec. 2.6). The importance of using pseudotime is demonstrated in Fig. 3.15.

In Fig.3.17, the pseudopressure functions in Fig.3.15 are replotted vs. inverse Horner pseudotime. Absolute permeability and skin factor was calculated from these plots and average pseudopressure estimated from m^* using MBH-functions. $p(\overline{m})$ was then calculated from the buildup $m(p)$ relation, which was extended to include the estimated $\overline{m}$.

The results of the analysis are presented in Table 3.4 and compared with the input model values and simulated average pressure. For the simulated examples the estimated average pressures correspond very closely to the simulated values, just as for a gas reservoir, but it still remains to show the general validity of the assumption $\overline{m} = m(\overline{p})$.

3.5 APPLICATION TO GAS CONDENSATE RESERVOIRS

Spivak and Dixon [20] in 1973 suggested that gas condensate reservoirs could be simulated analogous to black-oil reservoirs by assuming that the transfer between the gas and liquid phases could be handled by a r_{sg}-term similar to R_{so} used in black-oil simulation. In addition, they assumed that $R_{so} \equiv 0$, i.e., the oil phase does not contain any gas component.

At the same time, Fussell [21] presented a study showing that the K-values and phase densities can be considered functions only of pressure for many single-well performance predictions for gas condensate reservoirs. Cook et al. [22] proposed that volatile oil and gas condensate reservoirs could be simulated by a generalized β-model where the PVT variables were assumed to depend on a compositional parameter in addition to pressure. Later, Whitson and Torp [23] presented a method for calculating volume factors and solubility factors as functions of pressure for volatile oil and gas condensate reservoirs from a constant volume depletion experiment. Both solubility of gas component in oil phase and volatility of the oil component is then accounted for. However, in a recent work concerning two-phase flow Whitson does not consider gas condensate reservoirs "... because of the insufficient understanding of their PVT properties." [14].

The validity of the β-model for gas condensate reservoirs will not be discussed here, but if such reservoirs can be described by a three-component, three-phase model with only oil and gas flowing, i.e., Eqs.(3.2.1) - (3.2.3), most of the results from the previous sections should be directly applicable.

To give an example of this, one simulation of a drawdown/buildup process in a gas condensate reservoir was performed. PVT properties were taken from Ref.[23] and are shown in Table 3.3. Reservoir properties and relative permeabilities were the same as for the solution gas drive cases. The reservoir was produced with a constant surface gas rate, and pseudopressure was defined by Eq.(3.2.22) with α replaced by a. Note that for single phase gas flow, this pseudopressure function reduces to the real gas pseudopressure defined in Part 2 except for the constant factor $T_{sc}/2Tp_{sc}$.

The results from the simulation are shown in Figs. 3.18 - 3.22 and are very similar to the results from the solution gas drive simulations, with some exceptions:

- The oil saturation in block 1 continues to increase after shut-in, and at the end of simulation the gas saturation near the well is equal to zero. The mass production rate of gas component is in this case higher than the mass production rate of oil component. Hence, the continuing increase in oil saturation may be due to the fluid near the well being heavier during production, which in turn makes the critical point shift to a temperature higher than the reservoir temperature.

- The variations in $(c/\lambda)^{**}$ are somewhat different from $(c/\lambda)^{*}$, $(c/\lambda)^{**}$ being positive for all pressures. For buildup, $(c/\lambda)^{**} \approx c_t/\lambda_t$, indicating that, at least for this example, the correction term in Eq.(3.2.17) is negligible even if both R and r_{sg} are different from zero. The irregularities in the $(c/\lambda)^{**}$ and c_t/λ_t-curves correspond to the pressure points in the PVT table, and again show the sensivity to the calculated derivatives of b and β.

- For the simulated example, Raghavan's method for calculating buildup pseudopressure [8] does not seem to be as good as for the solution gas drive cases. For infinite reservoirs, the pseudopressure based on the drawdown S(p)-relation should be identical to the pseudopressure calculated with Raghavan's method if the "constant GOR" approximation is valid at shut-in. However,

in this case it seems that the size of Region 1 is significantly decreased since the deviation occurs for relatively small Δt. The point where the two pseudopressure curves start deviating from each other corresponds to the point where saturation calculated with Raghavan's method drops to zero in Fig. 3.19. The calculated pseudopressure thus seems to be more sensitive to inaccuracies in the GOR used than is the case for solution gas drive reservoirs. However, this may not be any problem with buildup from PSS. In the last plot, buildup pseudopressure is calculated from the drawdown $m(p)$-relation. Pseudotime is calculated from drawdown c_t/λ_t as in the solution gas drive examples.

3.6 EFFECT OF RELATIVE PERMEABILITIES

Application of the theory presented so far relies on the knowledge of relative permeabilities as functions of saturation. However, even if it is possible to define "average" relative permeability curves capable of describing the flow of the two phases, these are difficult to obtain. To investigate the effect of using incorrect relative permeabilities, the simulated example 4 was analysed using other relations than the ones used as input to the simulator. This was also done to investigate the possibility of estimating relative permeabilities from a two-phase pressure test.

The relative permeability curves were assumed to depend on two parameters; the pore distribution factor λ and the critical gas saturation S_{gc}. The three-phase drainage relations of Standing [16] were used. For $S_w = S_{iw} = $ constant, these relations simplifies to:

$$(3.6.1) \qquad k_{ro} = k_r^0 (S_o^*)^{2/\lambda+3}$$

$$(3.6.2) \qquad k_{rg} = k_r^0 (S_g^*)^2 \cdot \{ 1 - (S_o^*)^{2/\lambda+1} \}$$

where S_o^* and S_g^* are effective saturations defined by:

$$(3.6.3) \qquad S_o^* = \frac{S_o}{1 - S_{iw}}$$

$$(3.6.4) \qquad S_g^* = \frac{S_g - S_{gc}}{1 - S_{iw} - S_{gc}}$$

k_r^0 is the end-point relative permeability and is in all the calculations set equal to 0.7.

Simulator input for example 4 was $\lambda = 2.0$ and $S_{gc} = 0.05$ and corresponds to the solid lines in Fig. 3.23. In addition to these "correct" values, the example was analysed using 4 other combinations of λ and S_{gc}:

i) $\lambda = 2.0$, $S_{gc} = 0.00$

ii) $\lambda = 2.0$, $S_{gc} = 0.10$

iii) $\lambda = 1.0$, $S_{gc} = 0.05$

iv) $\lambda = 6.0$, $S_{gc} = 0.05$

The corresponding relative permeability curves are shown by the dashed and dotted curves respectively on the two plots in Fig. 3.23.

The resulting dimensionless pseudopressures for drawdown and buildup are plotted in Figs. 3.24 and 3.25, where in all cases the solid lines are calculated from the correct values. Drawdown pseudopressure is calculated with $S(p)$ calculated from Eq.(3.2.24) (method of Bøe et al. [11]), and buildup pseudopressure using Raghavan's method [8]. For buildup, pseudopressure is plotted v.s. dimensionless shut-in time based on $(c/\lambda)^*_i$; pseudotime is not used. The calculated c_t/λ_t, and hence the relation between Δt and Δt_a, will also change with the relative permeability relations used, but this effect is not studied.

The plots exhibit several interesting features:

i) Even if the variations in λ has a larger effect on the relative permeability curves for the present saturations than the variations in S_{gc}, the latter gives a more significant change in calculated pseudopressure. The reason for this is that the effect of the variations in k_{ro} and k_{rg} to a certain degree cancel each other when λ is changed.

ii) Qualitatively the calculated pseudopressure curves are very similar, and it is probably impossible to deduce from a test whether the relative permeabilities applied are correct. Hence,

it will be difficult to obtain good estimates of λ and S_{gc} from a test. On the other hand, if absolute permeability is calculated from the incorrect curves, the error in the result can be significant; the small changes in relative permeabilities used here causing as much as 20 - 25 % error.

iii) However, if <u>absolute</u> permeability is known, information about the expected slope will increase the possibilities of estimating λ and S_{gc} significantly.

The object of this section has only been to present some examples of using incorrect relative permeability relations when analysing a two-phase test and is not ment to be a detailed study. The results presented here, however, show that this is a field where further investigation is needed.

3.7 CONCLUSIONS

1) If the fluid flow can be described by the β-model given by
   Eqs.(3.2.1) - (3.2.7), multiphase-flow effects for a constant rate
   drawdown followed by a pressure buildup can, to a very good
   approximation, be adapted by the liquid model solutions. This is
   done by introducing an integral transformation of pressure also
   called a pseudopressure function. For buildup, a similar
   transformation - pseudotime - is applied to the shut-in time.

2) Provided that pressure can be assumed to be a strictly monotone
   function of radius and time for drawdown and buildup, separately,
   the pseudopressure function can be uniquely defined for all r and
   t by Eq.(3.2.22). For a given r and $t < t_p$, pseudopressure is
   then obtained by integrating first over time for $r = r_w$ and then
   over radius for the given time. The pseudopressure for a given
   buildup pressure is given by the corresponding pressure at the
   instant of shut-in.

3) If relative permeabilities are known as functions of saturation,
   the pressure-saturation relation needed in the integration along
   $r = r_w$ may be found from the producing GOR as suggested by
   Raghavan in Ref.[8], or, in the infinite-acting period, also from
   the relation of Bøe et al.[11]. In the infinite-acting period,
   the pressure-saturation relation in addition is approximately
   independent of position, and the integration over radius is not
   necessary.

4) All the simulated examples for a solution gas drive reservoir
   indicate that a good approximation to the saturation profile for
   all times may be obtained by assuming GOR to be independent of
   radius and equal to the producing GOR. This method is very
   similar to the Evinger/Muskat method [15], and for buildup it
   corresponds to applying the method proposed by Raghavan [8].

5) For drawdown in an infinite reservoir, the dimensionless pseudo-pressure function is equal to the liquid solution except for a small constant term. An estimate of this term may be obtained by the perturbation method presented in Part 2 for single-phase gas flow.

6) In pseudosteady state, the dimensionless pseudopressure profile very closely resembles the liquid solution profile, but the time variation is different. Drawdown c_t/λ_t may be calculated from flowing wellbore pressure and an estimate of the time variation in pseudopressure may be obtained by replacing μc with c_t/λ_t in the equations developed in Part 2.

7) If the producing time is sufficiently long, the buildup pseudopressure function will follow a straight line on a MDH plot, but with a larger slope than the liquid solution. An approximation to this slope may be obtained from the perturbation solution presented in Part 2 if the derivative of c_t/λ_t with respect to pseudopressure at shut-in can be estimated.

8) <u>Drawdown</u> c_t/λ_t may also be used to calculate the pseudotime transformation, and dimensionless buildup pseudopressure plotted against dimensionless shut-in pseudotime very closely follows the liquid solution also in cases where the compressibility is discontinuous.

9) Several buildup tests in a solution-gas-drive reservoir was simulated, and in all cases accurate estimates of initial or average pressure was obtained by applying the MBH-method to pseudopressure plotted v.s. pseudotime in a Horner plot.

10) One drawdown/buildup in an infinite acting gas condensate reservoir was simulated with the same conclusions as for solution-gas-drive reservoirs; the only exception being that buildup pseudopressure calculated from the constant GOR approximation was not as accurate as for the latter case.

11) Relatively small inaccuracies in the relative permeability relations used in the analysis can result in significant changes in the calculated formation permeability even if the pseudopressure curves are very similar. With relative permeability relations given by the relations of Standing [16], the pseudopressure curves are more sensitive to variations in critical gas saturation than pore distribution factor.

NOMENCLATURE

A	Drainage area
a, b, α, β	Defined by Eqs.(3.2.4) - (3.2.7)
B_g, B_o	Volume factors for gas and oil
$C_1(t)$, $C_2(t)$	Arbitrary functions of time (see Eqs.(3.3.8-9)
c_t	Total compressibility of reservoir fluids, defined by Eq.(3.2.19)
$f(p)$	Function of pressure used in the definition of the pseudopressure function (see Eq.(3.2.8))
GOR = a/α	Gas/oil ratio
h	Reservoir height
k	Absolute permeability
k_{rg}, k_{ro}	Relative permeabilities
k_r^o	Endpoint relative permeability
m	Pseudopressure

$$m_D = \frac{2\pi kh}{q_o}(m_i - m(r,t))$$ Dimensionless pseudopressure fall [1]

$$m_{Ds} = \frac{2\pi kh}{q_o}(m(r,t_p+\Delta t) - m(r_w,t_p))$$ Dimensionless pseudopressure rise during buildup [1]

m^*	Extrapolated value on Horner plot
p	Pressure

$$p_D = \frac{2\pi k k_{roi}h}{q_o B_{oi}\mu_{oi}}(p_i - p(r,t))$$ Dimensionless pressure fall [1]

p_{DLIN}	Dimensionless solution of the linear heat equation (liquid solution)

----

[1]   For a gas condensate reservoir, subscript o is replaced by g.

q_g, q_o Surface production rates

r Radius

$r_D = r/r_w$ Dimensionless radius

R_{so} Solubility of gas component in oil phase

r_{sg} Volatility of oil component

$S = S_o$ Oil saturation

S_g, S_{gc} Gas saturation, critical gas saturation

S_{iw} Irreducible water saturation

S_g^*, S_o^* Effective saturations, defined by Eqs.(3.6.3-4)

t Time

t_p Production time

$\Delta t = t - t_p$ Shut-in time

$t_{Di} = \dfrac{kt}{\varphi[(\frac{c}{\lambda})^*]_i r_w^2}$ Dimensionless time based on $[(c/\lambda)^*]_i$ <1>

$\Delta t_{Ds} = \dfrac{k(t-t_p)}{\varphi[(\frac{c}{\lambda})^*]_s r_w^2}$ Dimensionless shut-in time based on $[(c/\lambda)^*]_s$ <1>

Δt_a, Δt_{aD} Shut-in pseudotime, dimensionless shut-in pseudotime (See Eqs.(3.4.3) and (3.4.4))

$t_{DAi} = \dfrac{kt}{\varphi[(\frac{c}{\lambda})^*]_i A}$ Dimensionless time based on drainage area <1>

$y = \dfrac{\varphi r^2}{4kt}$ Boltzmann variable

φ Porosity

μ_g, μ_o Viscosities

<1>   For a gas condensate reservoir, $(c/\lambda)^*$ is replaced by $(c/\lambda)^{**}$

λ Pore distribution factor (see Eqs.(3.6.1-2))

$\lambda_t = \dfrac{k_{ro}}{\mu_o} + \dfrac{k_{rg}}{\mu_g}$ Total mobility

$\left(\dfrac{c}{\lambda}\right)^{*}, \left(\dfrac{c}{\lambda}\right)^{**}$ Generalized compressibility-mobility ratios defined by Eqs.(3.2.10-13)

$\bar{p}, \bar{m}, \bar{b}, \bar{\beta}$ Volume averaged values

Subscripts

D	Dimensionless
e	External
f	Flowing
g	Gas
i	Initial
o	Oil
s	Shut-in
w	Well
iw	Irreducible water

REFERENCES

[1] Muskat,M.: "Physical Principles of Oil Production," McCraw
     Hill, New York (1949), Second Edition: IHRDC, Boston (1981).

[2] Perrine,R.L.: "Analysis of Pressure Buildup Curves," Drill. and
     Prod. Prac., API (1956) 482-509

[3] Martin,J.C.: "Simplified Equations of Flow in Gas Drive
     Reservoirs and the Theoretical Foundation of Multiphase Pressure
     Buildup Analysis," Trans., AIME (1959) 216, 309-311.

[4] Weller,W.T.: "Reservoir Performance During Two-Phase Flow,"
     J.Pet.Tech. (Feb. 1966) 240-246, Trans., AIME 237.

[5] Earlougher,R.C.,Jr., Miller,F.G., and Mueller,T.D.: "Pressure
     Buildup Behavior in a Two-Well Gas-Oil System," Soc.Pet.Eng.J.
     (June 1967), 195-204, Trans., AIME 240.

[6] Levine,J.S. and Prats,M.: "The Calculated Performance of
     Solution-Gas-Drive Reservoirs," Soc.Pet.Eng.J.
     (September 1961) 142-152, Trans.,AIME 222.

[7] Fetkovich,M.J.: "The Isochronal Testing of Oil Wells," Paper SPE
     4529, Presented at the SPE-AIME 48th Annual Fall Meeting, Las
     Vegas, Nev., Sept. 30 - Oct. 3 (1973).

[8] Raghavan, R.: "Well Test Analysis: Wells Producing by Solution
     Gas Drive," Soc.Pet.Eng.J. (Aug. 1976) 196-208, Trans. AIME 261.

[9] Raghavan, R.: "Pressure Transient Analysis of a Vertically
     Fractured Well Produced by Solution Gas Drive," Soc.Pet.Eng.J.
     (Oct. 1977) 369-376, Trans. AIME 263.

[10] Verbeek,C.M.J.: "Analysis of Production Tests of Hydraulically
     Fractured Wells in a Tight Solution Gas-Drive Reservoir,"
     Paper SPE 11084, Presented at the SPE-AIME 57th Annual Fall
     Meeting, New Orleans, LA, Sept. 26-29, 1982.

[11] Bøe,A., Skjæveland,S.M., and Whitson,C.H.: "Two-Phase Pressure
     Test Analysis," Paper SPE 10224,
     Presented at the SPE-AIME 56th Annual Fall Meeting,
     San Antonio, Texas, Oct. 5-7, 1981.

[12] Agarwal,R.G.: "'Real Gas Pseudo-Time' - A New Function for
     Pressure Buildup Analysis of MHF Gas Wells," Paper SPE 8279,
     Presented at the SPE-AIME 54th Annual Fall Meeting,
     Las Vegas, Nev., Sept. 23-26, 1979.

[13] Skjæveland,S.M.: Private Communications.

[14] Whitson,C.H.: "Topics on Phase Behavior and Flow of Petroleum
     Reservoir Fluids," Thesis for the Degree Doctor of the Technical
     Sciences, Norwegian Institute of Technology, University of
     Trondheim, Trondheim (1983).

[15] Evinger,H.H. and Muskat,M.: "Calculation of Theoretical
     Productivity Factor," Trans. AIME (1942) 146, 126-139.

[16] Standing,M.B.: "Notes on Relative Permeability Relationships,"
     Division of Petroleum Engineering and Applied Geophysics,
     Norwegian Institute of Technology, University of Trondheim,
     Trondheim (1974).

[17] Nygård,R.: "Calculating Relative Permeabilities From Two-Phase
     Drawdown Tests," Thesis for the Cand.Techn. Degree,
     Rogaland Regional College, Stavanger (1982) (In Norwegian).

[18] Tjetland,G., Litlehamar,T., and Skjæveland,S.M.: "'TODVARS' - A Three-Phase, Two-Dimensional, Implicit Reservoir Simulator with Variable Saturation Pressure," Report No. T 12/82, Rogaland Research Institute, Stavanger (1982).

[19] Matthews,C.S., Brons,F., and Hazebroek,P: "A Method For Determination of Average Pressure in a Bounded Reservoir," Trans., AIME (1954) <u>201</u>, 182-191.

[20] Spivak.A. and Dixon,T.N.: "Simulation of Gas-Condensate Reservoirs," Paper SPE 4271, Presented at the SPE-AIME 3rd Symposium on Numerical Simulation of Reservoir Performance, Houston, Texas, Jan. 10-12 (1973).

[21] Fussell,D.D.: "Single-Well Performance Predictions for Gas Condensate Reservoirs," J.Pet.Tech. (July 1973) 860-870.

[22] Cook,R.E., Jacoby,R.H., and Ramesh,A.B.: "A Beta-Type Reservoir Simulator for Approximating Compositional Effects During Gas Injection," Paper SPE 4272, Presented at the SPE-AIME 3rd Symposium on Numerical Simulation of Reservoir Performance, Houston, Texas, Jan. 10-12 (1973) Also: "Numerical Simulation," SPE Reprint Series No.11, Society of Petroleum Engineers of AIME, Dallas (1973) 246-257.

[23] Whitson,C.H. and Torp,S.B.: "Evaluating Constant Volume Depletion Data," Paper SPE 10067, Presented at the SPE-AIME 56th Annual Fall Meeting, San Antonio, Texas, Oct. 5-7 (1981).

APPENDIX 3.1 SIMULATION EXAMPLES

6 simulations of a constant rate drawdown followed by a pressure buildup for a solution gas drive reservoir and one for a gas condensate reservoir were performed to demonstrate the applicability of the theory discussed. All simulations were performed with the two-dimensional, three-phase reservoir simulator, "TOOVARS" developed at Rogaland Research Institute [18]. In all examples one well was produced from the center of a circular, closed reservoir.

Reservoir parameters are identical in all examples and are shown in Table 3.1. Relative permeabilities were generated from Standing's drainage correlations [16], Eqs.(3.6.1) - (3.6.4), with pore distribution factor $\lambda = 2.0$. Critical gas saturation, S_{gc}, is 0.0 for for example 5 and 6 and 0.05 for all the other simulations. k_{rg} and k_{ro} as functions of saturation are shown in Fig.3.23.

Solution gas drive reservoir:

Except for the initial bubble point pressure equal to 4000 psi, the PVT properties are identical to those used in Ref.[11] and are presented in Table 3.2.

Example 1:

$p_i = 4300$ psi, $\quad q = 100$ stb/d, $\quad t_p = \Delta t = 100$ hrs,

$t_{pDi} = 1.79 \cdot 10^6$, $\quad t_{pDAi} = 0.142$, $\quad p_{wfs} = 3509$ psi

Example 2:

$p_i = 4001$ psi, $\quad q = 50$ stb/d, $\quad t_p = \Delta t = 100$ hrs,

$t_{pDi} = 5.02 \cdot 10^5$, $\quad t_{pDAi} = 0.04$, $\quad p_{wfs} = 3651$ psi

Example 3:

$p_i = 4001$ psi, $\quad q = 100$ stb/d, $\quad t_p = \Delta t = 100$ hrs,

$t_{pDi} = 5.02 \cdot 10^5$, $\quad t_{pDAi} = 0.04$, $\quad p_{wfs} = 3196$ psi

Example 4:

p_i = 4001 psi, q = 200 stb/d, t_p = Δt = 100 hrs,

t_{pDi} = 5.02·10^5, t_{pDAi} = 0.04, p_{wfs} = 1886 psi

Example 5:

p_i = 4001 psi, q = 100 stb/d, t_p = 10600 hrs, Δt = 100 hrs,

t_{pDi} = 5.32·10^7, t_{pDAi} = 4.23, p_{wfs} = 261 psi

Example 6:

p_i = 4001 psi, q = 200 stb/d, t_p = 1800 hrs, Δt = 100 hrs,

t_{pDi} = 9.04·10^6, t_{pDAi} = 0.72, p_{wfs} = 254 psi

Gas condensate reservoir:

The PVT properties, which is presented in table 3.3, were taken from
one of the examples in Ref. [23] (rich gas condensate, NS-1) with
initial dew point pressure 6000 psi.

p_i = 5999 psi, q_g = 4000 Mscf/d, t_p = Δt = 100 hrs,

t_{pDi} = 2.34·10^5, t_{pDAi} = 0.019, p_{wfs} = 2344 psi

APPENDIX 3.2 COMMENTS TO THE NUMERICAL CALCULATIONS

Several programs were written to analyse the simulator output. Two programs, based on the methods of Bøe et al. [11] and Raghavan [8], respectively, were used to calculate oil saturation and pseudopressure from simulated wellbore pressure. A similar program used simulated saturation in block 1 to calculate pseudopressure. $(c/\lambda)^{**}$, $(c/\lambda)^{*}$, and c_t/λ_t were calculated from simulated pressure and saturation as functions of time.

In all calculations, pseudopressure is defined by Eq.(3.2.22) and calculated as shown in Fig. 3.1, making $m_i = 0$ and $m_{wf} < 0$. Note that the pseudopressure for some r and t may be larger than m_i since $\alpha(p;t)$ generally is different from $\alpha(p;r_w)$, even if the pressure is the same.

Simple numerical methods were used: Linear interpolations; integrals were calculated from the trapezoidal rule; and the ordinary differential equation for saturation occuring in the method of Bøe et al. was solved with Euler's explicit method. For the solution gas drive case, the inverse of Eq.(3.2.2) was used when calculating S_o from Raghavan's method. If k_{rg}/k_{ro} (or k_{ro}/k_{rg}) in Eq.(3.3.2) becomes less than or equal to zero, S_g (or S_o) is set equal to zero. The derivatives involved in the expressions for $(c/\lambda)^{**}$, $(c/\lambda)^{*}$, and c_t/λ_t were calculated from a mid-point formula. Pseudotime was calculated directly from the c_t/λ_t-curves. A smoothing of the curves was tried without any significant difference in the resulting $m_{wDs}(\Delta t_{aD})$.

Well radius	0.33	ft
Radius of reservoir	660	ft
Reservoir height	15.5	ft
Absolute permeability	10.0	mD
Porosity	0.30	
Connate water saturation	0.30	
Initial gas saturation		
solution gas drive examples	0.00	
Initial oil saturation		
gas condensate example	0.00	

Table 3.1 Reservoir properties.

PVT properties saturated fluid (from Ref.[11]):

p (psi)	B_o (RB/STB)	μ_o (cp)	R_{so} (SCF/STB)	B_g (RCF/SCF)	μ_g (cp)	r_{sg} (STB/SCF)
193	1.058	1.350	44.286	.09479	.0113	.00
622	1.088	1.164	119.139	.02807	.0125	.00
1052	1.121	1.011	196.104	.01587	.0138	.00
1481	1.159	.881	278.240	.01083	.0152	.00
1911	1.202	.768	366.519	.008169	.0166	.00
2340	1.249	.671	461.531	.006581	.0181	.00
2769	1.302	.587	563.791	.005567	.0195	.00
3199	1.360	.515	673.783	.004888	.0210	.00
3700	1.434	.446	812.575	.004350	.0228	.00
4201	1.516	.391	963.478	.003979	.0246	.00
4701	1.605	.348	1127.453	.003711	.0263	.00
5202	1.702	.317	1305.561	.003507	.0281	.00
5631	1.791	.300	1470.383	.003367	.0295	.00
5703	1.806	.298	1499.003	.003346	.0298	.00

Initial bubble point pressure: 4000 psi

Properties of oil above bubble point pressure:

$$\frac{dB_o}{dp} = -1.6 \cdot 10^{-5} \text{ RB/STB-psi} \qquad \frac{d\mu_o}{dp} = 2.1 \cdot 10^{-5} \text{ cp/psi}$$

Table 3.2 Fluid properties. Solution gas drive examples.

PVT properties saturated fluid (from Ref.[23]):

p (psi)	B_o (RB/STB)	μ_o (cp)	R_{so} (SCF/STB)	B_g (RCF/SCF)	μ_g (cp)	r_{sg} (STB/SCF)
800	1.200	1.09	140	.0251	.0129	2.463E-5
1000	1.225	1.01	180	.0197	.0136	2.232E-5
1200	1.240	.96	220	.0165	.0143	2.174E-5
1400	1.280	.90	260	.0140	.0150	2.193E-5
1600	1.285	.85	300	.0123	.0157	2.222E-5
1800	1.310	.77	350	.0108	.0164	2.283E-5
2000	1.335	.74	400	.0095	.0171	2.370E-5
2200	1.360	.70	450	.0086	.0177	2.463E-5
2400	1.385	.66	500	.0078	.0184	2.577E-5
2600	1.410	.62	550	.0073	.0191	2.762E-5
2800	1.430	.58	600	.0068	.0198	2.994E-5
3000	1.460	.54	650	.0064	.0205	3.279E-5
3200	1.485	.51	710	.0060	.0212	3.650E-5
3600	1.550	.45	840	.0055	.0225	4.425E-5
4000	1.620	.40	980	.0050	.0239	5.405E-5
4400	1.675	.37	1130	.0047	.0253	6.667E-5
4800	1.730	.35	1310	.0045	.0267	8.065E-5
5200	1.790	.32	1500	.0043	.0280	9.804E-5
5600	1.850	.305	1700	.0041	.0294	11.628E-5
6000	1.915	.295	1910	.0040	.0308	13.514E-5
6400	1.980	.285	2120	.0039	.0321	15.625E-5
6800	2.045	.275	2330	.00385	.0335	17.857E-5

Initial dew point pressure: 6000 psi

Gas properties above dew point pressure:

$$\frac{dB_g}{dp} = -1.0 \cdot 10^{-5} \text{ RB/STB-psi} \qquad \frac{d\mu_g}{dp} = 3.5 \cdot 10^{-5} \text{ cp/psi}$$

Table 3.3 Fluid properties. Gas condensate example.

	Example	1	3	4	5	6
Calculated values	Slope, s (psi/cp-log⌣)	97.68	108.70	210.06	104.15	198.84
	m^* (psi/cp)	-8.904	113.6	166.5	-814.9	-255.0
	k (mD)	10.7	9.65	9.99	10.07	10.55
	Skin factor, S	0.2	-0.06	0.03	-0.06	0.10
	tDAi	0.152	0.038	0.039	4.259	0.758
	m_i (psi/cp)	-	113.6	166.5	-	-
	$p(m_i)$ (psi)	-	4001	4005	-	-
	$\bar{m}$ (psi/cp)	-76.77	-	-	-1039	-533.86
	$p(\bar{m})$ (psi)	4203	-	-	2750	3489
Model values	k (mD)	10.0	10.0	10.0	10.0	10.0
	S	0.0	0.0	0.0	0.0	0.0
	p_i (psi)	4300	4001	4001	4001	4001
	$\bar{p}$ (psi)	4230	3982	3965	2763	3478

Table 3.4 Results from an analysis of the Horner plots (Fig.3.17) generated from the simulated examples of a solution gas drive reservoir.
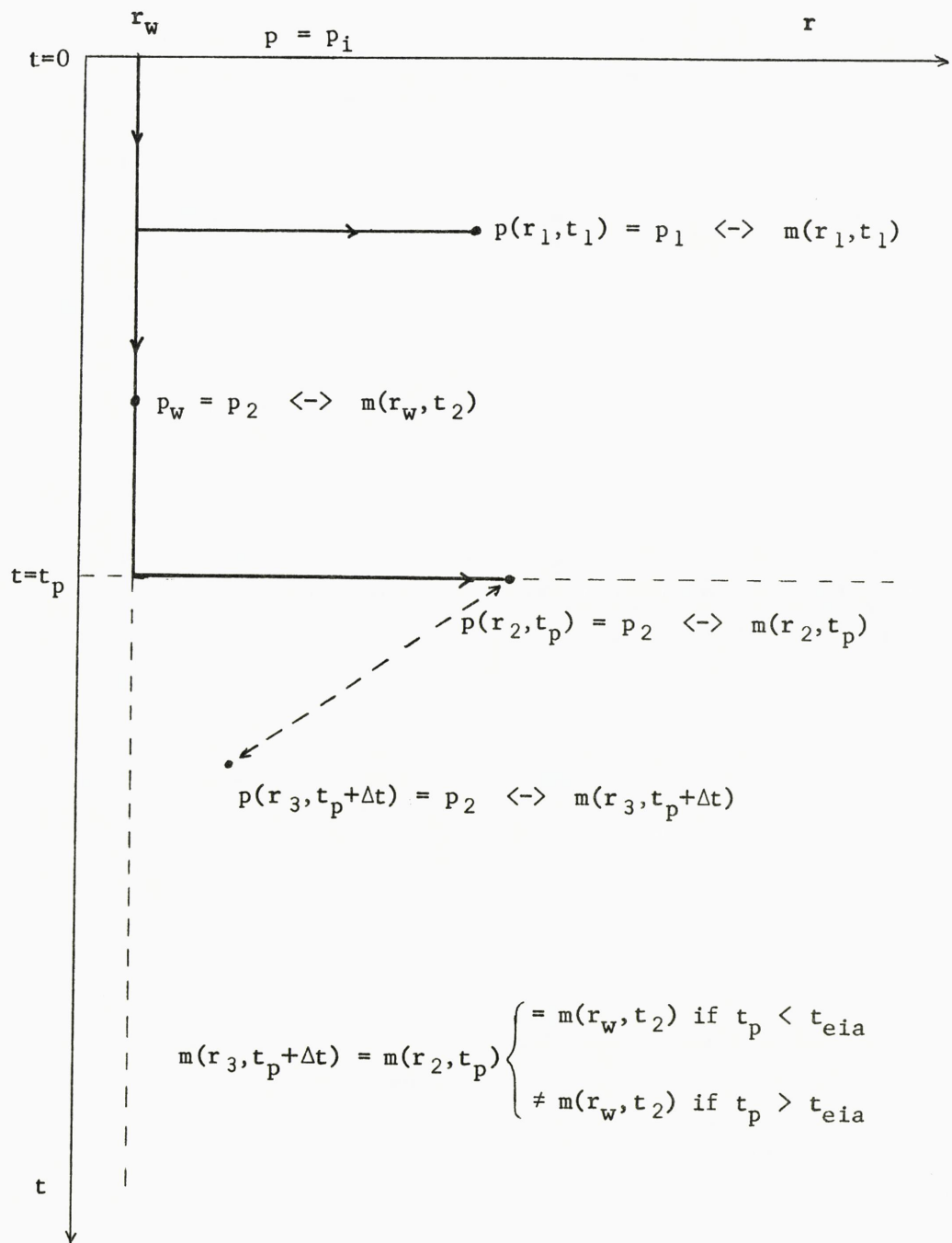
Fig. 3.1 Integration paths followed when pseudopressure is
calculated.

EXAMPLE 2

EXAMPLE 3

EXAMPLE 4

EXAMPLE 5

EXAMPLE 6

Fig. 3.2 Simulated oil saturation vs. pressure at different points in the reservoir. The plots show both drawdown and buildup relations, and the positive time direction is indicated with arrows.
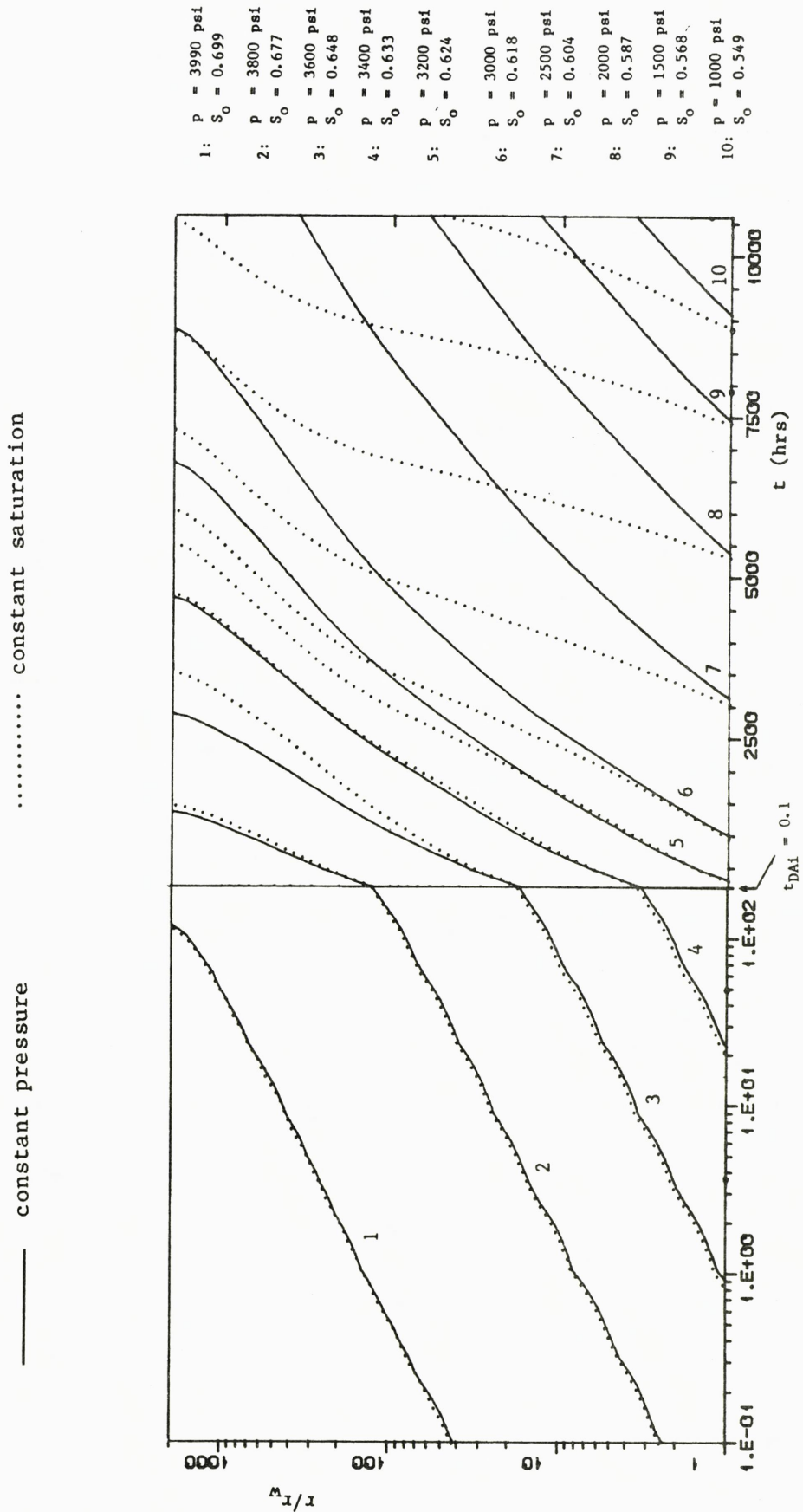
Fig. 3.3 Levels of constant pressure and oil saturation.
Drawdown example 5.
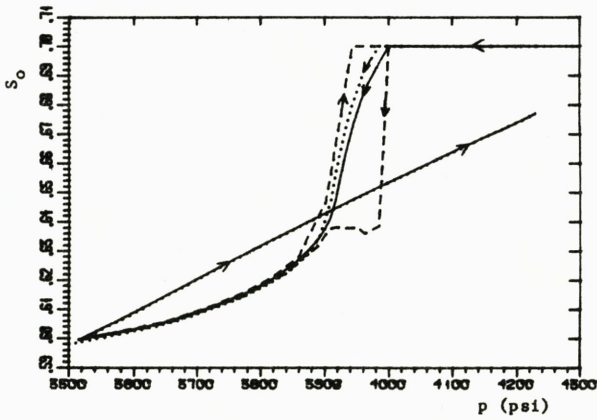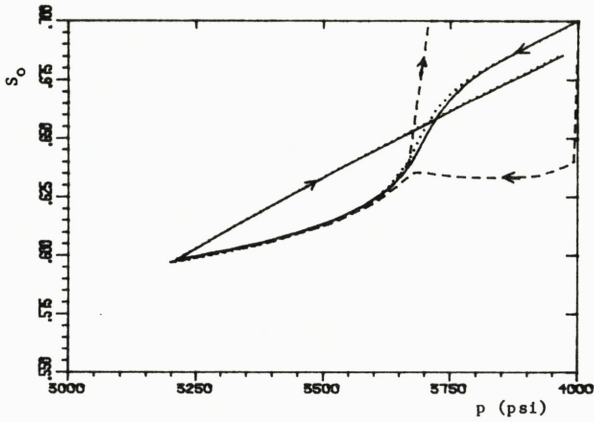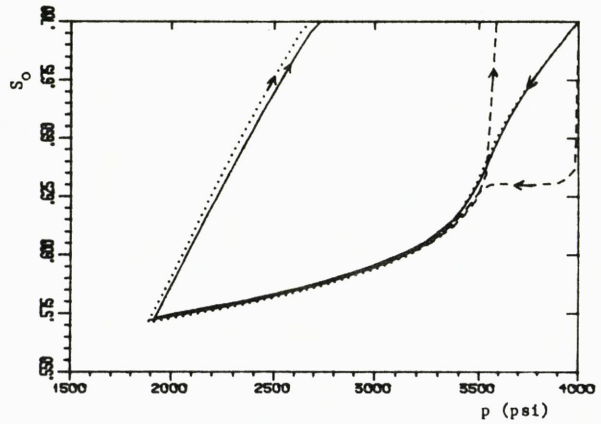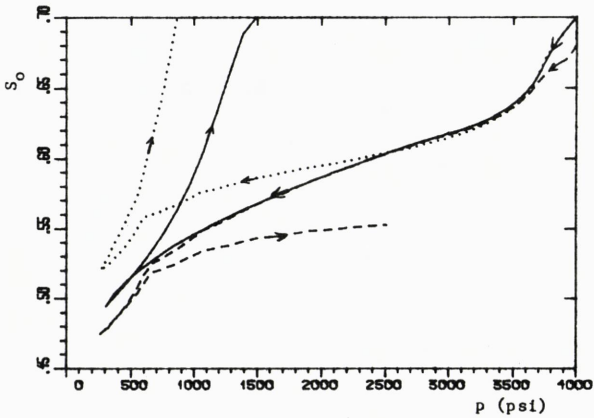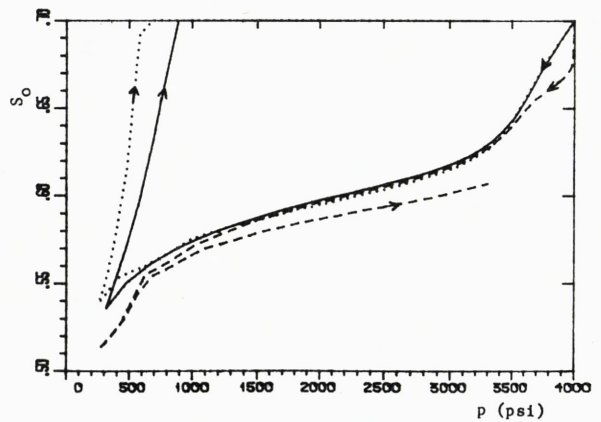
Fig. 3.4   Simulated oil saturation in block 1 compared with
           saturation calculated from Eq.(3.2.24) (method of
           Bøe et al.) and producing GOR (Raghavans method).
           Drawdown and buildup.

EXAMPLE 5
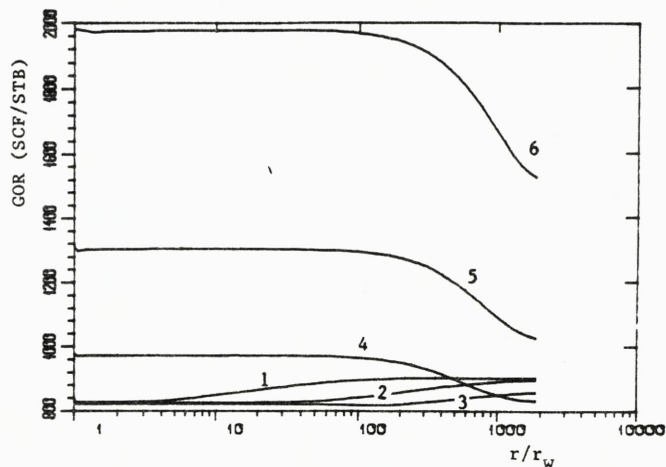
1	t =	1.04 hrs
2	t =	177 hrs
3	t =	1011 hrs
4	t =	5011 hrs
5	t =	7511 hrs
6	t =	10011 hrs

<u>Fig. 3.5</u>   Simulated GOR vs. dimensionless radius.   Drawdown.

EXAMPLE 3
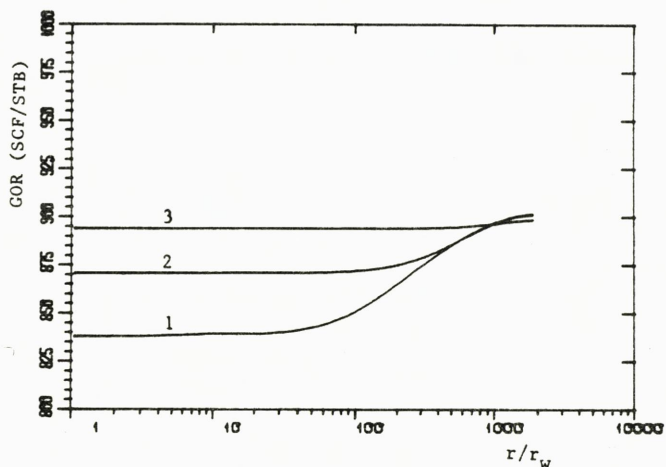
1	Δt =	1.14 hrs
2	Δt =	10.6 hrs
3	Δt =	100 hrs
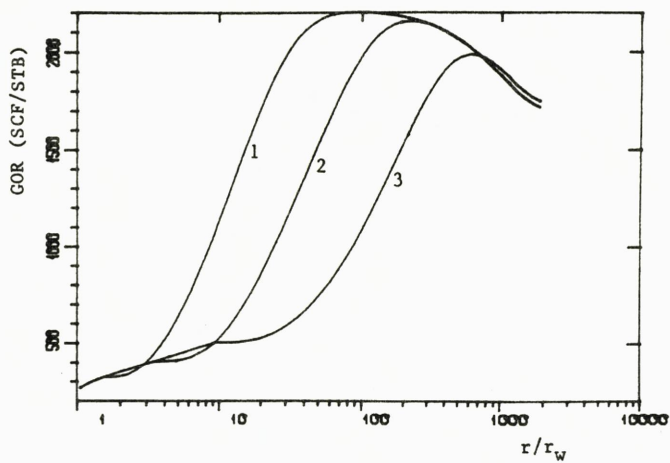
EXAMPLE 5

1	Δt =	0.75 hrs
2	Δt =	7.00 hrs
3	Δt =	100 hrs

<u>Fig. 3.6</u>   Simulated GOR vs. dimensionless radius.   Buildup.
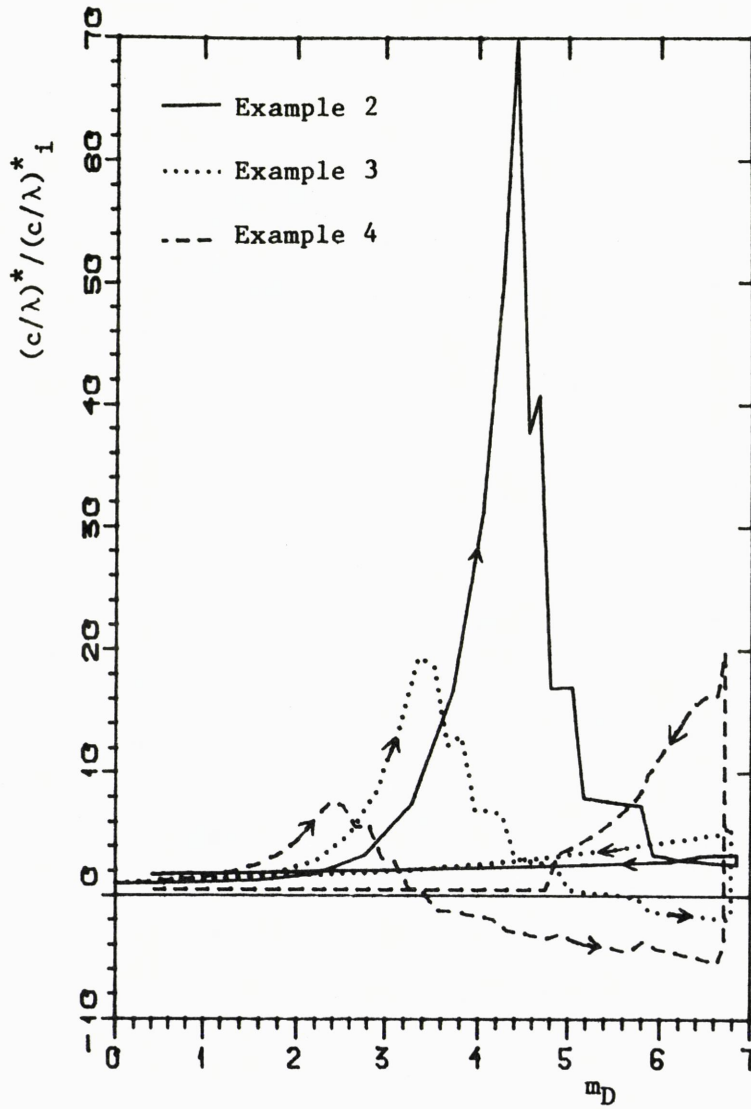
Fig. 3.7 $(c/\lambda)^*/(c/\lambda)^*_i$ vs. m_D for example 2,3,and 4,
drawdown and buildup. Effect of rate.
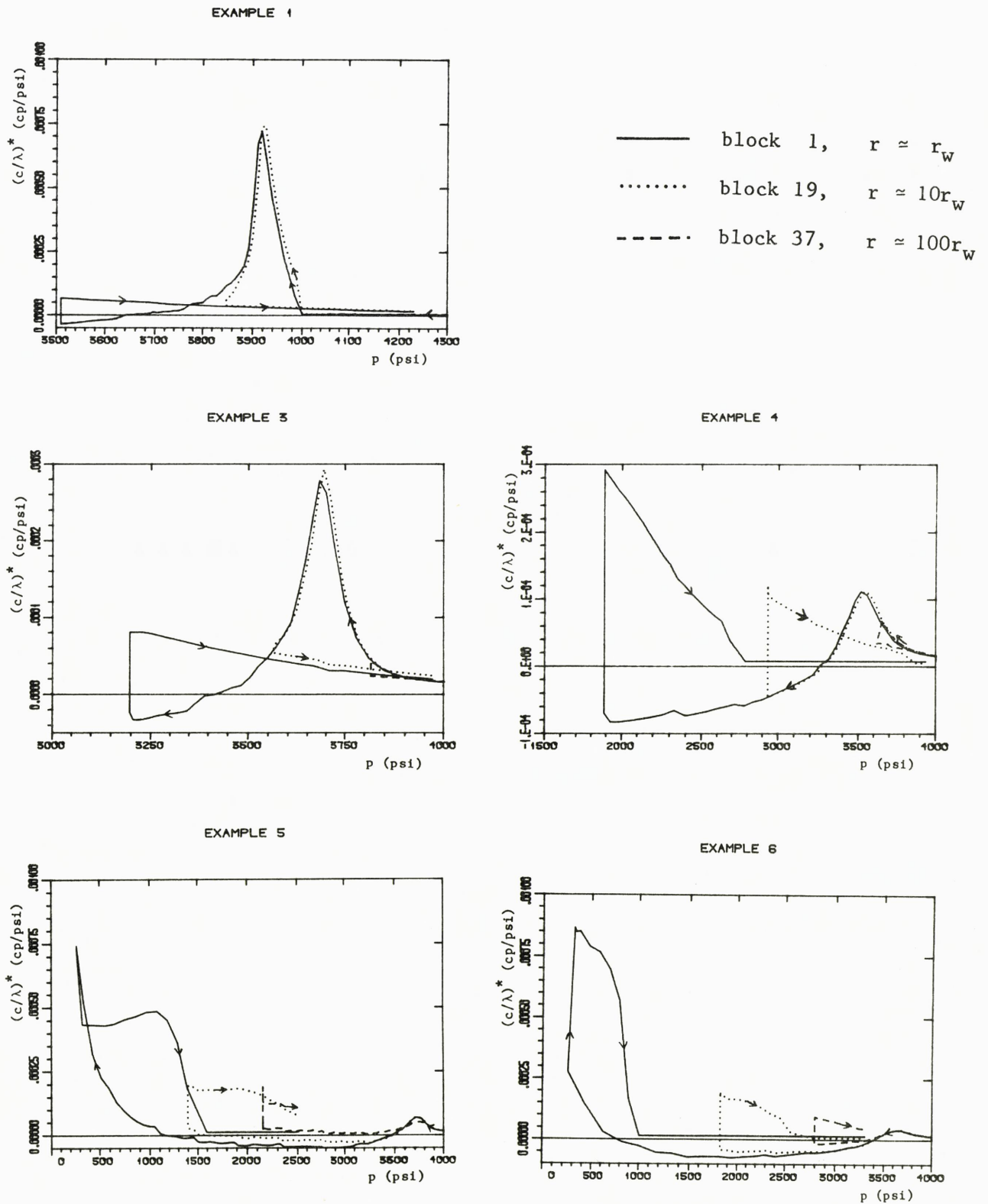
EXAMPLE 1

EXAMPLE 3

EXAMPLE 4
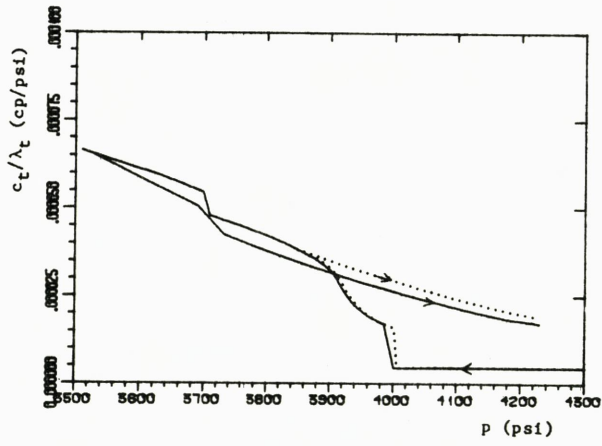
EXAMPLE 5

EXAMPLE 6

		block 1,	$r \simeq r_w$
....		block 19,	$r \simeq 10r_w$
- - - -		block 37,	$r \simeq 100r_w$
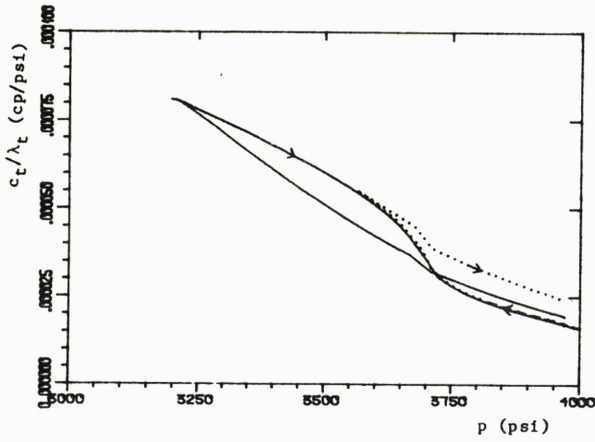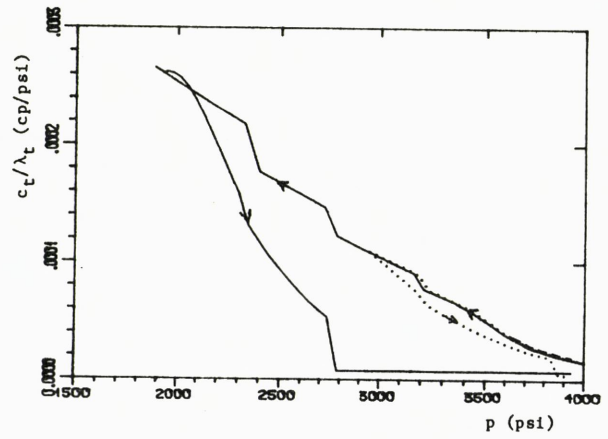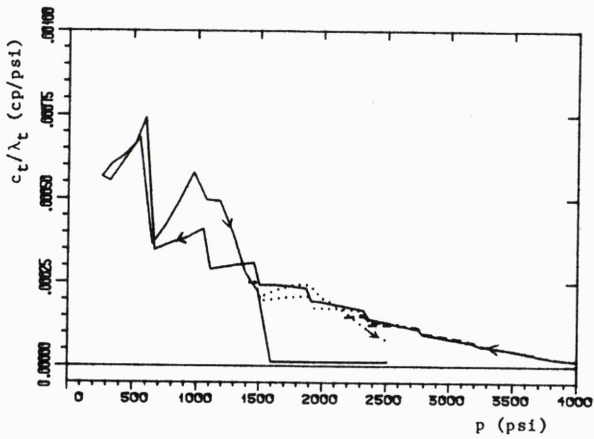
Fig. 3.8 $(c/\lambda)^*$ vs. pressure at different points in the reservoir.
Drawdown and buildup.
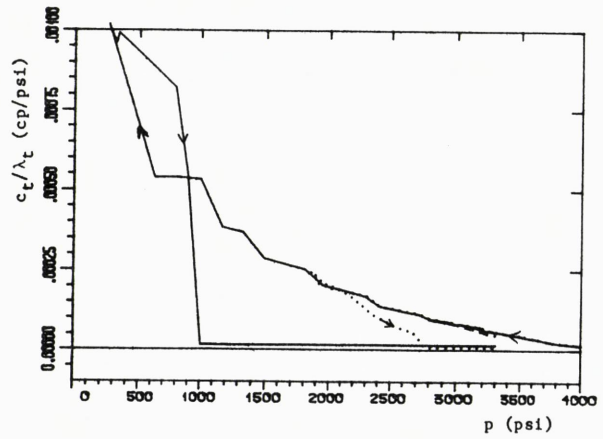
Fig. 3.9 c_t/λ_t vs. pressure at different points in the reservoir.
Drawdown and buildup.

EXAMPLE 3
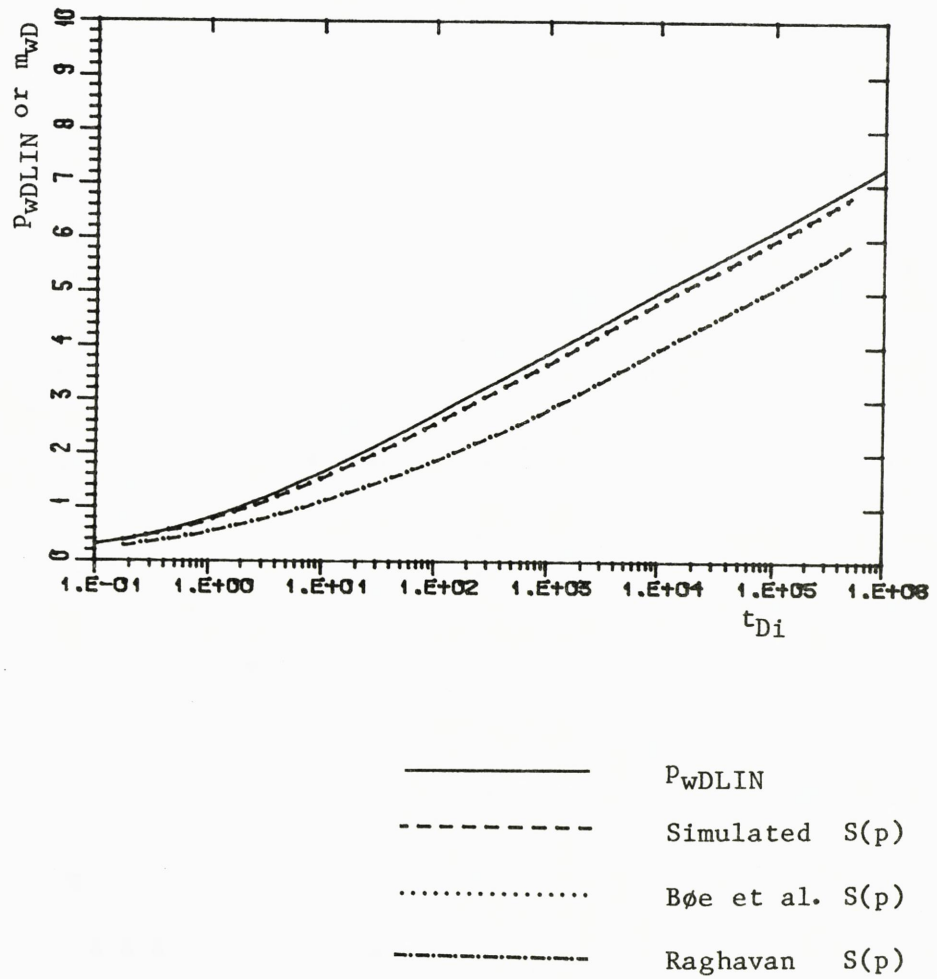
Fig. 3.10 Dimensionless pseudopressure functions vs. dimensionless
producing time, t_{Di}. Pseudopressure calculated from
the pressure-saturation relation of Bøe et al. (Eq.(3.2.24)
and Raghavan (Eq.(3.3.2) compared with pseudopressure
calculated from simulated S(p) in block 1.
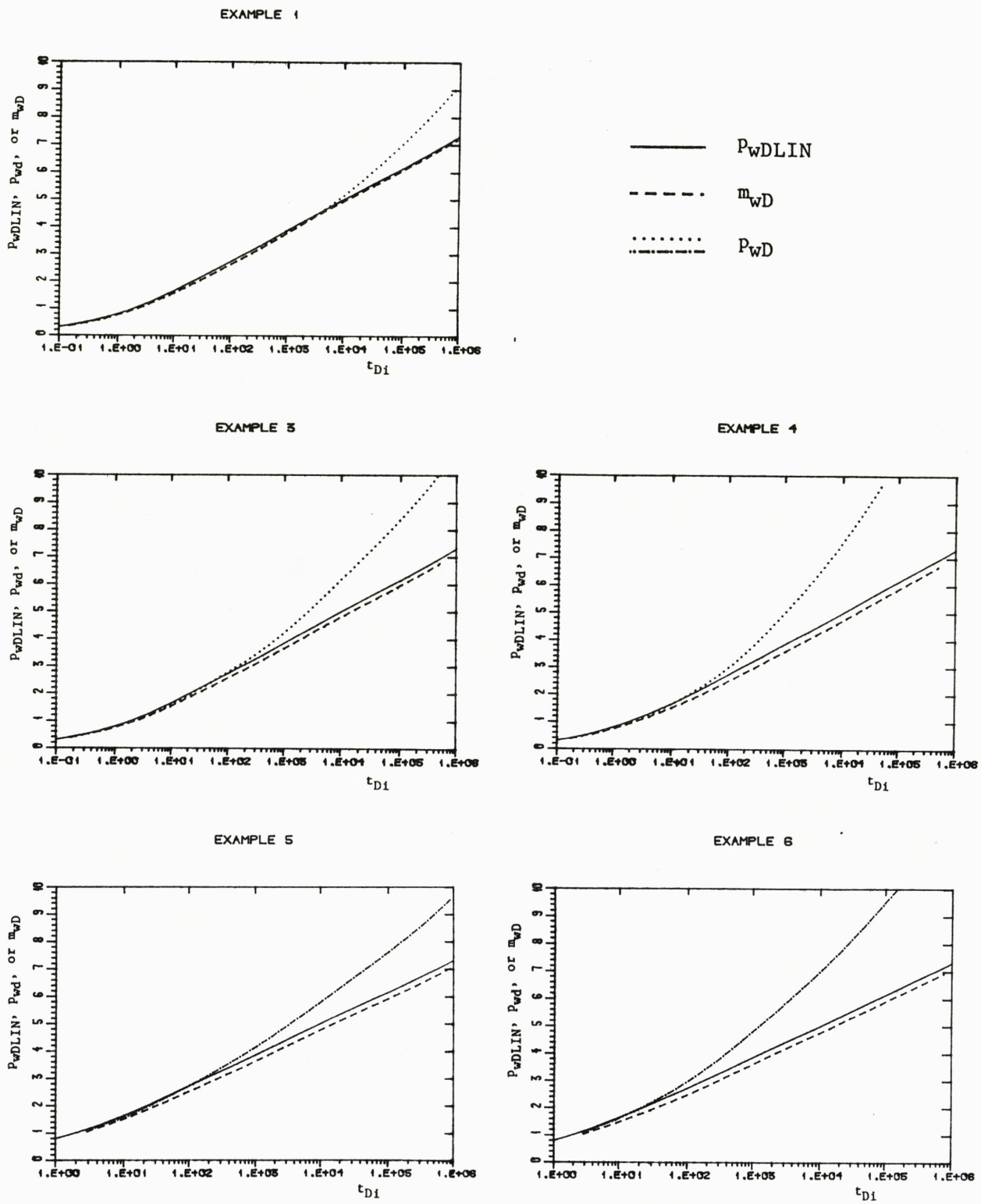
Fig. 3.11 Dimensionless pressure and pseudopressure functions vs. dimensionless producing time, t_{Di}. Pseudopressure is calculated from simulated $S(p)$ in block 1.

Example 5

t = 177 hrs

$(t_{DAi} = 0.07)$
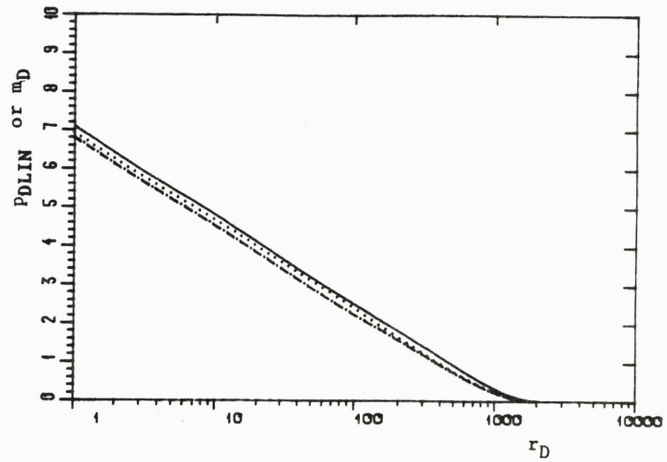
Example 6

t = 1800 hrs

$(t_{DAi} = 0.72)$
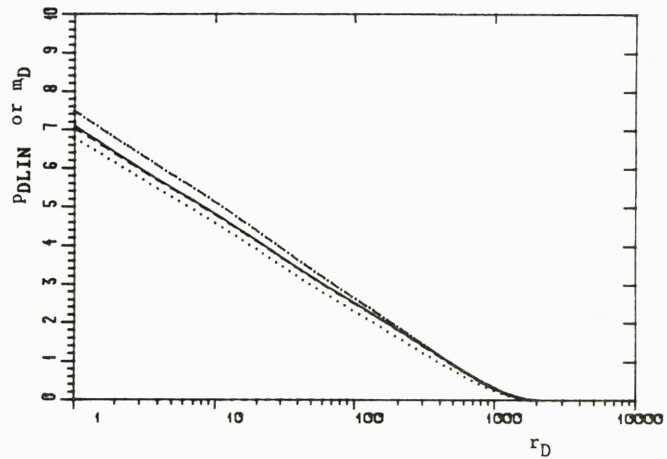
Example 5

t = 10600 hrs

$(t_{DAi} = 4.23)$
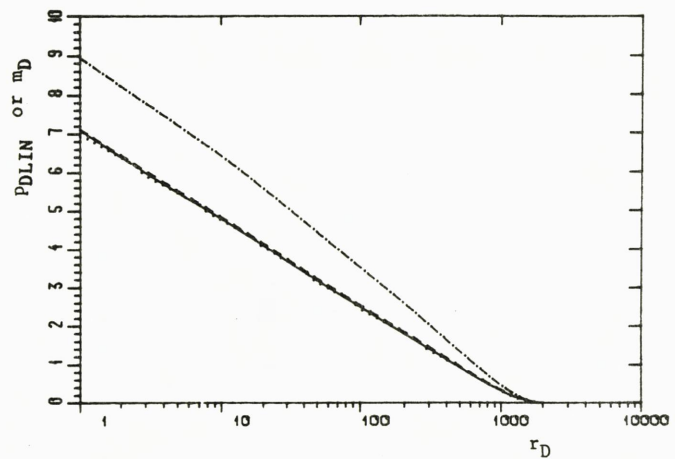
——————— p_{DLIN}

—·—·—·— m_D calculated from simulated S(p) in block 1

— — — — m_D calculated from simulated S(p) profile

·········· m_D calculated from producing GOR and Eq.(3.3.2)

Fig. 3.12 Dimensionless pseudopressure profiles compared with the
liquid solution. p_{DLIN} and m_{DLIN} are defined relative
to the respective solutions at the outer boundary.

EXAMPLE 5
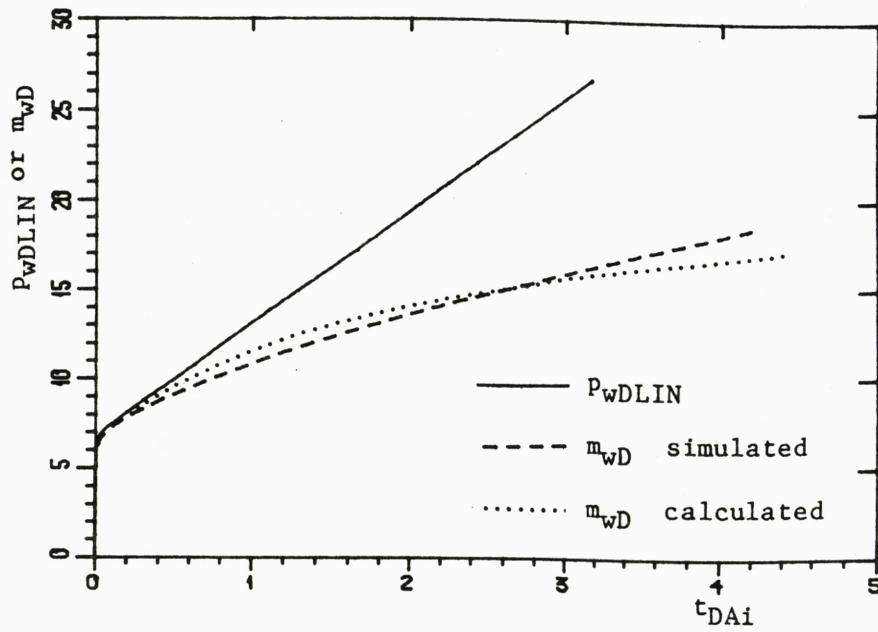
EXAMPLE 6
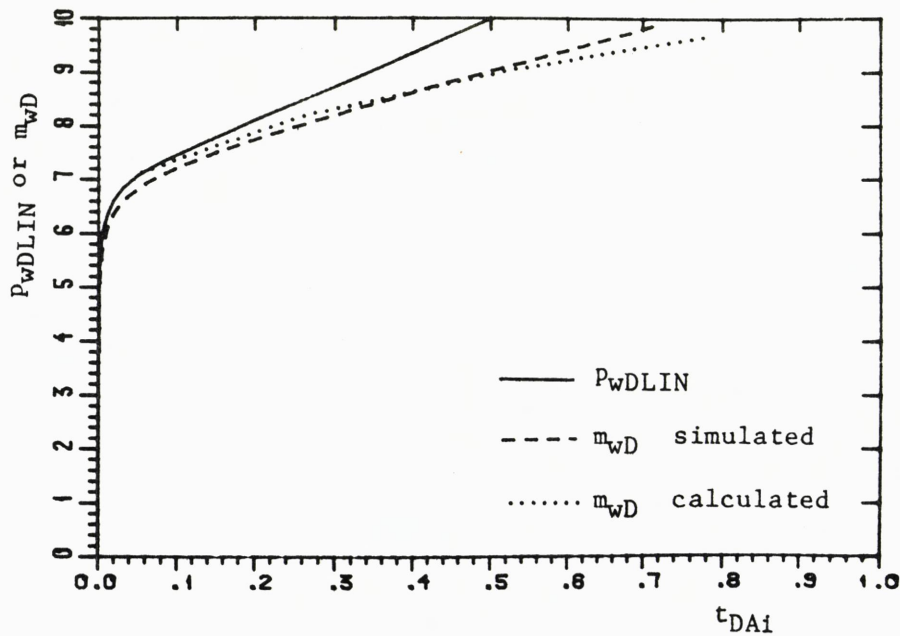
Fig. 3.13 Dimensionless pseudopressure vs. t_{DAi} compared with the
liquid solution. "Simulated" m_D is calculated from
simulated wellbore pressure and oil saturation in block 1.
"Calculated" m_D is calculated from Eq.(3.3.6) and
an equation corresponding to Eq.(2.5.10).

EXAMPLE 1

Legend:

—— P_{wDLIN}

– – – m_{wDs} calculated from drawdown
$S(p)$ in block 1

–·–·– m_{wDs} calculated from buildup
$S(p)$ in block 1
(method of Bøe et al.)

········ m_{wDs} calculated from producing
GOR at shut-in
(Raghavan's method)

EXAMPLE 3

EXAMPLE 4
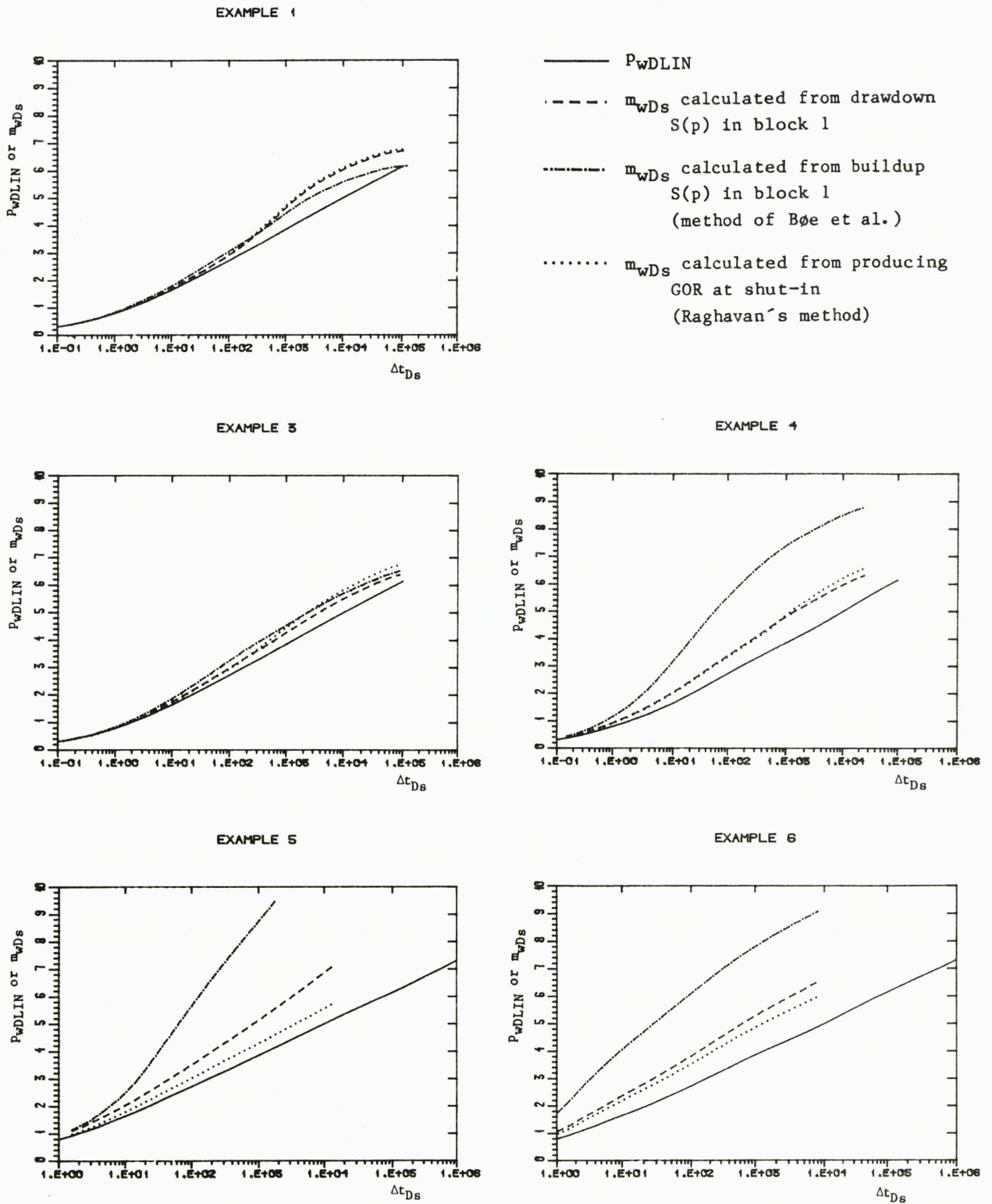
EXAMPLE 5

EXAMPLE 6

Fig. 3.14 Dimensionless pseudopressure rise during buildup vs.
dimensionless shut-in time, Δt_{Ds}, compared with
(drawdown) liquid solution.

EXAMPLE 1
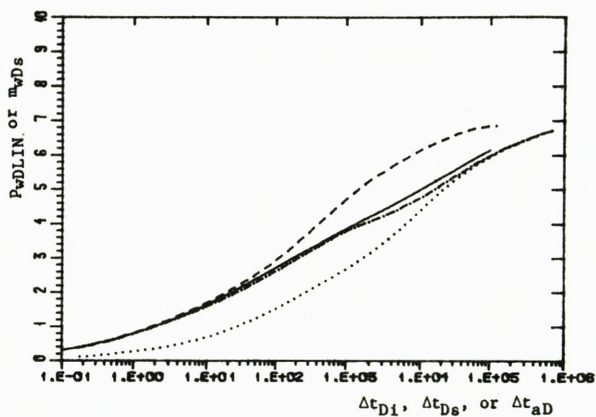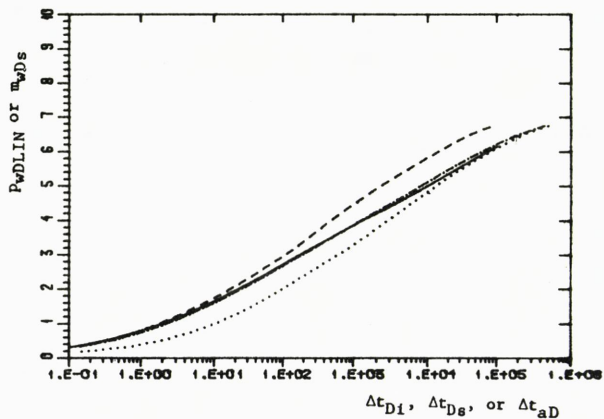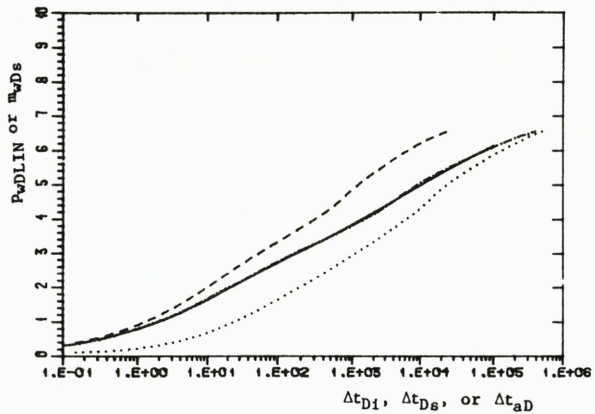
EXAMPLE 3
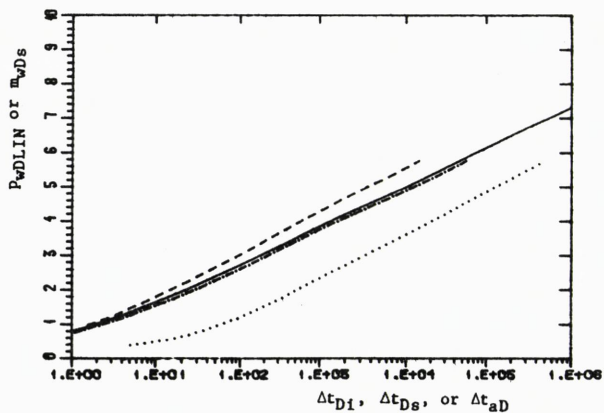
EXAMPLE 4

EXAMPLE 5

EXAMPLE 6
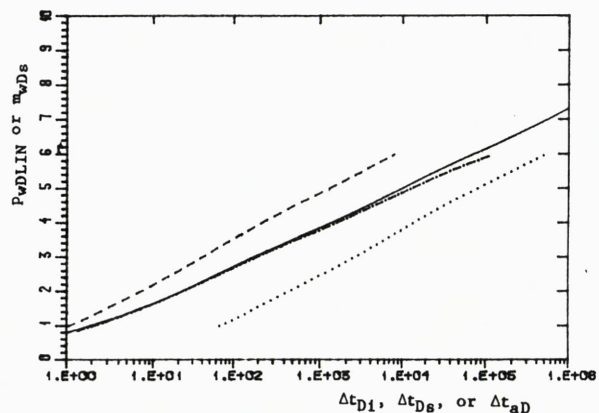
Fig. 3.15 Dimensionless pseudopressure rise during buildup
calculated from producing GOR at shut-in (Raghavan's
method) vs. dimensionless shut-in times, Δt_{Di} and Δt_{Ds},
and dimensionless shut-in pseudotime, Δt_{aD},
compared with (drawdown) liquid solution.

Drawdown.

Pseudopressure calculated from
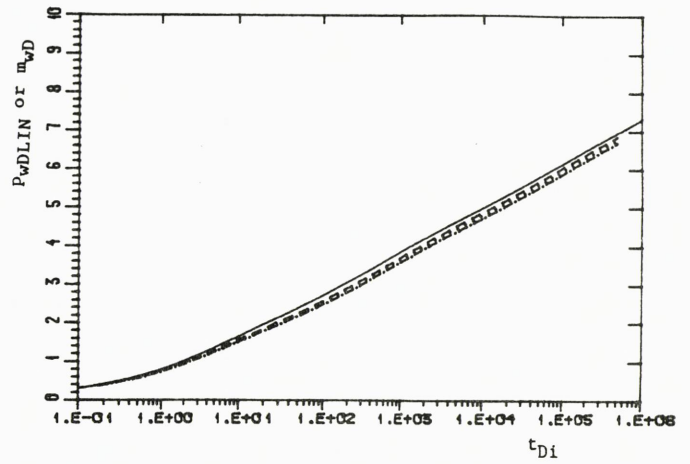
drawdown S(p) in block 1

Buildup.

Pseudopressure calculated from

drawdown S(p) in block 1
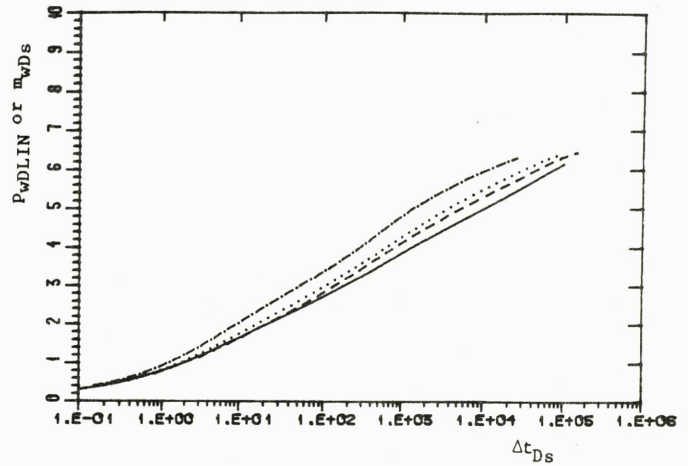
Buildup.

Pseudopressure calculated from

buildup S(p) in block 1
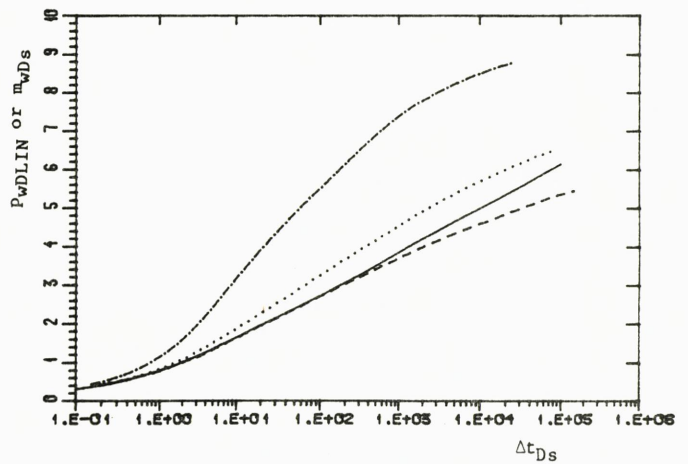
Fig. 3.16 Pseudopressure functions compared with liquid solution,

example 2, 3, and 4. Effect of rate.
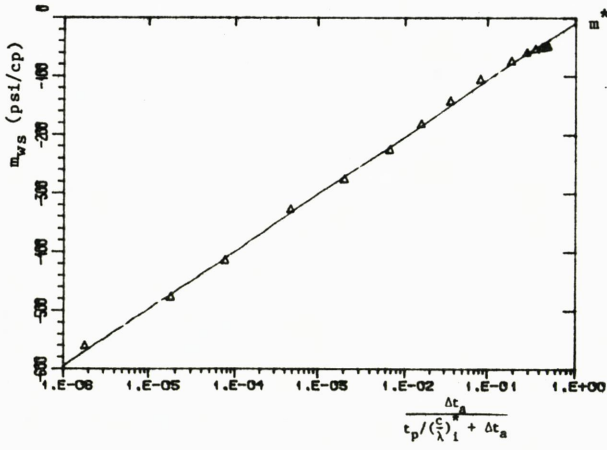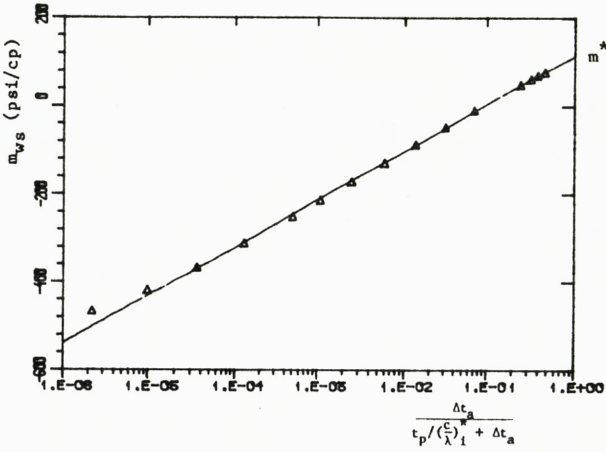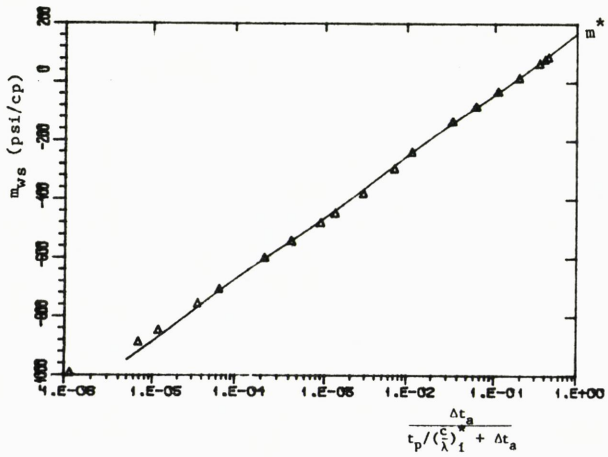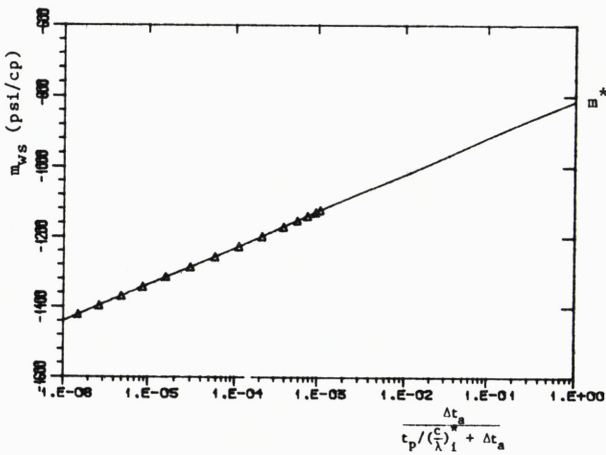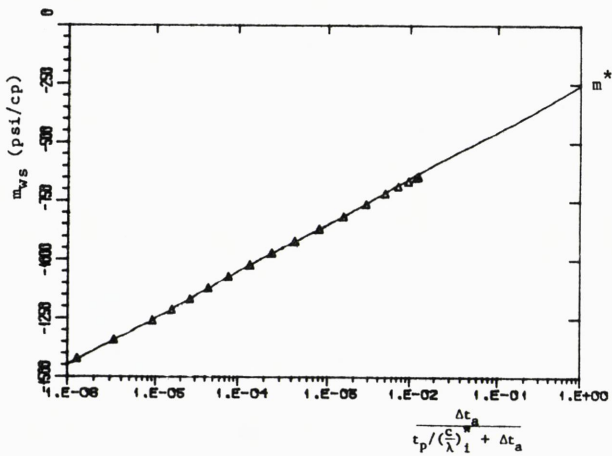
Fig. 3.17 Pseudopressure calculated from producing GOR at shut-in (Raghavan´s method) vs. inverse Horner pseudotime.
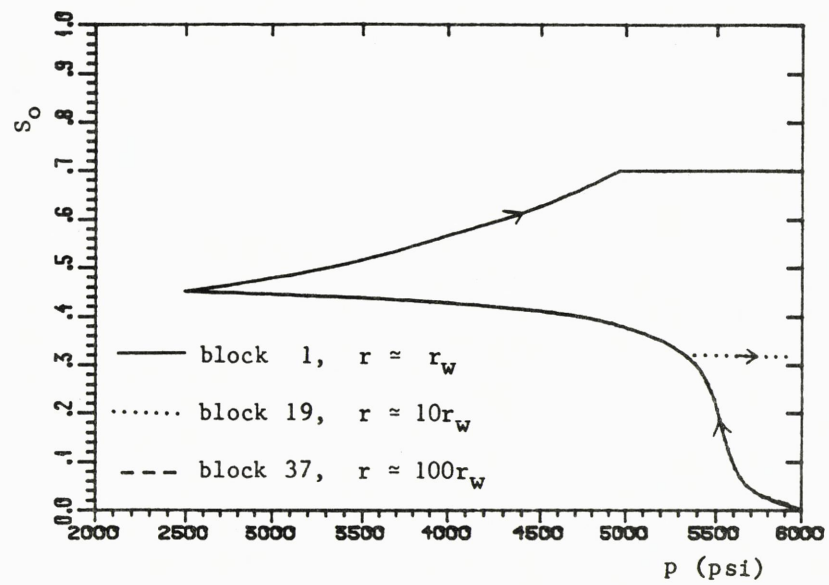
Fig. 3.18 Gas condensate example. Oil saturation vs. pressure at
          different points in the reservoir. Drawdown and buildup.
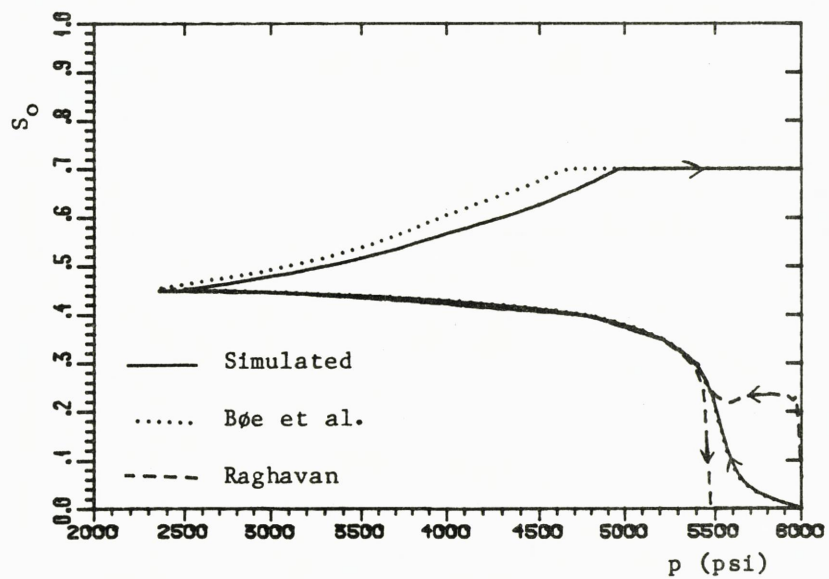
Fig. 3.19 Gas condensate example. Simulated oil saturation in block 1
          compared with saturation calculated from Eq.(3.2.24) (method
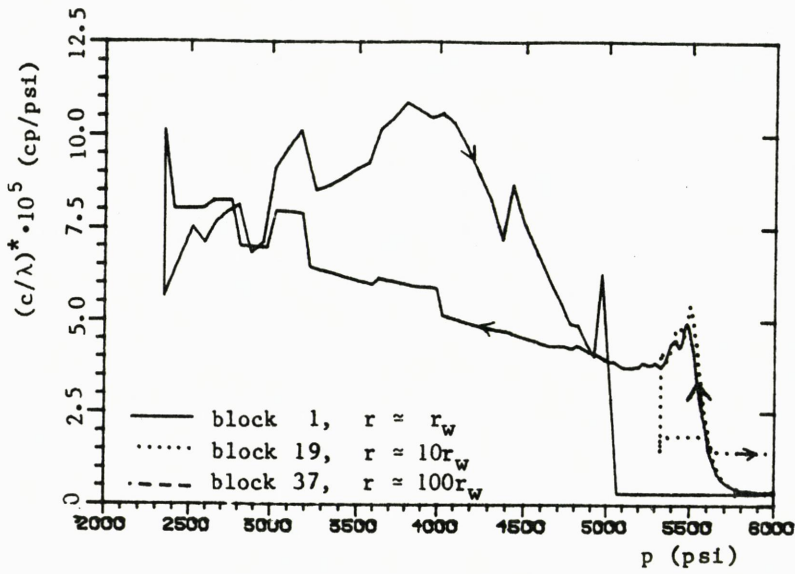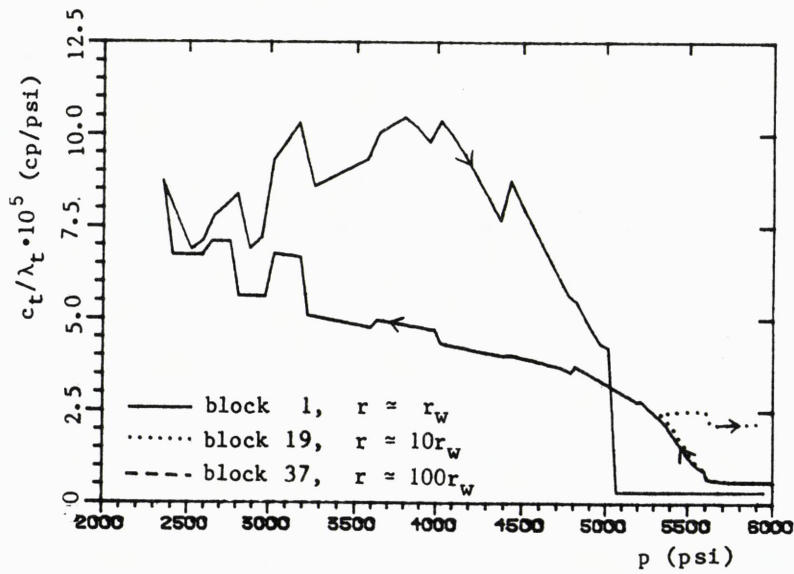   of Bøe et al.) and producing GOR (Raghavan´s method).
          Drawdown and buildup.

Fig. 3.20 Gas condensate example. $(c/\lambda)^*$ vs. pressure at different
         points in the reservoir. Drawdown and buildup.

Fig. 3.21 Gas condensate example. c_t/λ_t vs. pressure at different
         points in the reservoir. Drawdown and buildup.
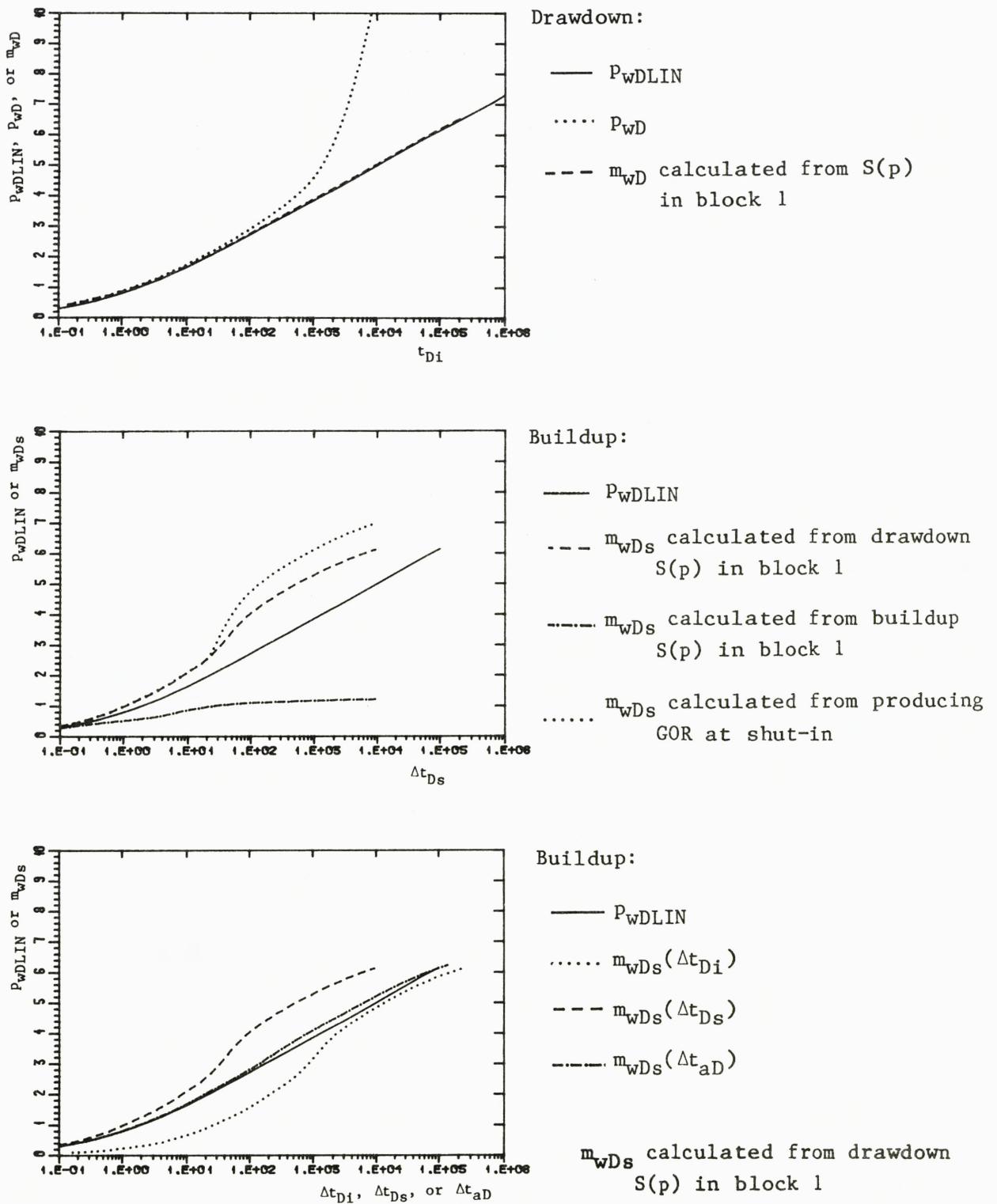
Fig. 3.22 Gas condensate example. Dimensionless pressure and
        pseudopressure functions compared with the liquid solution.
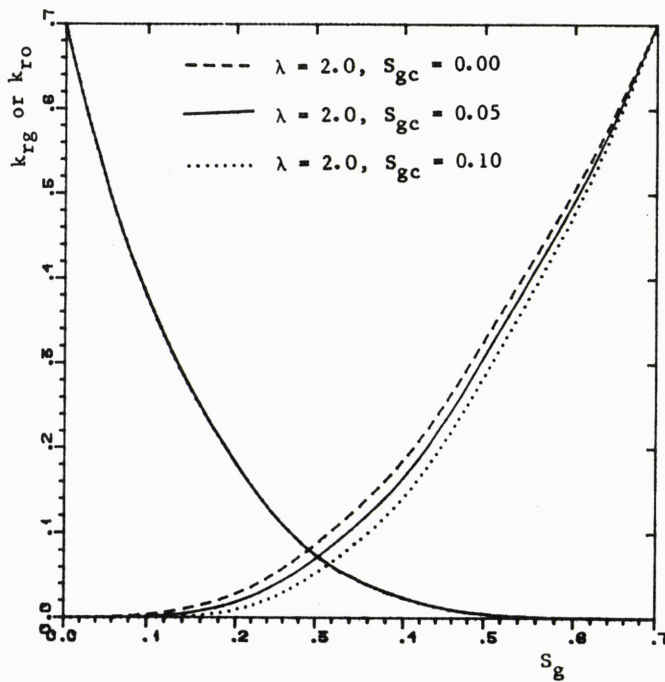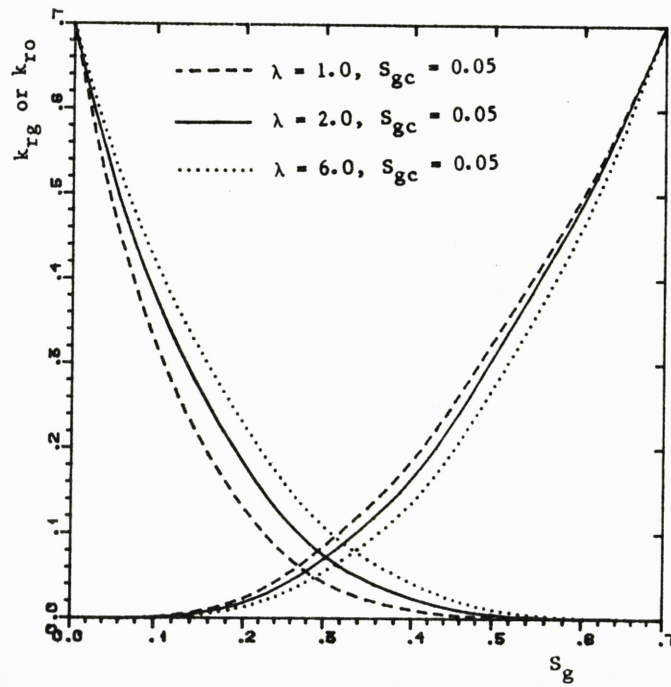
Fig. 3.23 Relative permeabilities calculated from Standing's
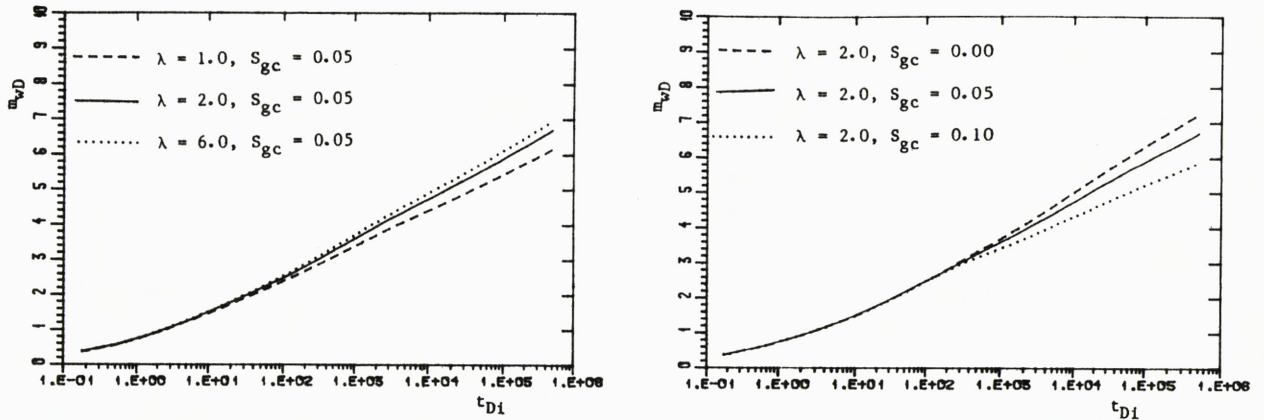correlations [16].

Fig. 3.24 Dimensionless pseudopressure fall vs. dimensionless
          producing time, t_{Di} example 4. Effect of using
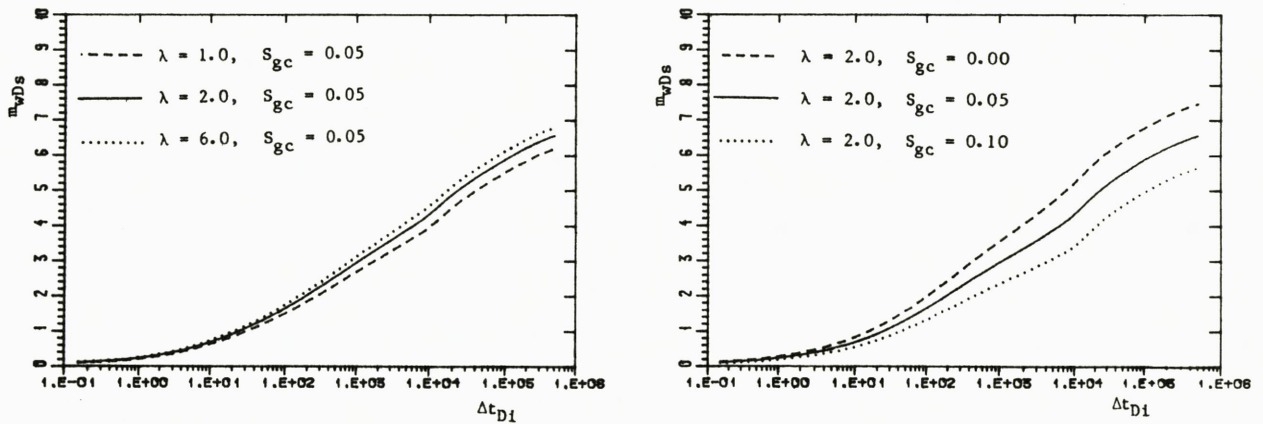   different relative permeabilities.

Fig. 3.25 Dimensionless pseudopressure rise during buildup vs.
          dimensionless shut-in time, Δt_{Di} example 4. Effect of
          using different relative permeabilities.

REPORTS PUBLISHED BY THE

DEPARTMENT OF APPLIED MATHEMATICS

UNIVERSITY OF BERGEN

BERGEN, NORWAY

No. 1. A. Kildal and S. Tjøtta.
On acoustic streaming in magneto-
hydrodynamics, February 1964.

No. 2. G. Berge.
On the stability of a magnetized
plasma with a continuous density
force field, June 1964.

No. 3. J. Falnes.
Coaxial waveguide consisting of a
circular metal tube surrounding a
coaxial unidirectionally
conducting sheet, August 1965.

No. 4. K.B. Dysthe.
On nonlinear interaction between
two beams of plane electromagnetic
waves in an anisotropic medium,
December 1964.

No. 5. K.J. Overholt.
Extended Aitken acceleration.
March 1965.

No. 6. G. Berge.
On the stability of a rotating
plasma from the two fluid equations
including finite radius of gyration
effects, May 1965.

No. 7. A. Svardal.
On acoustical streaming between two
coaxial cylinders, May 1965.

No. 8. K.B. Dysthe.
On convective and absolute
instability, November 1965.

No. 9. L. Engevik.
On linear and non-linear hydro-
magnetic vortex motion generated
by the interaction of a gravity
wave with a solid boundary, April 1966.

No. 10. S. Tjøtta.
Some non-linear effects in sound
fields, July 1966.

No. 11. L. Engevik.
On a stability problem in
hydrodynamics. Part I,
November 1966.

No. 12. L. Engevik.
On the stability of plane
inviscid Couette flow,
November 1966.

No. 13. L. Engevik.
On a stability problem in
hydrodynamics. Part II,
January 1967.

Report NTNF. L. Storesletten.
On non-linear magneto-hydro-
dynamic wave motion in dissipative media,
September 1967.

No. 14. K.B. Dysthe.
Self-trapping and self-focusing of
electromagnetic waves in a
plasma, May 1968.

Report no. 15 not written.

No. 16. K.B. Dysthe.
Force on a small inclusion in a
standing acoustic wave, July 1968.

No. 17. A. Svardal and S. Tjøtta.
Oscillatory viscous flows in the
vicinity of a cylinder, June 1969.

No. 18. A.H. Øien and J. Naze Tjøtta.
Kinetic theory of a weakly coupled
and weakly inhomogeneous gas,
June 1969.

No. 19. M.S. Espedal.
Hydrodynamic equations for a
F.L.R. plasma, August 1969.

No. 20. J. Naze Tjøtta and A.H. Øien.
Kinetic theory of a weakly
coupled and weakly inhomogeneous
plasma in a magnetic field,
August 1969.

No. 21. K.S. Eckhoff.
On stability.
Part I: General theory,
November 1969.

No. 22. K.S. Eckhoff.
On stability.
Part II: Linear problems,
December 1969.

No. 23. K.S. Eckhoff.
On stability.
Part III: The energy principle
in MHD, December 1969.

No. 24. K.B. Dysthe.
On the stability of a
cylindrical surface-film,
December 1969.

No. 25. M.S. Espedal.
The effects of ion-ion collision on
a ion-acoustic plasma pulse,
April 1970.

No. 26. A.H. Øien.
Derivation of kinetic equations of
a plasma using a multiple time and
space scale method, September 1970.

No. 27. K.S. Eckhoff.
On stability.
Part IV: Nonlinear partial
differential equations,
October 1970.

No. 28. O. Faltinsen and S. Tjøtta.
Interaction between sound waves
propagating in the same direction,
April 1971.

No. 29. T. Leversen and J. Naze Tjøtta.
Solution of a stationary Fokker-
Plank equation, June 1971.

No. 30. E. Mæland.
Application of the Galerkin's
method on the problem of cellular
convection induced by surface
tension gradients, November 1971.

No. 31. S. Nissen-Meyer.
A note on the problem of reversi-
bility of mathematical models.
(Preliminary issue.),
December 1971.

No. 32. L. Hinderaker.
On the foundations of the method
of matched asymptotic approxi-
mations to two meeting orthogonal
boundary-layers, December 1971.

No. 33. A. Bertelsen, A. Svardal
and S. Tjøtta
Non-linear streaming effects
associated with oscillating
cylinders, December 1971.

No. 34. S. Nissen-Meyer.
Some theorems on the problem of
reversibilty of mathematical
models.
(This report is a revised issue
of report no. 31.), April 1972.

No. 35. I. Eidhammer.
A minimum resource sorting method,
June 1972.

No. 36. T.O. Espelid.
On the behaviour of the secant
method near a multiple root,
September 1971.

No. 37. H.B. Drange.
The linearized Boltzmann collision
operator for cut-off potentials,
December 1972.

No. 38. J. Naze Tjøtta and S. Tjøtta.
Sur le transport de masse produit
par des oscillations en milieu
compressible, dissipatif et
inhomogene, December 1972.

No. 39. M. Aksland.
On the twodimentional birth and
death process with mutation,
January 1973

No. 40. A. H. Øien.
Kinetic theory for evolution of
a plasma in external electro-
magnetic fields toward a state
characterized by balance of
forces transverse to the
magnetic field, April 1973.

No. 41. H.B. Drange.
On the Boltzmann equation with
external forces. April 1973.

No. 42. J. Naze Tjøtta and
S. Tjøtta.
On the mass transport induced
by time-dependent oscillations
of finite amplitude in a
nonhomogeneous fluid.
I General results for a
perfect gas, May 1973.

No. 43. L. Engevik.
Perturbation about neutral
solutions occuring in shear
flows in stratified, incom-
pressible and viscid fluids,
June 1973.

No. 44. J. Naze Tjøtta and
S. Tjøtta.
On the mass transport induced by
time-dependent oscillations of
finite amplitude in a
nonhomogeneous fluid.
II General results for a liquid.
August 1973.

No. 45. G.Dahl and S. Storøy.
Enumeration of vertices in the
linear programming problem,
October 1973.

No. 46. M. S. Espedal.
The effects of trapped and
untrapped particles on an
electrostatic wave packet.
December 1973.

No. 47 M. S. Espedal.
A procedure to solve the Fokker-
Planck - Poisson equations
consistently, April 1974

No. 48. E. Mjølhus.
Application of the reductive per-
turbation method to long hydromag-
netic waves parallel to the
magnetic field in a cold plasma,
May 1974.

No. 49. K. S. Eckhoff.
The propagation of discontinuities
for linear hyperbolic partial
differential equations, August 1974.

No. 50. T. O. Espelid.
An algorithm for internal merging
of two subsets with small extra
storage requirements, September 1974.

No. 51. E. Mæland.
Mass transport induced by wave
motion in a rotating fluid,
October 1974.

No. 52. I.S. Helland.
A random exchange model with
constant decrements,
December 1974.

No. 53. A. H. Oien.
On the evolution of a two
component, two temperature, fully
ionized plasma in electromag-
netic fields, January 1975.

No. 54. K.S. Eckhoff.
Stability problems for linear
hyperbolic systems, May 1975.

No. 55. K. S. Eckhoff.
On stability in ideal compres-
sible hydrodynamics, May 1975.

No. 56. L. Storesletten.
A note on the stability of
horizontal shear flow of an
inviscid compressible fluid,
July 1975.

No. 57. K. S. Eckhoff and
L. Storesletten.
On the stability of shear flow in
a rotating compressible and
inviscid fluid, July 1975.

No. 58. E.N. Håland and G. Berge.
Dynamic stabilization of the
m = 1 instability in a diffuse
linear pinch, July 1975.

No. 59. E. Mæland.
Mass transport induced by wave
motion in a stratified and
rotating fluid, August 1975.

No. 60. T. O. Espelid.
On replacement-selection and
Dinsmore's improvement, August 1975.

No. 61. L. Storesletten.
A note on the stability of
steady inviscid helical gas
flows, January 1976.

No. 62. E. Mæland.
A time-dependent model of
coastal currents and upwelling,
June 1976.

No. 63. A. H. Oien.
Corrections to classical kinetic
and transport theory for a two-
temperature, fully ionized plasma
in electromagnetic fields,
June 1977.

No. 64. S. D. Flåm.
Convergence in law of a series of
φ-mixing random variables implies
convergence in probability,
August 1977.

No. 65. A. H. Oien.
Kinetic equation for an electron
gas (non-neutral) plasma in
strong fields and inhomogenities,
June 1978.

No. 66. H. Hobæk and S. Tjøtta.
Theory of parametric acoustic
arrays, July 1978.

No. 67. T.O. Espelid.
On floating-point summation,
December 1978.

No. 68. E.N. Håland.
Stability of an inverted pendulum
with hard spring and oscillating
support, December 1978.

No. 69. S. Storøy.
An efficient least distance algo-
rithm based on a general quadratic
programming method, November 1979.

No. 70. L. E. Engevik.
Amplitude evolution equation for
linearly unstable modes in
stratified shear flows, November 1979.

No. 71. F. Oliveira-Pinto.
Argument reduction for elementary
mathematical functions : An
overview, July 1980.

No. 72. A. H. Oien.
A quasi moment description of the
evolution of an electron gas
towards a state dominated by a
reduced transport equation,
September 1980.

J. Berntsen.
User-documentation. Program HALF.
A subroutine for numerical
evaluation of three-dimensional
complex integrals, spring 1983.

No. 73. S.I. Aanonsen.
Numerical computation of the
nearfield of a finite amplitude
sound beam, September 1983.

No. 74. L.K. Sandal.
Influence of equilibrium flows
on viscous tearing modes,
December 1983.

No. 75. Ø. Pettersen.
The nearfield of a high frequency
amplitude shaded baffled piston.
An analytical/numerical investi-
gation, July 1981.

No. 76. Ø. Pettersen.
Numerical solution of the
Buckley-Leverett equation with a
general fractional flow function,
November 1984.

No. 77. T. Mannseth.
Sound propagation in the Pekeris
waveguide with application to
directional sources.
November 1984.

No. 78. T. Barkve.
A study of the Verigin problem
with application to analysis of
water injection tests.
March 1985.